

Alma Mater Studiorum – Università di Bologna

DOTTORATO DI RICERCA IN
Scienze Biotecnologiche e Farmaceutiche

Ciclo XXX

Settore Concorsuale: 03/D1

Settore Scientifico Disciplinare: CHIM/08

Design, Synthesis and *in vitro* Characterization of
Novel Topoisomerase II Inhibitors and Poisons

Presentata da: Elirosa Minniti

Coordinatore Dottorato

Prof. Santi Mario Spampinato

Supervisore

Prof.ssa Anna Minarini

Supervisore

Dott. Marco De Vivo

Co-supervisore

Prof. Neil Osheroff

Esame finale anno 2018

Contents

Preface	v
Abstract	vii
Chapter 1 – Introduction	1
1.1 Cancer Therapy.....	1
1.2 DNA topology.....	4
1.3 Eukaryotic DNA topoisomerases.....	7
Chapter 2 – Polyamines and cancer	29
2.1 Polyamine metabolism and transport.....	30
2.2 Polyamine-drug conjugates.....	33
Chapter 3 – Effect of etoposide derivatives on DNA cleavage mediated by human topoisomerase IIα	35
3.1 Etoposide derivatives.....	35
3.2 Drug design.....	41
3.3 Methods.....	43
3.3.1 Chemistry.....	43
3.3.2 Biology.....	44
3.3.3 Computational study.....	44
3.4 Results and discussion.....	48
3.5 Conclusion.....	52
3.6 Experimental section.....	53
3.6.1 Biology.....	53
3.6.2 Molecular modeling.....	54

Chapter 4 – Inhibition of human topoisomerase II α by xanthone

derivatives	55
4.1 Xanthone derivatives.....	55
4.2 Drug design.....	64
4.3 Methods.....	66
4.3.1 Chemistry.....	66
4.3.2 Biology.....	69
4.3.3 Computational study.....	69
4.4 Results and discussion.....	70
4.5 Conclusion.....	80
4.6 Experimental section.....	80
4.6.1 Chemistry.....	80
4.6.2 Biology.....	87
4.6.3 Molecular modeling.....	90

Chapter 5 - Inhibition of human topoisomerase II α by merbarone

derivatives	91
5.1 Merbarone derivatives.....	91
5.2 Drug design.....	96
5.3 Methods.....	98
5.3.1 Chemistry.....	98
5.3.2 Biology.....	100
5.3.3 Computational study.....	100
5.4 Results and discussion.....	100
5.5 Conclusion.....	104
5.6 Experimental section.....	105
5.6.1 Chemistry.....	105
5.6.2 Biology.....	108
5.6.3 Molecular modeling.....	110

Chapter 6 – Inhibition of human topoisomerase IIα by 4-Amino-2-pyrido-bicyclic pyrimidines derivatives	112
6.1 4-Amino-2-pyrido-bicyclic pyrimidines derivatives.....	112
6.2 Drug design.....	115
6.3 Methods.....	117
6.3.1 Chemistry.....	117
6.3.2 Biology.....	120
6.4 Results and discussion.....	120
6.5 Conclusion.....	123
6.6 Experimental Section.....	123
6.6.1 Chemistry.....	123
6.6.2 Biology.....	128
Abbreviations.....	130
Bibliography.....	131

Preface

This PhD thesis has been carried out at the Department of Pharmacy and Biotechnology, Alma Mater Studiorum-University of Bologna (Italy), under the supervision of Prof. Anna Minarini and Dott. Marco De Vivo (Istituto Italiano di Tecnologia) and during the period abroad under the supervision of Prof. Neil Osheroff (Vanderbilt University).

The dissertation research presented here is focused on the design, synthesis and evaluation of new poisons and inhibitors of topoisomerase II α for the treatment of cancer.

This PhD work is focused on four main projects: i) study of etoposide derivatives conjugates with different polyamine chain with the aim of obtaining a selective delivery to the cancer cells; ii) design, synthesis and characterization of new xanthone derivatives that block the activity of topoisomerase II α ; iii) design, synthesis and characterization of new merbarone derivatives that enhance topoisomerase II-mediated DNA cleavage; iv) design, synthesis and characterization of 4-amino-2-pyrido-bicyclic pyrimidine derivatives targeting the topoisomerase II α .

The thesis is organized in different chapters: the first chapter is a brief introduction about the physiopathological aspects and the current approaches for the treatment of cancer. Chapter 2 described the role of the polyamines in targeted cancer therapy.

Chapters 3-6 describe each class of compounds that act against topoisomerase II on the basis of which we designed and synthesized the new molecules. In particular, they include the drug design approaches, the synthetic methods, the biological evaluation assays and the computational study of the new synthesized compounds. Result and discussion section and experimental procedure are also reported.

I would like to first thank my research advisors, Prof. Anna Minarini, Dott. Marco De Vivo and my co-supervisor Prof. Neil Osheroff for the helpful discussions, guidance and encouragement in the project realization.

I would also like to thank Jo Ann Byl (Vanderbilt University) for the valuable support and assistance.

Thanks to Prof. Michela Rosini (University of Bologna) for encouragement.

To Prof. Claudia Sissi and her group (University of Padova) for biological investigations on etoposide and merbarone derivatives.

Abstract

Cancer is a term used for diseases characterized by out of control cell-growth and rapid creation of abnormal cells able to grow beyond their usual borders, invading adjoining parts of the body and spreading to other organs. Several biochemical targets have been recognized to play a fundamental role in its development. In particular, in cancer therapy, DNA topoisomerases have raised much interest as potential anticancer targets. Topoisomerases are ubiquitous enzymes essential for cell survival that regulate the topological state of DNA. They modulate DNA supercoiling and remove DNA knots and tangles. There are two major classes of topoisomerases, type I and type II, that are distinguished by the number of DNA strands that they cleave and the mechanism by which they alter the topological properties of the genetic material. Type II topoisomerases regulate the topological state of DNA in the cell by generating transient double-stranded breaks in the double helix. The catalytic cycle of the enzyme is initiated by binding the two double-stranded DNA segments. In order to maintain genomic integrity while the DNA is cleaved, topoisomerase II forms a covalent attachment, known as the “cleavage complex”, which is normally short-lived and is present at low steady-state levels in order to be tolerated by normal cells.

Considering the key role of this enzyme for cell surviving, in this thesis project new small entities have been designed and synthesized in order to provide molecules able to block the activity of topoisomerase II by inhibiting the overall catalytic activity of the enzyme or by enhancing the concentration of the cleavage complex. To this aim, four different scaffolds known to act against topoisomerase II were selected: i) 4'-demethylepipodophyllotoxin, ii) xanthone, iii) thiobarbituric acid, and iv) 4-amino-2-pyrido-bicyclic pyrimidine moieties.

All the new derivatives were investigated in biological assays and computational studies to evaluate their inhibitory activity and to identify their mechanism of action against topoisomerase II α .

Chapter 1-Introduction

1.1 Cancer therapy

Cancer, by definition, is a disease of genes. It is the second most common cause of morbidity and mortality world-wide, with millions of new cases of the common cancers, such as breast, colorectal, prostate and lung. Neoplasia, from Latin to indicate “new growth”, is an abnormality of cellular differentiation, maturation, and control of growth. In the early 1950s, Rupert Willis, a British pathologist, defined the neoplasia as an abnormal mass of tissue, the growth of which is uncontrollably faster than the one of the surrounding normal tissues.¹ Furthermore, neoplasia is characterized by three different peculiarities: 1) excessive cellular proliferation that usually produces an abnormal mass, or tumor; 2) uncoordinated growth, arose without any particular reasons; 3) persistence of excessive cell proliferation and growth even after the cause that caused the change has been removed.¹

Cancers can develop in different tissues of the body and can have different forms, in fact there are more than a hundred distinct types of cancer that differ in their behavior and response to treatments. There are five main categories of cancers, grouped according to the type of cell they start from:

- carcinomas: cancers that begin in the skin or in tissues that cover body organs;
- myeloma: cancers that originate in the plasma cells of bone marrow;
- sarcomas: rare kind of cancers. These tumors are most common in the bones, muscles and blood vessels;
- leukaemias and lymphomas: cancers of the blood and lymph glands, respectively.²

The incidence of this disease changes within the different genders: skin cancer is the most common type of malignancy for both men and women, the second most common type in men is prostate cancer, while in women is breast cancer. After heart disease, cancer is the second leading cause of death globally, and was responsible for 8.8 million deaths in 2015. Unfortunately, the number of new cases is expected to rise by about 70% over the next two decades.³

From a pathological standpoint, tumors are of two types, benign or malignant. The first one is not considered cancer; it usually grows slowly and cannot invade other tissues. It can form in different parts of the body but remains confined in the initial location. Once it is removed, does not usually recur. Malignant tumors are called cancers. They are able to invade surrounding tissues of the body different from the original site (the primary tumor) in order to provide origin to secondary tumors, or metastases. Malignant cells can pass more easily through smaller gaps, and can reach other tissues through bloodstream or lymphatic channels. These secondary tumors may grow, invade and damage nearby tissues, and spread again.⁴

In order to decrease the mortality rate due to cancer, much effort has been made to develop new therapies. Depending on the type and the localization of the disease, or the presence of metastases, the age and the health of the patient, there are different types of cancer treatments. Among them, there are surgery, radiation, chemotherapy, biological therapies (*e.g.*, immunotherapy and hormone therapy) and bone-marrow transplantation.

Surgery can be used to remove the entire tumor when is confined in one area or can be used to remove some of a cancer mass. Tumor removal may be the only treatment, or it may be combined with radiation therapy and/or chemotherapy.

Radiation therapy is a treatment with high-energy x-rays or proton radiations to destroy cancer cells and slow tumor growth, while inflicting minimal harm on nearby healthy tissue.

Chemotherapy is a valid option in modern cancer treatment, and many clinically available anticancer drugs are currently used to treat some type of leukaemias, lymphomas and solid tumors.^{5, 6} The chemical entities used during the chemotherapy are able to interfere with the cell division process, through the infliction of damage to DNA or proteins. A novel approach in chemotherapy field is the molecular-targeted therapy, which has the goal of achieving antitumor effects by selectively acting toward cancer cells. This kind of treatment differs from standard chemotherapy in several ways. First, targeted therapies act on selective molecular targets that are associated with the cancer. Furthermore, these treatments are designed with the aim of interacting specifically with their target, while standard chemotherapies were chosen because they kill cells. Classic chemotherapy agents are cytotoxic (they are able to kill tumor cells), contrary to targeted

therapies that are often cytostatic and act by blocking tumor cell proliferation. Molecular-targeted agents now account for ~70% of all anticancer agents currently under development. In fact, the great majority of recent standard therapies for cancers of various organs include molecular-targeted therapies.⁷ There are many different targeted therapies that have been approved for use in cancer treatment. These therapies include monoclonal antibodies, tyrosine kinase inhibitors, and antisense inhibitors of growth factor receptors. Some targeted therapies block specific enzymes and growth factor receptors involved in cancer cell proliferation. These drugs, in some cases, are called signal transduction inhibitors. As an example, the epidermal growth factor receptor inhibitor (EGFRi) erlotinib (Tarceva), is used in the treatment of non-small lung cell cancer.

DNA as target for anticancer drugs

DNA represents a molecular target for many drugs that are used in cancer therapy, and is viewed as a non-specific target for cytotoxic agents. A large number of chemotherapeutic anticancer drugs are compounds that interact with DNA directly or prevent the proper relaxation of DNA (through the inhibition of topoisomerases). Drugs that act at the DNA level can be classified in four different groups:

- alkylating agents react with electron-rich atoms in biologic molecules to form covalent bonds. There are several nucleophilic groups in DNA, in particular the 7-nitrogen of guanine. Alkylating agents are divided into two types: those that react directly with biological molecules and those that form a reactive intermediate, which then reacts with biological molecules. A large number of chemical compounds are alkylating agents under physiologic conditions, and a variety of them have antitumor activity. *E.g.*, mechlorethamine or cisplatin;
- intercalating agents are a class of polyaromatic compounds that can insert or intercalate between two base pairs of duplex DNA.⁸ Some drugs prefer to approach the helix *via* the DNA minor groove, while others prefer to interact with the DNA major groove. Several cancer antibiotics, such as the antitumor agents actinomycin D and adriamycin, operate by intercalating into the DNA;
- antimetabolites are compounds that are able to interfere with DNA production by stopping cell division and the growth of tumors. These substances often have

structure that are similar to naturally occurring molecules used in nucleic acid synthesis. Antimetabolites are used for a variety of cancer therapies including leukaemia, breast, ovarian and gastro-intestinal cancers. Among them, methotrexate is an example and represents an analogue of folic acid;

- drugs interacting with protein-DNA complexes are compounds that inhibit the action of enzymes involved in DNA replication, by changing nucleic acid topology. These enzymes are known as topoisomerase I and topoisomerase II. Camptothecin and epipodophyllotoxin derivatives are the important representative drugs belonging to these categories.

1.2 DNA topology

DNA refers to the molecule located in the nucleus of a cell that contains the genetic instructions used in the cellular development, function, and reproduction of all known living organisms.⁹ The DNA structure model proposed by Watson and Crick in 1953 was immediately endorsed by many biologists because it solved the problem of the nature of genetic information and the mechanism for the transmission of this information from one generation to other.¹⁰ Each human cell contains ~2 meters of DNA that are compacted into a nucleus that is ~10 μm in diameter. An important property of DNA structure is known as supercoiling, due to the induction of torsional stress in the DNA. It is coiled in the form of a double helix, with both strands of the DNA coiling around an axis. The further coiling of that axis upon itself produces DNA supercoiling. Conversely, if there is no net bending of the nucleic acid axis upon itself, the DNA is said to be in a relaxed state. Thus, in order to be replicated the two strands must be separated to act as templates for the new daughter strands.

Topological properties of DNA are those that can only be changed when the double helix is broken. Supercoiled DNA has three fundamental parameters: twist (Tw), writhe (Wr), and linking number (Lk). Tw indicates the total number of double helical turns in a given segment of DNA. Wr represents the number of times the double helix crosses itself if the molecule is projected in two dimensions. Lk is a numerical term that describes the sum of the Tw and the Wr and represents the total linking within a DNA molecule and

can only be varied when the double helix is broken. From a mathematical point of view, these characteristics can be expressed as: $Lk = Tw + Wr$ (Figure 1.1).¹¹

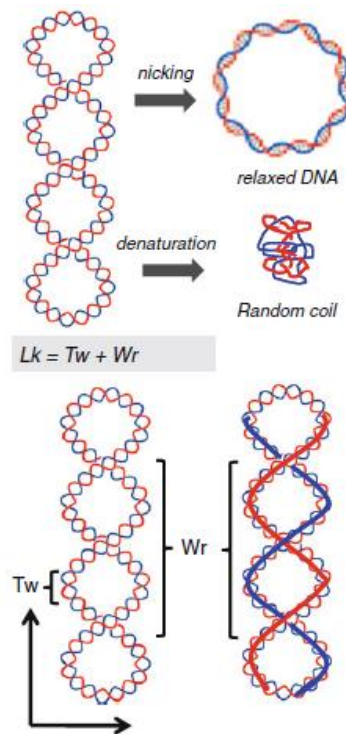


Figure 1.1. Basic topological tenets of DNA.¹¹

Lk is an invariant value that cannot be changed without opening the system. Thus, the only way to change Lk is to introduce a break in one or both DNA strands, rotate the two DNA strands relative to each other, and reseal the break.¹² The equation describe above predicts the existence of either positive or negative superturns.

When the superhelix winds in the same direction as the double helix itself, the superturns are positive ($Wr > 0$) because the double-helix turns are themselves positive per definition. Thus, the nucleic acid shows an excess of topological links compared to a relaxed DNA of the same size ($Lk > Tw$). However, if the super-helix winds in the opposite direction, the superturns are negative ($Wr < 0$) and the DNA exhibits a linking deficit ($Lk < Tw$). By definition, a relaxed circular DNA molecule that is 1050bp in term of length should have an $Lk = +100$ ($1050\text{bp} \div 10.5\text{bp/turn}$). Nonetheless, relaxed DNA does not generally exist in nature. In all living systems, from bacteria to humans, DNA is underwound by ~6%. This means that for every ~1.050bp, there are ~94 turns of the helix as opposed to the expected

~100 turns. This difference is described by the term ΔLk , which represents the actual linking number of a molecule minus the linking number of the DNA if it were completely relaxed (Lk_0). For the example described above, $\Delta Lk = Lk(94) - Lk_0(100) = -6$.¹²⁻¹⁶ However, because molecules can have different sizes, the term ΔLk is dependent on the length of the DNA. Thus, in order to compare levels of supercoiling between molecules, the term σ (specific linking difference or more commonly, superhelical density) is used. It is independent of DNA length and can be calculated using the equation: $\sigma = \Delta Lk \div Lk_0$.¹² Thus, for the example mentioned above, $\sigma = \Delta Lk(-6) \div Lk_0(100) = -0.06$. The σ value for underwound DNA is always negative, even if negative supercoiled DNA still has a positive Lk value; for overwound DNA, it is always positive.¹²

An important consideration is that the duplex DNA molecule contains all of the genetic information.^{11, 14-16} Therefore, to replicate or express this information, the two strands of DNA must be separated. Furthermore, because underwinding the genome increases the single-stranded character of the double helix, negative supercoiling simplifies strand separation.^{17, 18}

Whereas negative supercoiling enhances many processes that involve nucleic acids, DNA overwinding (*i.e.*, positive supercoiling) inhibits them. The linear movement of enzymes, such as helicases and polymerases, compresses the turns of the double helix into a shorter region (Figure 1.2).¹⁴⁻¹⁶ Therefore, the double helix becomes overwound; the positive supercoiling that results makes it harder to open the two strands of the double helix and eventually blocks essential nucleic acid processes.¹⁷⁻¹⁹

Another important aspect of DNA topology is the relationships between separate DNA segments. During recombination and replication processes, DNA strands become knotted (intramolecular links formed within the same DNA molecule) or tangled (intermolecular links formed between daughter DNA molecules), respectively.¹⁸⁻²⁰ DNA knots prevent essential nucleic acid processes by making it impossible to separate the two double strands. Furthermore, tangled DNA molecules can not be segregated during mitosis or meiosis.¹⁸⁻²⁰ It follows that both of these topological relationships have to be resolved in order to prevent cell death.

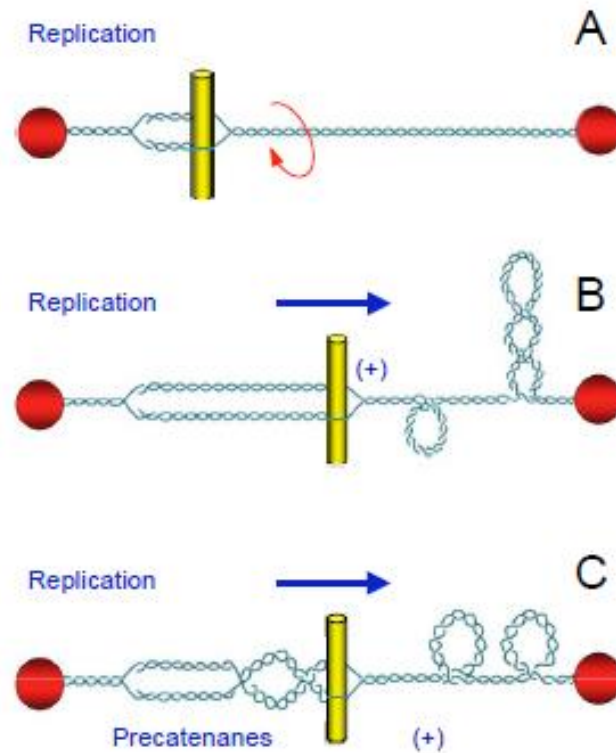


Figure 1.2. Topological challenges of DNA due to cellular processes. Nuclear processes induce changes in DNA topology. DNA replication is used as an example. Although chromosomal DNA is globally underwound in all cells, the movement of DNA tracking systems generates positive supercoils (A). The ends of chromosomal DNA are anchored to the chromosome scaffold (red spheres) and are not free to rotate. Therefore, the linear movement of tracking systems through the immobilized double helix compresses the turns into a shorter segment of the generic material and induces acute overwinding (*i.e.*, positive supercoiling) ahead of the fork (B). In addition, the compensatory underwinding (*i.e.*, negative supercoiling) behind the replication machinery allows some of the torsional stress that accumulates in the pre-replicated DNA to be translated to the newly replicated daughter molecules in the form of precatenanes (C). If these precatenanes are not resolved, they ultimately lead to the formation of intertwined (*i.e.*, tangled) duplex daughter chromosomes.¹²

1.3 Eukaryotic DNA topoisomerases

An important class of enzymes, known as topoisomerases, resolves topological problems associated with DNA. Topoisomerases are essential for cells survival, because they regulate the higher-order structural state of the DNA. They play a crucial role in different cellular processes, including DNA replication, transcription, recombination and chromosome segregation²¹, by introducing transient breaks into the DNA double helix. This large class of enzyme is characterized by the presence of active site tyrosine residues that initiate DNA cleavage by a nucleophilic attack on the phosphate of the nucleic acid backbone. This

process always takes place with the formation of a transitory phosphodiester bond between one end of the nicked DNA and a tyrosine residue in the enzyme.^{22, 23} The covalent topoisomerase-DNA complex, known as “cleavage complex”, is important in terms of mechanism of action of the enzyme for two different reasons. First of all, the covalent linkage is able to save the bond energy of the sugar-phosphate DNA backbone; thus no energy source is required from outside for topoisomerase-mediated DNA cleavage or religation.²⁴ Second, the covalent bond conserves the integrity of the genetic material during the cleavage event. Religation of the DNA is highly favored and the DNA sequence remains unchanged at the end of the catalytic cycle.¹³

Topoisomerases are ubiquitous enzymes and they are expressed in all organisms.^{22, 25} There are two major classes of topoisomerases, type I (TOP1) and type II (TOP2), which are distinguished by the number of DNA strands that they cleave. Type I topoisomerases act by generating a transient single-stranded break in the DNA duplex, while type II topoisomerases change DNA topology by introducing a double-strand break in the DNA duplex. Additionally, topoisomerases are further divided into three different subtypes (A, B, C) on the basis of their amino acid sequences, DNA interactions and/or global structure.^{19, 26-29}

Type I topoisomerases

In higher eukaryotes, DNA topoisomerase I is an essential enzyme for cellular metabolism. In association with topoisomerase II, is responsible for relaxing the torsionally strained supercoils that are generated during both transcription and DNA replication. They are monomeric enzymes and require no high-energy cofactor for their activities.³⁰ Thus far, two subfamilies of type I enzymes have been characterized: type IA and type IB, which are functionally distinct. Both act by creating transient single-stranded breaks in the DNA. However, for type IA enzymes, this action is followed by passage of the opposite intact segment through the break, while for type IB enzymes, it is followed by controlled rotation of the helix around the break.^{22, 27, 31} The type IA can only relax negative supercoils and does not go to complexation. These enzymes require Mg^{2+} divalent metal ions for the scission of the nucleic acid^{22, 27, 31}, and they catalyze different reactions, such as the knotting, unknotting, and interlinking of single-stranded circles.²⁷ In contrast, type IB

enzymes are very efficient at relaxing both negative and positive supercoils, do not require divalent metal ions for DNA scission, and bind covalently to the 3'-terminal phosphate of the DNA, rather than the 5' phosphate end found for the type IA enzymes. In conclusion, type I enzyme can modulate DNA under- and overwinding, but cannot remove knots or tangles from double-stranded DNA (Figure 1.3). To solve these topological forms of DNA, the presence of type II topoisomerases is required.

Type II topoisomerases

Type II topoisomerases all share similar characteristics. They are homodimeric enzymes with a monomer molecular mass ranging from ~160 to 180 kDa.^{32, 33} These enzymes act by binding both 5' termini of the double helix through a phosphotyrosine bond, and cleave the opposing strands.²⁷ This class of enzymes relaxes supercoiled, untangled (decatenated), and unknotted DNA (Figures 1.3). Furthermore, the reactions require Mg^{2+} and ATP for overall catalytic activity and rapid kinetics.

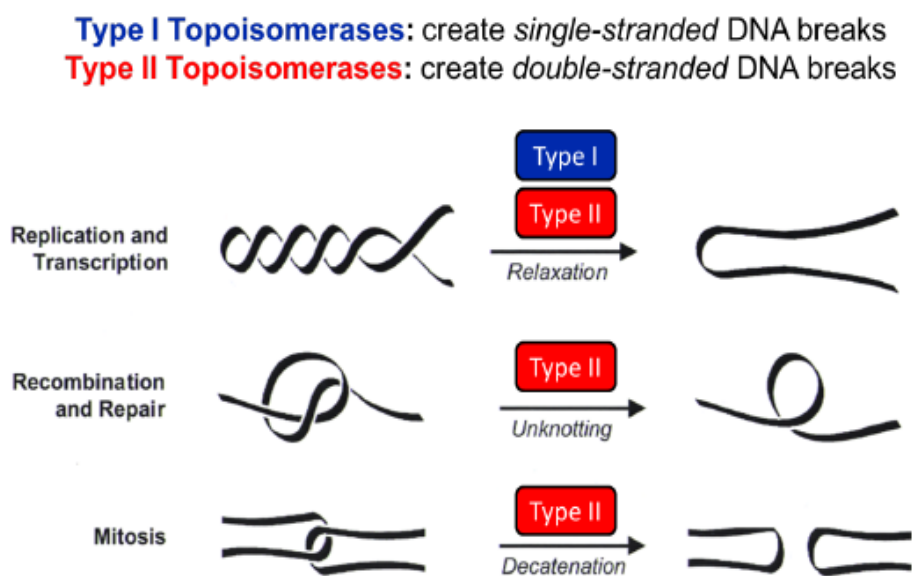


Figure 1.3. Topological challenges overcome by topoisomerases. A schematic is shown to indicate some of the cellular process in which topological challenges of DNA can occur and the role of topoisomerases to resolve the problems. (Figure produced by the Osheroff lab.)

Regarding the structure of the topoisomerase II polypeptide, each protomer can be characterized by three distinct domains (Figure 1.4):

- the N-terminal domain (N-gate), which is represented by the first 660 amino acids of the enzyme, is homologous to the B subunit of DNA gyrase. This portion of the enzyme contains the Gyrase, Hsp90, Histidine Kinase, MutL (GHKL) domain, which binds the ATP^{22, 34-36};
- the sequence between amino acids ~660 and ~1200 represents the cleavage/ligation region (DNA-gate or catalytic core), which is homologous to the A subunit of DNA gyrase and contains the active site tyrosine residue (the winged-helix domain, WHD), which is required for the formation of the covalent bond with DNA during scission. It also contains the topoisomerase/primase (TOPRIM) domain, which coordinates the divalent metal ion^{22, 35, 37};
- the C-terminal domain (CTD) is not conserved and differs from species to species. This is a highly charged variable region of the enzyme, which contains sites of phosphorylation and the nuclear localization sequences.^{37, 38}

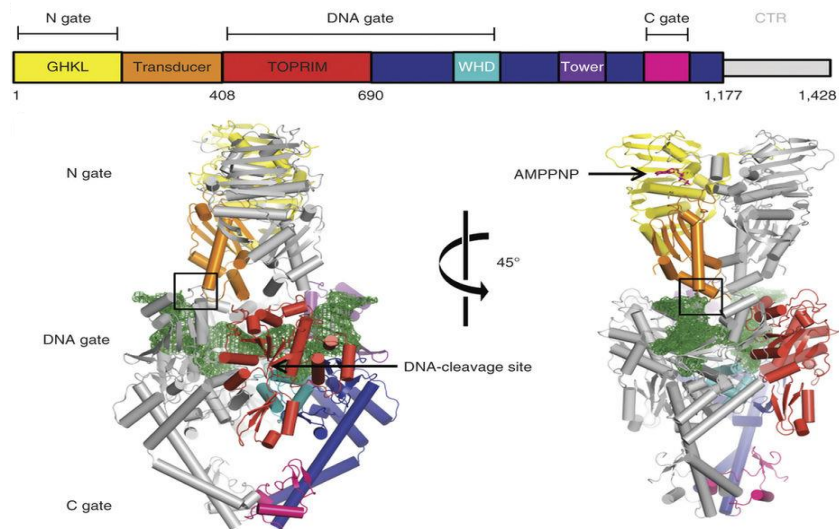


Figure 1.4. Domain organization and structure of eukaryotic topoisomerase II. Domain arrangement indicating the functional regions of type II topoisomerase (TOP). A model of ternary complex of yeast topoisomerase II (BOTTOM).³⁹

Lower eukaryotes and invertebrates encode only one type II topoisomerase, contrary to vertebrates that express two similar isoforms of topoisomerase II, known as topoisomerase II α and topoisomerase II β . These two subfamilies share a large amino acid sequence identity (~70%), but are encoded by two separate genes (17q21-22 and 3p24, respectively) and differ in molecular mass (170 and 180 kDa, respectively). Despite the fact that they share similar enzymatic properties, there are a number of differences regarding their cellular regulation, expression and physiological functions.^{22, 26, 40} Topoisomerase II α is essential for the survival of proliferating cells, and its concentration is particularly high during periods of cell growth.⁴¹⁻⁴³ In addition, the concentration of this isoform increases 2-3 fold during G2/M phases of the cell cycle. In contrast, the concentration of topoisomerase II β is relatively constant over both cell and growth cycle.⁴⁴⁻⁴⁶

Since only the type II α is associated with replication forks and remains tightly bound to chromosomes during the mitosis, it is considered the isoform that functions in growth-related processes, such as DNA replication and chromosome segregation.^{19, 44} Overexpression of this isoform is also used as a cancer cell marker.^{29, 47-51} Levels of topoisomerase II α are practically non-existent in quiescent and differentiated tissues, while rapidly proliferating cells contain ~500.000 copies.^{43, 48}

The β isoform is not required at the cellular level, but it is essential for neuronal development.⁵²⁻⁵⁴ This isoform has a key role in the transcription of hormonally and developmentally regulated genes.^{21, 55, 56} Despite the above, there are several unanswered questions about the specific contribution of both isoforms to cancer therapy versus leukemogenesis. Evidence suggests that topoisomerase II α is more involved in cytotoxicity^{57, 58}, while topoisomerase II β seems to play a more important role in triggering drug-induced cancers.⁵⁸ Because both isoforms are mechanistically similar, unless stated otherwise, will be collectively referred to as topoisomerase II or type II enzyme.

Catalytic cycle of type II topoisomerases

As discussed above, topoisomerase II is able to remove negative or positive superhelical twists from DNA and resolve intermolecular tangles and intramolecular knots from the double helix.^{22, 25} Over the years, all the steps of the topoisomerase II catalytic cycle have been analyzed in order to better understand enzyme function and the interaction of

topoisomerase II with anticancer drugs. This catalytic cycle can be divided into six discrete steps (Figure 1.5); a description of each step follows.

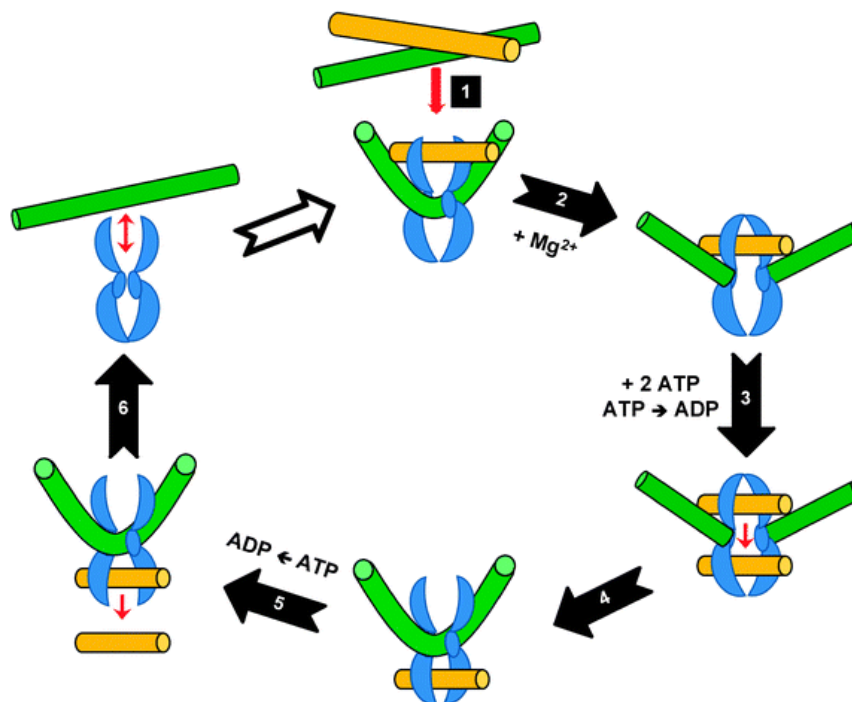


Figure 1.5. Catalytic cycle of topoisomerase II. The G-segment is indicated in green, while the T-segment in yellow.⁶⁴

Step 1- DNA binding: the catalytic cycle is initiated by the binding of the enzyme to two segments of DNA at a crossover. During this step of the cycle, the presence of the cofactor ATP is not necessary, although stimulation of binding has been reported in the presence of the divalent cations.⁵⁹ While specificity of topoisomerase II is determined by the primary structure of DNA, levels of enzyme binding and consequential catalytic activity seems to be regulated by the topological state of the double helix. In fact, topoisomerase II is able to discriminate topological structures (negatively or positively supercoiled nucleic acids over relaxed molecules) and interacts preferentially with them (as determined by levels of DNA binding and cleavage) over relaxed substrates.^{60, 61} This ability to discern the topology of DNA probably is due to the ability of topoisomerase II to recognize the DNA crossovers, that may be either intramolecular or intermolecular, as found in supercoiled and in catenated molecules respectively.⁶¹ Even if the exact mechanism by which the enzyme recognizes the crossover is not known, it seems that it binds the two DNA segments in

sequential order by first binding the segment that is cleaved.^{61, 62} Furthermore, the phosphorylation state of topoisomerase II plays an important role in modulating the recognition of DNA topology. In contrast to supercoiled DNA for which phosphorylation of the enzyme is not important, the catalytic activity on relaxed or linear DNA is stimulated 2-3-fold following phosphorylation of the enzyme by casein kinase.⁶³

Step 2- pre-strand passage DNA cleavage/religation: the first segment bounded by the enzyme, called the “Gate-” or “G-segment”, is cleaved by a covalent attachment of the active site tyrosine of topoisomerase II and serves as the site of DNA cleavage. The second segment, “Transport”- or “T-segment”, positioned in the N-gate domain, is bound and transported through the transiently cleaved G-segment. Strand scission is catalyzed by the active site tyrosine residue of each topoisomerase II protomer.⁶⁵ The role of a divalent metal ion(s) is essential in this process. Evidence suggests that many different divalent metal ions can support DNA cleavage mediated by topoisomerase II. However, only Mg^{2+} has been shown to support the full catalytic activity of the enzyme.⁵⁹ Recent study suggests that the topoisomerase II α utilizes a non-canonical “two-metal-ion” mechanism (Figure 1.6), in which one of the metal ions interacts with the 5'-oxygen.

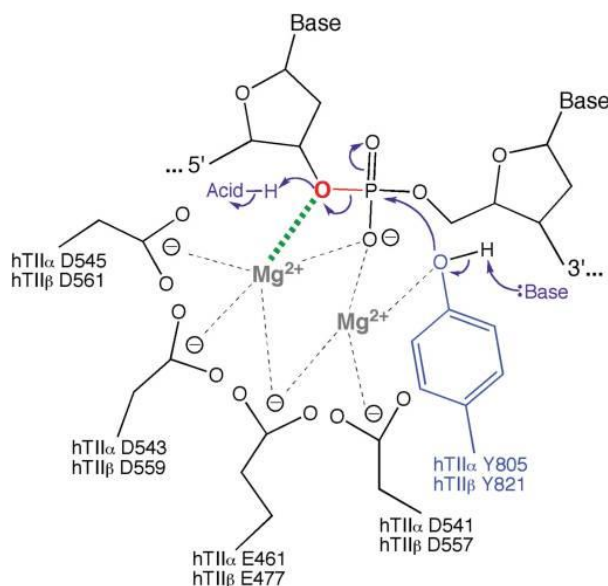


Figure 1.6. Mechanism of DNA cleavage mediated by topoisomerase II. The type II enzyme utilizes a two-metal ion mechanism similar to that utilized by primases and polymerases.¹³

The role of the second metal ion is not well understood. However, it likely creates critical interactions with the active site tyrosine and may stabilize the DNA transition state and/or

contribute to the deprotonation of the active site tyrosine.⁶⁶ It was also proposed that one ion promotes the leaving and attacking of the ribose 3'-OH during DNA cleavage and religation. While, the second metal plays a role in anchoring the DNA.⁶⁷ Thus, the cleavage reaction moves the two cut sites four-base pairs apart from one another across the major groove; a new 5'-terminal phosphate moiety is generated on each strand of the G-segment through a trans-esterification reaction.

Step 3- DNA strand passage: the binding between topoisomerase II and its ATP cofactor generates a conformational change that consequently triggers double-stranded DNA passage.⁶⁸ This reordering of structural elements induces dimerization of the ATPase domains, which regulates the rate of DNA cleavage and T-segment transport. Thus, the ATP during the catalytic cycle can be considered as a cofactor that helps co-ordinate the opening and closing of additional subunit interfaces to prevent aberrant subunit dissociation and chromosome fragmentation. Structural studies of human topoisomerase II indicate that the enzyme shows a selective interaction with the adenosine ring and that binding is not affected by the loss of the 2'-hydroxyl group (the K_m value for dATP is approximately twice that of ATP).^{60, 69} Finally, the triphosphate portion of the high-energy cofactor promotes DNA strand passage. Hydrolysis of ATP is not required for single enzyme turnover, but it accelerates the rate of T-segment translocation ~20-30-fold. Kinetic studies suggest that P_i release is involved in this reaction, showing that the two ATPs bound by type II topoisomerase are hydrolyzed at the same time and that strand passage is probably accompanied by the release of P_i from the first hydrolysis event.^{70, 71}

Step 4- post-strand passage DNA cleavage/religation: topoisomerase II establishes DNA cleavage/religation equilibrium also after the DNA translocation event. The topoisomerase II-DNA cleavage complex formed in this step, is characterized by a kinetic pathway that is comparable to that of pre-strand passage. However, but the one formed in the presence of ATP is intrinsically 2-4-fold more stable than that generated prior to ATP binding.^{60, 72}

Step 5- ATP-hydrolysis: the opening of the protein clamp and the release of the nucleic acid products is triggered by the hydrolyzation of the ATP. Evidence shows that the hydrolysis of the high-energy cofactor by topoisomerase II takes place in the presence or in the absence of the nucleic acid, although it is considerably faster in the presence of DNA. Thus, it is difficult to understand the precise linkage between the ATP hydrolysis and the strand

passage. It seems that each round of DNA strand passage consumes no more than two ATP molecules, but it is still unknown if the binding and hydrolysis of a single molecule is sufficient to support the complete catalytic reaction of the enzyme.^{69, 73}

Step 6- enzyme recycling: the T-segment is released from the enzyme at the end of the cycle. Thanks to the hydrolyzation of another molecule of ATP, the G-segment is then released and the enzyme is free to dissociate and initiate catalysis on a new DNA substrate.⁶⁹

Cleavage-ligation balance

Topoisomerase II-DNA cleavage complexes, which are central to the catalytic cycle of the enzyme, normally are short-lived and reversible.^{20, 74} Since type II topoisomerases are essential for proliferating cells and generate double-stranded DNA breaks as part of their mechanism, they represent a real danger to human cells. Because of its dualistic behavior, topoisomerase II is essential to cell viability but has the capacity to fragment the genome, levels of cleavage complexes are maintained in a critical balance so that they are tolerated by the cell (Figure 1.7).^{20, 74} When levels of cleavage complexes are too low, daughter chromosomes remain entangled following replication. Thus, chromosomes cannot segregate properly during mitosis and cells die because of mitotic failure.

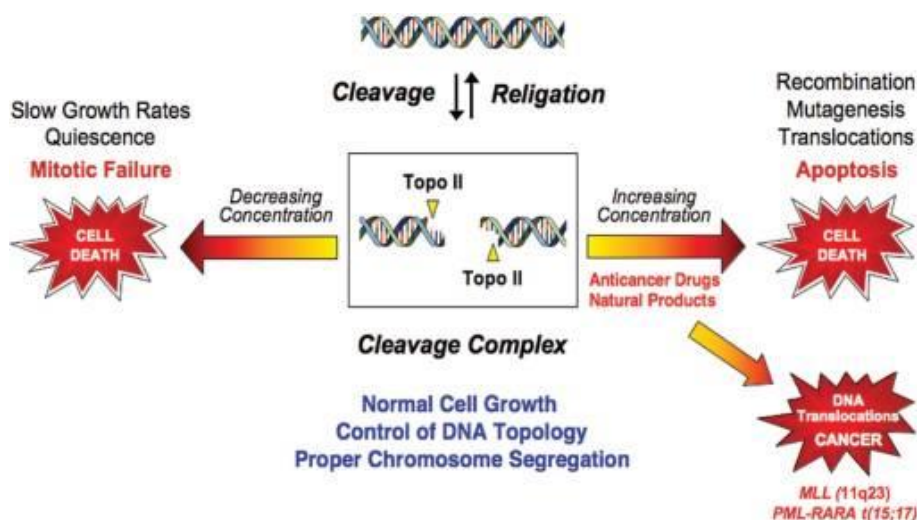


Figure 1.7. Shifting the equilibrium of topoisomerase II-DNA cleavage.¹³

When levels of cleavage complexes rise too high, cells also die but for other reasons. In this case, the transient cleavage intermediates are converted to permanent strand breaks.

It seems that permanent strand breaks are generated when replication forks, transcription complexes or DNA tracking enzymes such as helicases attempt to traverse the covalently bound protein “roadblock” in the genetic material. Finally, the resulting damage and induction of recombination/repair pathways also can induce mutations, chromosomal translocations and other aberrations. When topoisomerase II-initiated permanent DNA breaks are present in sufficient numbers, they can initiate cell death pathways.^{13, 49, 75, 76}

Drug interaction domains

Different approaches have been utilized to better clarify drug interaction domains on topoisomerase II. In the first, the mutation of specific amino acid residues that led to drug resistant mutant type II enzymes have been generated and identified.⁷⁷ The result was the discovery that the drug interaction domain on topoisomerase II (at least for quinolone-based agents) has been conserved during evolution from the bacterial to the eukaryotic type II enzyme.⁷⁸ No clear picture has emerged from mutagenesis studies alone, because of the lack of detailed structural information for mutant type II enzymes and because many mutant enzymes display altered enzymatic properties or characteristic drug interaction domain.⁷³ A second approach was used to determine whether DNA cleavage-enhancing drugs utilize a common site of action on the enzyme and used a biochemical strategy that complemented the above genetic studies. One significant finding from this approach was the discovery that most anticancer drugs share an overlapping interaction domain on topoisomerase II.⁷⁹ However, since several mutant type II enzymes display differential resistance between drug classes,^{80, 81} it is clear that the specific sequence of amino acid residues responsible for binding different anticancer agents within this domain differs from drug to drug. A third approach utilized a photoactivatable form of amsacrine (*m*-AMSA) and showed that the site of drug action in the cleavage complex is close to or at the site of DNA scission.⁸²

Topoisomerase II poisons vs inhibitors

Compounds that alter the catalytic activity of topoisomerase II can be separated into two categories: topoisomerase II poisons and topoisomerase II catalytic inhibitors. Chemicals that act by increasing the level of topoisomerase II-DNA cleavage complexes belong to the first class. They are named “poisons” because they convert the enzyme into a cellular toxin that initiates the mutagenic and lethal consequences described above.^{75, 83} Notwithstanding that many topoisomerase II poisons can inhibit overall activity, the increased levels of cleavage complexes induced by these compounds in the cell is a “gain of function”, which is a dominant phenotype.^{20, 84}

Alternatively, chemicals that kill cells by robbing them of the essential activities of the type II enzyme are said to be catalytic inhibitors. They can block topoisomerase II activity by a variety of mechanisms, which can have important consequences for cells. Whereas drugs that block ATP binding (novobiocin), DNA cleavage, or strand passage (merbarone) inhibit the catalytic reactions of topoisomerase II, those that disrupt topoisomerase II-DNA binding (aclerubicin) impair both the structural and catalytic roles of the enzyme. Furthermore, drugs that allow ATP binding but block the hydrolysis of the high-energy cofactor (ICRF-193), trap the enzyme on the DNA.^{50, 74, 85-89}

Mechanism of topoisomerase II poisons

Topoisomerase II poisons represent a large class of anticancer drugs currently in clinical use.⁴⁹ These drugs encompass a diverse group of natural and synthetic compounds that are used to treat a variety of human malignancies. Topoisomerase II poisons are subdivided into two different groups: interfacial and covalent poisons.⁴⁹ Compounds that operate by the first mechanism are chemicals that form noncovalent interactions with topoisomerase II at the protein-DNA interface within the vicinity of the active site tyrosine. They physically block the ability of topoisomerase II to ligate the cleaved DNA strand by intercalating into the cleaved scissile bond.^{20, 49, 66, 74, 84, 90} Furthermore, their actions against the enzyme are not changed by reducing agents, such as dithiothreitol, and they induce similar levels of enzyme-mediated DNA cleavage whether they are added to the binary topoisomerase II-DNA complex or are incubated with the enzyme prior to the addition of nucleic acid

substrates.^{91, 92} Two of the most important non-intercalating interfacial topoisomerase II poisons are etoposide and teniposide, both of which are epipodophyllotoxins (Figure 1.8).

In contrast to interfacial topoisomerase II poisons, compounds that act by the second mechanism contain protein-reactive groups and are referred to as “covalent or redox-dependent poisons”. They require redox activity to facilitate their actions against topoisomerase II and they adduct to the enzyme at the amino acid residues outside of the active site. Consequently, their activity is abrogated in the presence of reducing agents. Finally, these compounds enhance DNA cleavage when added to the protein-DNA complex, but display the distinguishing feature of inhibiting topoisomerase II activity when incubated with the enzyme prior to the addition of DNA. Likely, this may reflect the fact that closing the N-terminal protein gate prevents DNA binding. Many dietary polyphenols such as epigallocatechin gallate, which is found in green tea, as well as several quinone-based toxins, exemplify redox-dependent topoisomerase II poisons (Figure 1.8).^{93, 94}

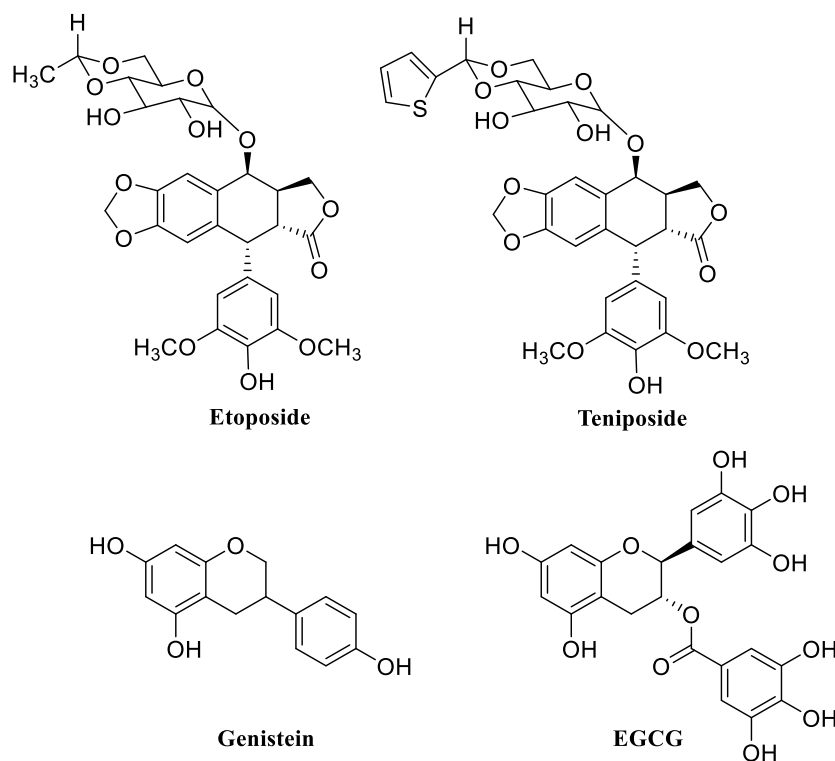


Figure 1.8. Structures of selected interfacial and covalent poisons.

Quinone-based metabolites. These compounds are produced in the body as a result of metabolism and are highly reactive, since they are able to generate reactive oxidative species (ROS) and covalently modify proteins. Evidence suggests that the target of these covalent poisons on topoisomerase II are the amino acids Cys170, Cys392 and Cys405 located on the N-terminal domain and residue Cys455 located in the catalytic core of topoisomerase II α .⁹⁵ Etoposide and paracetamol are two drugs that can be converted in quinone-based metabolites. In particular, etoposide is metabolized by CYP3A4 to etoposide catechol, which is further oxidized into an etoposide quinone (Figure 1.9). This product is able to increase the levels of topoisomerase II-DNA by up to 12-fold in comparison to etoposide. Paracetamol can be metabolized into *N*-acetyl-*p*-benzoquinone imine (NAPQI) (Figure 1.9) which is a potent topoisomerase II poison that acts by increasing levels of enzyme-mediated DNA cleavage by a direct interaction with the cleavage complex.⁹⁶

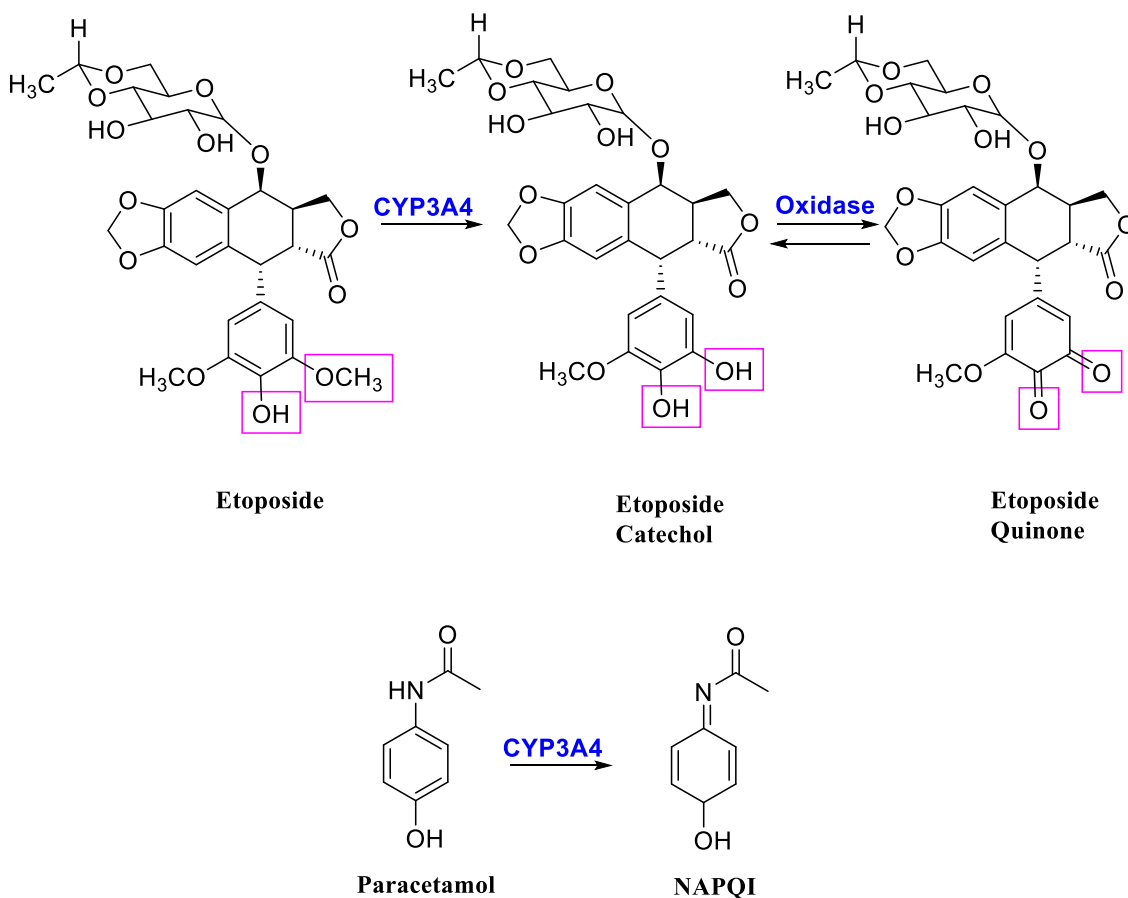


Figure 1.9. Metabolism of etoposide and paracetamol.

involves the sulphonamide substituent at the 1' position and the hydroxyl group of Thr744, while the second hydrogen bond takes place between the carbonyl oxygen of Gly747 and the NH group of the sulfonamide moiety. There were also found hydrophobic interactions between the substituent on the 3' position and amino acid Phe754.⁹⁶ Considering these results, a series of derivatives was developed by introducing different substituent on the scaffold on the *m*-AMSA (compound **A**). Other studies revealed that the acridine scaffold intercalates with DNA base pairs via π interactions, while the side chain interacts with the minor and major grooves. These finding suggested that these compounds do not act as topoisomerase II poisons, but follow a catalytic inhibitory action by inhibiting the ATP binding site or DNA cleavage (Figure 1.11).⁹⁶

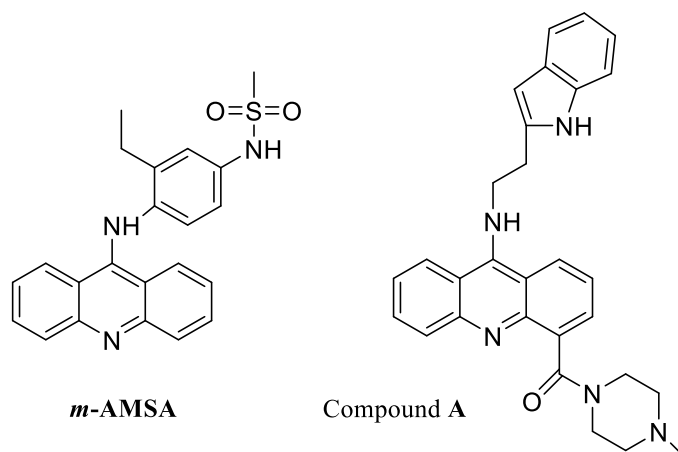


Figure 1.11. Structures of *m*-AMSA and compound **A**.

Podophyllotoxins analogues. As mentioned above, one of the most important podophyllotoxin analogues is etoposide (Figure 1.8). This drug is used for the treatment of many different types of cancer, such as testicular cancer, small cell lung cancer, lymphomas, sarcomas and ovarian cancer. In 2009, the detailed interactions between topoisomerase II, DNA, and etoposide was revealed.⁹⁸ In the ternary complex, two etoposide molecules bind between the base pairs (+1/+4 and -1/+5) near the two cleaved scissile phosphates. This interaction is mediated by direct contacts with surrounding residues of topoisomerase II. Clearly, the enzyme-DNA-etoposide association stabilizes the cleavage complex by physically blocking the topoisomerase II-mediated resealing of DNA.⁹⁸ The etoposide molecule consists of three parts: a glycosidic group substituted at the

C4 position, a polycyclic core (rings A-D) and a pendant aromatic ring (E-ring) (Figure 1.12).

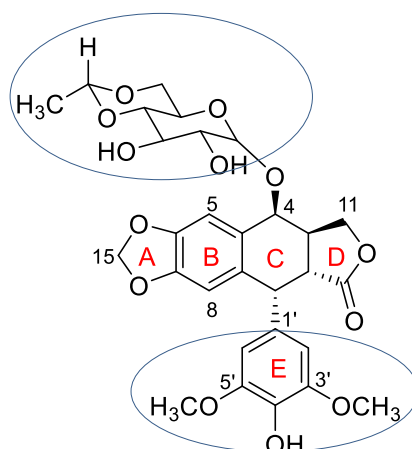


Figure 1.12. Structure of etoposide with its essential ring.

In 2011, Wu and co-workers (Figure 1.13) published a crystal structure of human topoisomerase II β in complex with DNA and etoposide. This structure revealed that etoposide is positioned inside the catalytic core of each subunit of the enzyme, stabilizing the cleavage complex.⁹⁸

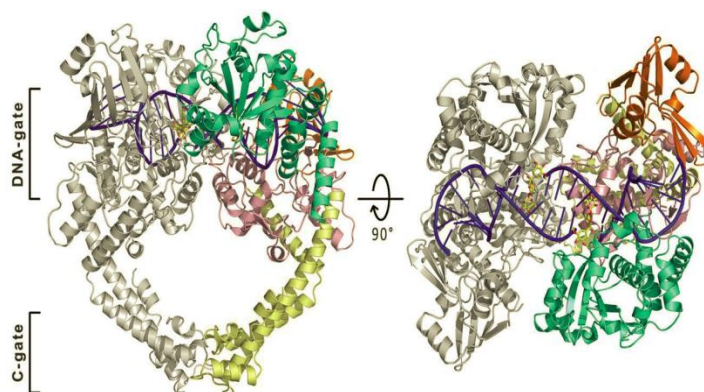


Figure 1.13. Structure of the human topoisomerase II β in complex with DNA and etoposide. DNA is blue, one topoisomerase II β ^{core} is in gray. The essential ring of etoposide are shown.⁹⁸

Teniposide, introduced in the clinic in 1993, is identical to etoposide except it contains a thiophene moiety at the 8' position of the glycosidic group (Figure 1.8). Over the years, many others podophyllotoxin derivatives have been designed as topoisomerases II poisons which shows the importance of etoposide in chemotherapy for a large variety of solid and hematological tumors. Several of them have been tested clinically, such as TOP-53, GL331,

and tafluposide, but unfortunately, none of them ever reached the market.⁹⁹⁻¹⁰¹ The anticancer potential of this class of compounds, despite these failures, is well known, in fact oncologists and medicinal chemists continue to pay a large interest to them. Thus, novel podophyllotoxin derivatives continue to be identified and characterized; among them, the most promising anticancer drug is F14512. It represents the lead molecule of the polyamine conjugates, designed to increase DNA interactions and selectively target tumor cells through an active polyamine transport system (PTS).¹⁰²

Several poisons are able to intercalate into the DNA double helix. Among them, doxorubicin and other anthracyclines, mitoxantrone, *m*-AMSA, amonafide and a number of other compounds that are not currently in clinical use (ellipticine).⁴⁹ Non-intercalating topoisomerase II poisons include the epipodophyllotoxins (etoposide and teniposide) and fluoroquinolones, which are mainly active against prokaryotic type II topoisomerase.⁴⁹ These compounds do not interact strongly with DNA, suggesting that enzyme drug interactions might have a key role in their ability to block topoisomerase II covalent complexes.^{84, 103}

Mechanism of topoisomerase II inhibitors

Catalytic inhibitors of topoisomerase II include a large group of compounds, such as merbarone¹⁰⁴, aclarubicin¹⁰⁵, suramin¹⁰⁶, bisdioxopiperazines¹⁰⁷, and xanthenes.¹⁰⁸ The most characterized catalytic inhibitors of eukaryotic topoisomerase II are the bisdioxopiperazines analogues, *e.g.*, dexrazoxane (Figure 1.14).⁸⁶ Although the mechanism of action of these drugs is thought to differ from that of topoisomerase II poisons, the manner by which these agents inhibit the enzyme and their mechanism of cytotoxicity are less significantly understood.⁸⁷

Compounds that inhibit ATP hydrolysis and trap the enzyme in a closed clamp. After strand passage, the enzyme hydrolyzes ATP, the N-terminal clamp opens and the strand that has been cleaved by topoisomerase II is released. Bisdioxopiperazines (Figure 1.14) inhibit the activity of the enzyme, by blocking ATP hydrolysis by topoisomerase II and consequently blocking the opening of the N-terminal clamp.⁸⁸ Thus, the generation of a closed clamp interferes with DNA metabolism.^{88, 109} Furthermore, studies demonstrate that the

dioxopiperazine compounds interact with the ATPase domain and consequently, inhibit ATPase activity.

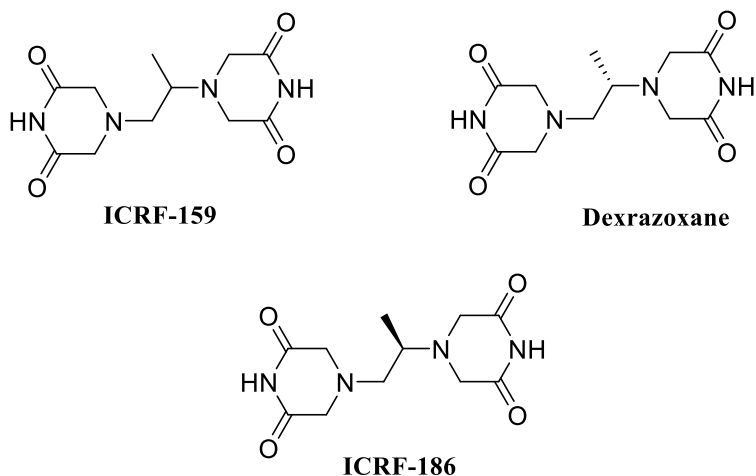


Figure 1.14. Bisdioxopiperazine analogues. Structures of ICRF-159, dexrazoxane and ICRF-186.

Compounds that bind to the ATP binding site. These compounds prevent binding of the ATP molecule, which has a key role in the catalytic cycle of the enzyme. This class of compounds contains several natural chemical structures, such as coumarin, gambogic acid, salvacine, and emodin (Figure 1.15). Modeling studies suggest that gambogic acid interacts with the ATP binding site by forming several hydrogen bonds.¹¹⁰ Salvacine is a compound isolated from *Salvia prionitis* and it is a potent antitumor inhibitor *in vivo* and *in vitro* and is currently in clinical evaluation for the treatment of cancer. A binding mode of this drug showed that it is a competitive inhibitor able to bind the ATP binding site of the enzyme.¹¹⁰

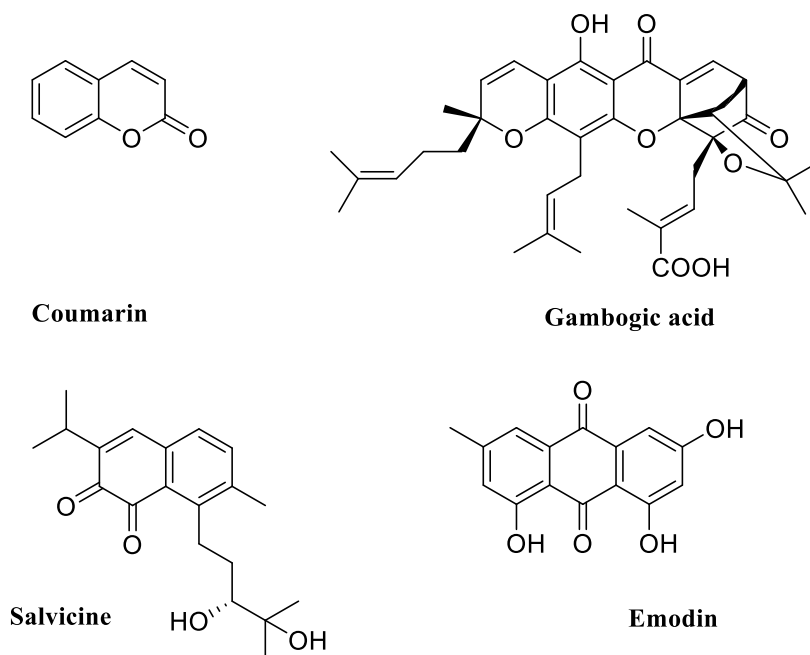


Figure 1.15. Selected small molecules that bind to the ATP binding site structure of gambogic acid, salvicine and emodin.

Compounds that block cleavage of the DNA. These compounds are able to inhibit the ability of topoisomerase II to cleave the DNA molecule. The most important compound in this series is merbarone (Figure 1.16). It is one of the most successful topoisomerase II inhibitors, under phase I and phase II clinical evaluation for treatment of different types of cancer.¹¹⁰ However, clinical trials were halted due to lack of sufficient antitumor activity and nephrotoxicity issues.⁸⁵

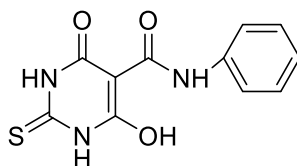


Figure 1.16. Structure of merbarone.

Compounds that prevent binding of topoisomerase II to DNA. This group of catalytic inhibitors prevent binding of the type II enzyme to DNA. Aclarubicin (Figure 1.17) is an anthracycline antibiotic used in clinical practice for the treatment of acute myeloblastic leukaemia and lymphoma. Like other anthracyclines, aclarubicin has multiple targets. In

fact, the drug has been shown to stimulate DNA cleavage by eukaryotic topoisomerase I.¹¹¹ For this reason is unclear to what extent the antitumor activity of this drug is due to its activity against topoisomerase II.^{112, 113} Despite these encouraging results, this drug induces late cardiac events in adult patients with refractory leukaemia.¹¹⁴

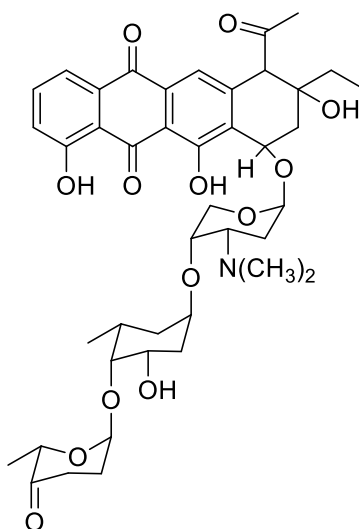


Figure 1.17. Structure of aclarubicin.

Thus far, the clinical use of catalytic topoisomerase inhibitors as antineoplastic agents is limited to aclarubicin and dexrazoxane. Both of these compounds are more active against hematological malignancies and show limited activity toward solid tumors. A notable property of most catalytic topoisomerase inhibitors is their capacity to modulate the cytotoxic effects of other anticancer agents.⁸⁵

Topoisomerase II-associated leukaemia and side effects

Notwithstanding the importance of topoisomerase II as target for cancer chemotherapy, secondary effects can accompany treatment with topoisomerase II poisons. Evidence suggests that DNA cleavage mediated by the enzyme can induce chromosomal translocations that can lead to specific leukaemias.^{115, 116} In 2-3% of patients treated with topoisomerase II-targeted drug, such as etoposide, a therapy-related acute myeloid leukaemia (AML) was diagnosed. Most of these leukaemias are characterized by translocations with breakpoints in the mixed lineage (MLL) gene at chromosomal band

11q23. Thus far, in close proximity to topoisomerase II-DNA cleavage sites that are induced by the drug etoposide, different breakpoints in the MLL gene have been identified.^{76, 117-119} About 80% of infants (< 1 yr of age) with AML and acute lymphoblastic leukaemia (ALL) show chromosome translocations that involve the MLL gene.^{120, 121} The chromosomal translocations associated with these types of cancers have been observed *in utero*, indicating that infant leukaemias are initiated during gestation.¹²⁰ Evidence suggests that several bioflavonoids available in the diet can induce cleavage of the MLL gene in human myeloid and lymphoid progenitor cells and in cell lines. This finding provides evidence that dietary flavonoids may be directly involved in causing genetic damage.¹²² Compounds that show the highest *in vitro* topoisomerase II-DNA cleavage activity tend to show the greatest tendency to generate breaks in the MLL gene in cultured cells. Thus, the topoisomerase II activity has a double effect: from one side it is essential for normal cell growth and can be targeted to treat a number of human malignancies, from the other side it can be disadvantageous when targeted by photochemicals, or by anticancer drugs, possibly leading to leukaemia.

The specific contributions of topoisomerase II α and topoisomerase II β to cancer therapy *vs* leukemogenesis are unclear. Evidence suggests that topoisomerase II α plays a more important role in cytotoxicity^{57, 58}, while topoisomerase II β may play a major role in causing drug-induced cancers.⁵⁸ Thus, while targeting topoisomerase II has been extremely successful in a variety of settings (*i.e.*, anticancer and chemopreventive), there is still the need to identify new agents that preferentially target topoisomerase II α , since no isoform-specific topoisomerase II-targeted drugs are available.

Topoisomerase II-targeted anticancer drugs

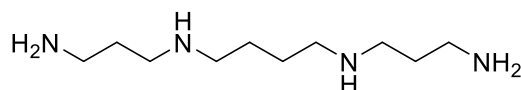
Due to its vital cellular functions, topoisomerase II represents the primary cytotoxic target for some of the most active drugs currently available for treatment of human cancers and for bacterial diseases. Nowadays, the research goal is to reduce the risks of secondary malignancy and other toxicities. Different studies suggest that the anticancer and leukemogenic effect of some compounds, that act against type II topoisomerases, are believed to result from their ability to poison the enzyme. As discussed above, the enzyme expresses two different isoforms, topoisomerase II α and II β . Both are believed to be

targeted by anticancer and dietary topoisomerase II poisons, but the individual contribution of the single isoforms to the side effects are not well-defined.¹²³ Recent evidence suggests that topoisomerase II α may be the primary cytotoxic target of these agents. This isoform is more responsive to some topoisomerase II poisons *in vitro* and when expressed in yeast than is the β isoform.^{40, 124} Furthermore, as described above, levels of the α isoform are remarkably elevated in proliferating cells, while levels of topoisomerase II β do not change significantly with growth status.^{58, 125}

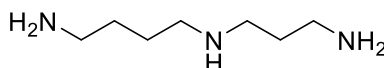
At the present time, six topoisomerase II-targeted anticancer agents are approved for use in the United States, and additional drugs are prescribed elsewhere in the world.¹³ These agents all act as interfacial topoisomerase II poisons and function primarily by inhibiting enzyme-mediated DNA ligation.

Chapter 2-Polyamines and cancer

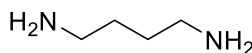
Polyamines are natural compounds occurring *in vivo* as low molecular weight aliphatic polycations, first discovered in 1678 by Antonie van Leeuwenhoek in the human seminal liquid.¹²⁶ Many physiological processes are tightly linked to the cellular level of some polyamines, such as the tetramine spermine, the triamine spermidine and the diamine putrescine (Figure 2.1).



Spermine



Spermidine



Putrescine

Figure 2.1. Structures of naturally occurring polyamines: spermine, spermidine and putrescine.

These molecules are essential cellular component from all species and they have various functions. They are required for proper cell growth. In fact, cells where polyamine production has been prevented by mutation, or blocked by inhibitors, require exogenous polyamines for continued survival.¹²⁷ Because they have a positive charge on each nitrogen atom at physiological pH, they are “supercations”, equivalent to one or two calcium or magnesium ions. They are able to bind *via* ionic bonds and electrostatic interactions to many negatively charged molecules such as nucleic acids, proteins, phospholipids and are able to modulate the activity of proteins and organelles. Furthermore, structural studies indicate that polyamines interact with individual rather than multiple DNA molecules.¹²⁸ In order to further investigate their actions polyamines are the subject of intensive research. It has been suggested that the charge distribution of spermine makes this molecule able to stabilize the DNA helix against thermal or radiation damage following the formation of bonds with the phosphate groups of the two strands of the nuclei acid. Thanks to their

capacity to interact with DNA and modulate DNA-protein interactions, polyamines are suggested to be cell cycle modulators. Furthermore, it was shown that the concentration of polyamines varies in the different phases of the cell cycle. However, these changes are different across the various cell types studied and alterations in specific polyamine concentrations may not correlate with changes in the activities of their biosynthetic enzymes.¹²⁹ Additionally, alterations in specific polyamine concentrations during the G1 phase leads to greater concentrations of the cell cycle inhibitor proteins p21, p27, and p53, which blocks the cell cycle. Given the importance of these molecules in regulating cell proliferation, it is clear that they play a role in the growth and maintenance of cancer cells.¹³⁰

2.1 Polyamine metabolism and transport

Under normal physiological conditions, polyamines are regulated by a complex network of biosynthetic, catabolic, and transport mechanisms.¹³¹⁻¹³³ They are present in concentrations in the μM range in eukaryotic cells. There are three main sources for polyamines in organisms: food, cellular synthesis and microbial synthesis in the gut. Polyamines are synthesized from the amino acids L-arginine and L-methionine *via* a series of six interdependent enzyme reactions. The first step is the synthesis of L-ornithine, precursor of putrescine, from arginine by the mitochondrial enzyme arginase. In contrast, methionine is used for the synthesis of spermine and spermidine (Figure 2.2). Putrescine is formed from the decarboxylation of ornithine by ornithine decarboxylase (ODC). ODC expression is regulated by transcription, post-transcriptional processing, changes in translational efficiency, and altered stability of the protein.¹³⁴ Spermidine and spermine synthases are used for the synthesis of spermidine and spermine, respectively. These synthases are stable enzymes that are expressed constitutively with little inducibility.¹²⁷ The activity of these last two enzymes is regulated by the bioavailability of the substrate, *i.e.*, decarboxylated S-adenosylmethionine, which then serves as propyl-aminic group donor and is itself produced from the enzyme S-adenosylmethionine decarboxylase (SAM-DC). Since the synthesis of polyamines is a non-reversible process, the cell has developed a mechanism to prevent the accumulation of spermine and spermidine by using the spermine/spermidine *N*¹-acetyltransferase enzyme (SSAT). It is very highly regulated and plays a crucial role in

polyamine homeostasis. Furthermore, this enzyme is able to cause a loss of spermidine and spermine, by converting them in putrescine. Under resting conditions, SSAT activity in the cell is very low.¹³⁵ Its levels and activity may increase in response to a higher polyamine content, for example following exogenous administration. SSAT uses acetyl-CoA as cofactor to yield acetylated spermine and spermidine. The N¹-acetyl derivatives are the preferred substrates of FAD-dependent polyaminoxidase (PAO), which converts spermine in spermidine into putrescine. Furthermore, acetyl polyamines are easily removed from the intracellular compartment, because they are able to permeate the membrane more efficiently.¹³⁶ Metabolism of polyamines *via* SSAT and PAO leads to the formation of secondary products, such as 3-acetamidopropanol and H₂O₂, in stoichiometric amounts, which are both able to induce toxicity and cell death.^{137, 138}

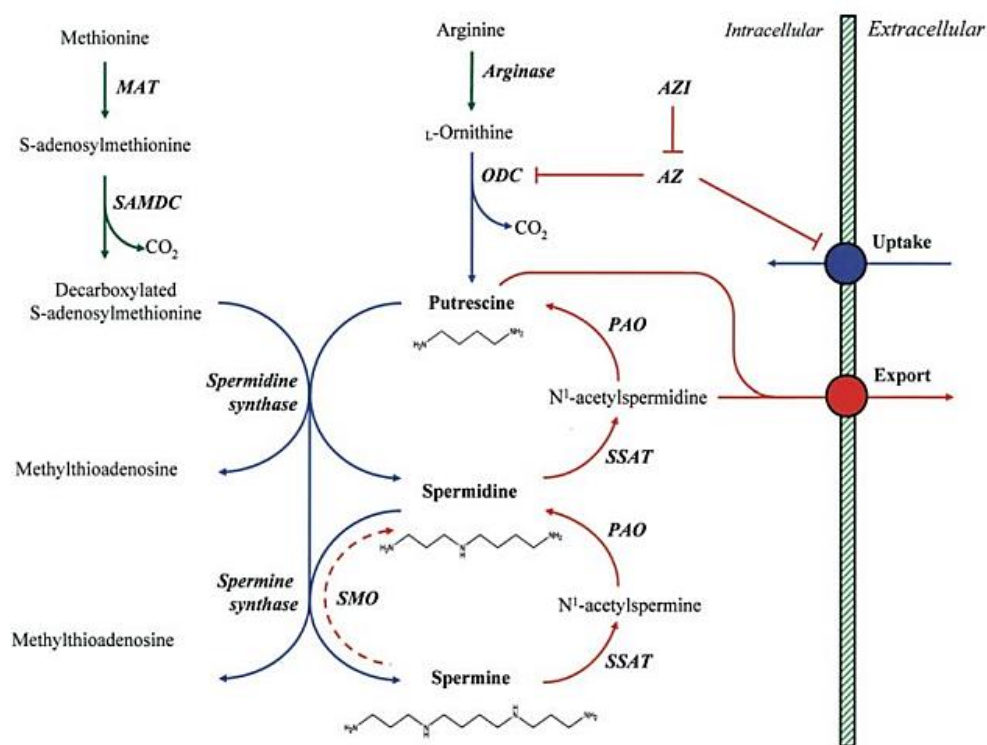


Figure 2.2. Pathways of polyamine metabolism.¹³⁶

Although less well characterized than the biosynthetic pathway, polyamine transport is also involved in the regulation of intracellular polyamine levels. Their transport between the inside and the outside of the cell contributes to their homeostasis. A polyamine transporter system (PTS) may be located in the plasma membrane or in organelle membranes and polyamine transport is carrier mediated, energy-dependent, and saturable. Evidence suggests that in the mammalian cell there are at least two separate transporters, one for putrescine (and possibly other diamines) and one for spermidine and spermine. The putrescine-PTS is a sodium dependent transporter, while the spermine/spermidine-PTS is sodium independent. Currently, there are three proposed mechanisms of internalizations of these macromolecules. The first model suggests that polyamines are transported into the cell by a not yet identified transporter, which is powered by negative membrane potential. The second hypothesis describes a mechanism by which the polyamines are introduced into the cell through a receptor-mediated endocytosis after their binding to heparan sulphate on a molecule of glypican 1 (GPC1).¹³⁹ The last hypothesizes a caveolin-1-dependent internalization of polyamines that are bound to an unknown polyamine membrane receptor.¹⁴⁰

Cancer cells have high demand for polyamines to support their rapid growth and endogenous synthesis is insufficient to their needs. Thus, to provide sufficient levels of polyamines to sustain rapid cell division, they introduce polyamine from the extracellular environment by using the polyamine transporter. In fact, the activity of the PTS was found higher in proliferating cells than in resting cells and the uptake of polyamines by tumor tissues was superior to normal tissues.¹⁴¹ Several findings demonstrate that the selectivity of the PTS is not restricted to natural polyamines.¹⁴² Differences in the level of transporter activity between normal and malignant cells provide a mechanism for cell-selective drug delivery by using polyamine-drug conjugates. The uptake of polyamines provides a vector for tumor cell delivery through the PTS and reduces the toxicity on normal cells associated with classic chemotherapy.

Unfortunately, although it is well known that polyamines are essential in cancer and that their transporter is overexpressed in cancer cells, little data currently is available about the structure and functioning of the PTS. Thus, it is still difficult for researchers to develop a rational design for PTS-targeting drugs.

2.2 Polyamine-drug conjugates

Several examples of polyamine-conjugated anticancer drugs such as chlorambucil, nitroimidazoles, or camptothecin have contributed to validating the concept of PTS targeting. In 1992, Holley and co-workers¹⁴³, synthesized one of the first compounds of polyamine-conjugates compounds, the chlorambucil-spermidine (Figure 2.3). Chlorambucil is one of the best-tolerated *per os* alkylating agents and is used for the treatment of some types of leukaemia. However, its use is strongly limited by the induction of haematological suppression. Conjugation of chlorambucil to spermidine should increase both its accumulation and its cell type specificity. Furthermore, since polyamines have a high affinity for DNA, the insertion of spermidine should also facilitate the targeting of this derivative to DNA (increase of the affinity towards the nucleic acid of 10.000).¹⁴³

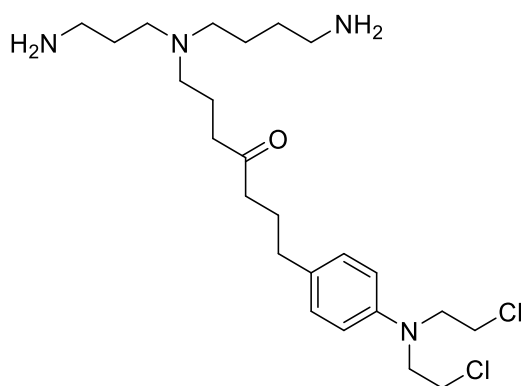


Figure 2.3. Structure of chlorambucil-spermidine conjugate.

Later, Bailly and co-workers¹⁰² synthesized the spermine-epipodophyllotoxin conjugate F14512 (Figure 2.4). It is considered as the most promising anticancer drug in this category, since it shows all the required properties for polyamine conjugates. In particular, it is able to increase cytotoxicity and DNA binding affinity than etoposide, uptake through PTS and *in vivo* reduced toxicity. The spermine tail of F14512 plays a key role as a cell delivery vehicle as well as a DNA anchor.¹⁰² The drug is currently in phase II clinical trials for the treatment of acute myeloid leukaemia and shows a favorable safety profile. Moreover, the combination of F14512 and cisplatin is synergistic and more powerful than the co-administration of etoposide and cisplatin.¹⁴⁴

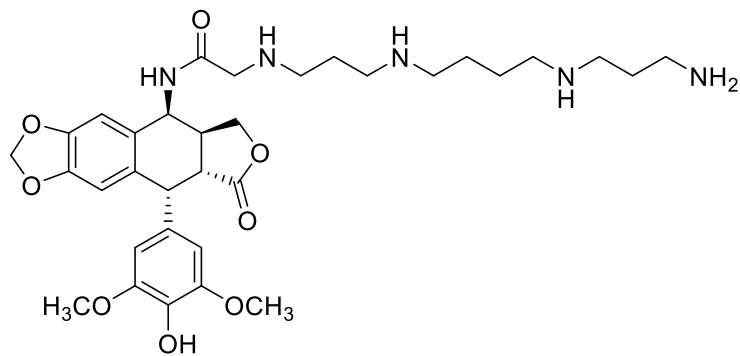


Figure 2.4. Structure of etoposide-spermine conjugate, F14512.

Findings suggest that one of the weak points of polyamine-based compounds is their potential metabolism by PAO, as it reduces the PTS selectivity of these derivatives in culture *via* compound degradation. Since this enzyme targets primary amines and it also metabolizes polyamine-based derivatives containing primary amines, compounds with a protected primary amine could be able to avoid the metabolic effects of PAO activity.¹⁴⁵

In conclusion, a greater knowledge of the mammalian PTS could help in the development of new polyamine conjugates in the future. Thus far, results for the uptake of these derivatives *via* PTS are obtained indirectly. It is therefore, not definitive that they use the PTS for the internalization in the cell.

Chapter 3-Effect of etoposide derivatives on DNA cleavage mediated by human topoisomerase II α

3.1 Etoposide derivatives

Etoposide is a semisynthetic derivative of podophyllotoxin, an antimetabolic agent that has been used as an herbal remedy for more than a millennium.^{146, 147} Etoposide gained its approval by the FDA in 1983.²⁹ It is a successful anticancer agent currently used for the treatment of a large variety of solid and hematological tumors, in particular in small cell lung cancer and in refractory testicular tumors in combination therapy, as well as in second-line therapy for acute myeloid leukaemia in combination with cytarabine and/or mitoxantrone.^{146, 148-150} As described in the first chapter, it kills cells by increasing the equilibrium level of topoisomerase II-cleaved DNA complexes. This drug, as well as other anticancer agents, is able to affect both human topoisomerase II α and II β .^{13, 20, 49, 91, 151} Several findings, including mutagenesis, binding, and kinetic studies show that interactions between the enzyme and etoposide are essential for drug activity, because they mediate the formation of the cleavage complex.^{77, 92} It was demonstrated that the molecule binds weakly to DNA in absence of topoisomerase II.¹⁵² On the other hand, mutation of specific residues in topoisomerase II α changes the ability of the drug to increase levels of enzyme-DNA cleavage complexes.^{73, 74, 153, 154} From a structural point of view, etoposide can be divided into three distinct structural domains: a glycosidic group (at the C₄ position), a polycyclic ring system (A-D rings), and a pendant ring (E-ring) (Figure 3.1). Among these, the A-, B-, and E- rings of etoposide play an important role in promoting the interaction between drug and the enzyme. STD ¹H NMR, conducted by Pitts and co-workers, confirmed that the C₁₅ geminal protons of the A-ring, the C₅ and C₈ protons of the B-ring, the C_{2'} and C_{6'} protons and the 3'- and 5'-methoxy protons of the pendant E-ring are essential substituents to contact the enzyme in the binary topoisomerase II-drug complex.¹⁵⁵ Otherwise, no kind of interactions have been observed for C₁ and C₄ protons of the C-ring, C₂ and C₃ protons between C- and D- ring, C₁₁ protons of the D-ring and for all the glycosidic moiety. Modifications on the A-ring or on the E-ring substituents significantly change the activity of the drug.¹⁵⁵ To better understand the key role of these substituents in establishing the interactions with the enzyme, four new derivatives, retroetoposide,

demethylepipodophyllotoxin (DEPT), retrodemethylepipodophyllotoxin (retroDEPT) and D-ring diol have been analyzed in the above-mentioned study (Figure 3.1).

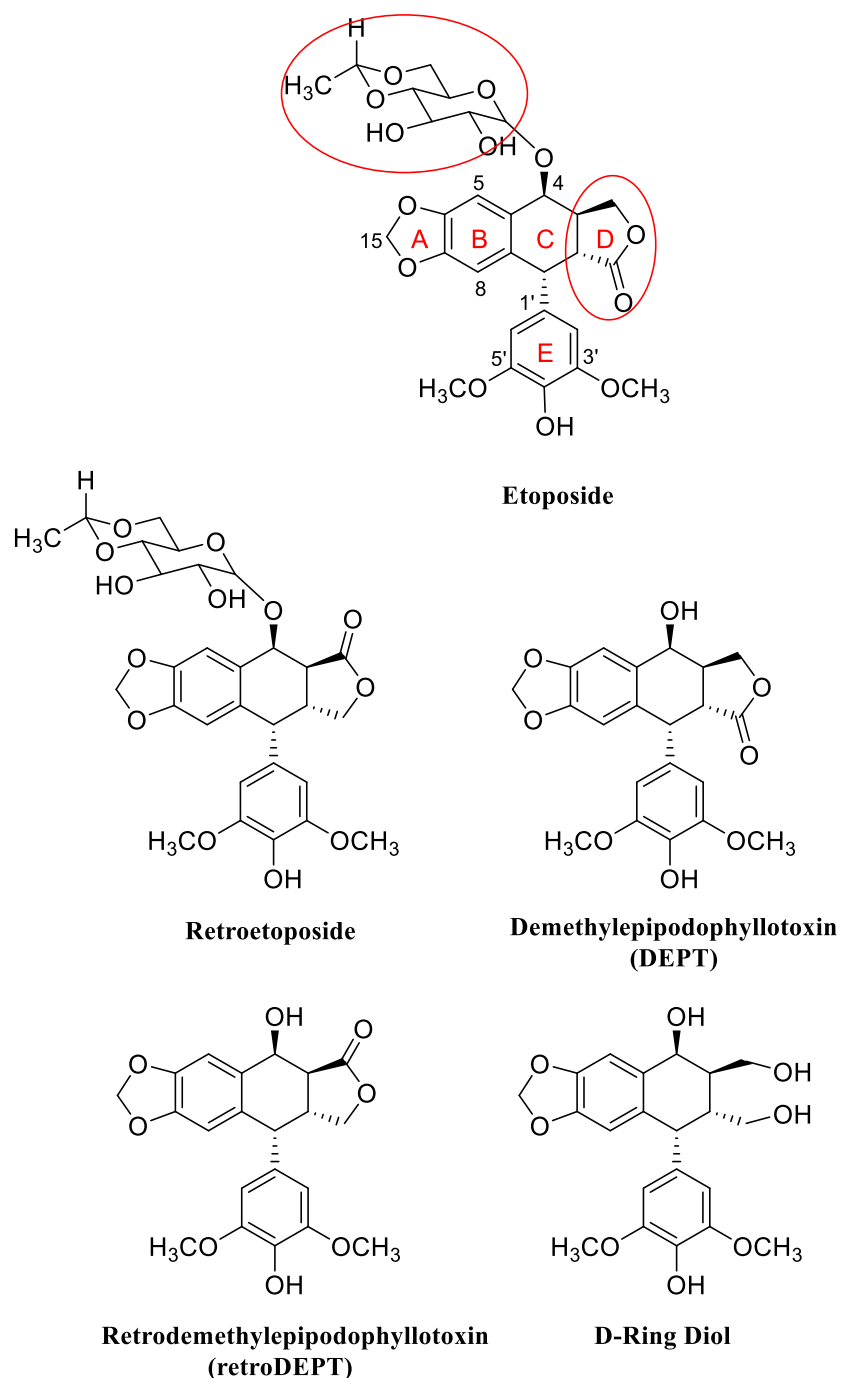


Figure 3.1. Structures of etoposide and etoposide derivatives with substitutions on C-ring and D-ring.

Compared to etoposide, the changes affected the C₄ glycosidic moiety and the shift of the lactone carbonyl group from the C₁₃ to C₁₁ position in the D-ring or the opening of the D-

ring. These compounds have been tested to underline the role played by the D-ring in mediating etoposide function. Results have confirmed that changing this ring results in a decreased ability to stimulate enzyme-mediated DNA cleavage. In retroDEPT, which shows both modifications (C₄ glycosidic moiety and D-ring), the activity is more reduced compared to the others, except the D-ring diol one. Hence, the double modifications have additive negative effects. The D-ring diol displays no ability to stimulate DNA cleavage.^{84, 155} Although etoposide is routinely used in clinic, it is responsible for many side effects, including myelosuppression and neurotoxicity at short term, and the risk of secondary leukaemia at longer term.⁷⁷ These side effects could be associated with a genetic cause¹⁵², but epipodophyllotoxin-mediated leukemogenesis is not directly linked to drug cytotoxicity.¹⁵³ Findings showed that in a total of 2-3% of patients treated with etoposide, treatment-related leukaemias characterized by 11q23 chromosomal rearrangements arise. It appears that drug-induced cleavage of nucleic acid by topoisomerase II might lead to the formation of chromosomal translocation break points (in particular 11q23 translocation with rearrangements of the MLL oncogene), causing the expression of the oncogenic factors responsible for secondary leukaemia.^{73, 156, 157}

Another issue concerns the poor oral bioavailability of etoposide, which led to the development of new analogues of this compound. Most of the modifications were made in the glycosidic moiety (C-ring) and the E-ring¹⁵⁸⁻¹⁶¹ and many of these modified the activity of etoposide. In particular, most substitutions radically modified drug potency or efficacy, but it is still unknown if these alterations are caused by changes in drug uptake/efflux or metabolism.

In addition to etoposide, in 1993 the FDA has approved teniposide for clinical use (Figure 3.2).^{146, 148} This is another podophyllotoxin derivative in which the 8"-methyl group of etoposide glycosidic moiety is substituted by a thiophene moiety. It is used primarily in the treatment of leukaemias and lymphomas (primarily childhood). Teniposide is 10-fold more active than etoposide in killing cancer cells. Because teniposide and etoposide display similar activity against topoisomerase II, its higher *in vitro* cytotoxic potency is probably due to better cellular uptake of teniposide. Despite that, toxicities are identical to those of etoposide, such as myelosuppression, hair loss, nausea and mucositis. In addition,

teniposide is even less water soluble than etoposide and findings suggest that allergic reactions are more frequently with the use of teniposide rather than etoposide.¹⁴⁶

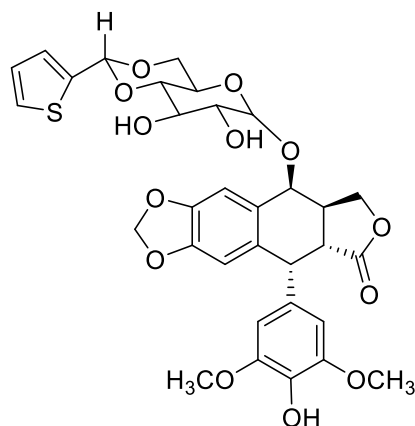


Figure 3.2. Structure of teniposide.

In 1996, Utsugi synthesized a new potent antitumor podophyllotoxin derivative named as TOP-53 (Figure 3.3) in which the glycosidic moiety was substituted with a flexible aminoalkyl side chain. Despite having the same core structure as etoposide and teniposide, TOP-53 was 4-fold more potent than these two molecules at generating chromosomal breaks and it showed a better uptake and pharmacokinetics in animal lung tissues.¹⁶² Despite the preclinical success of TOP-53, the cellular targeting of topoisomerase II by this drug has not been fully addressed.

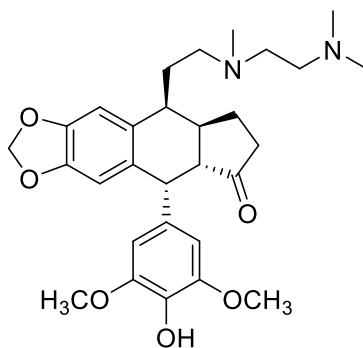


Figure 3.3. Structure of TOP-53.

In 2007, Wilstermann and co-workers characterized the effects of various substituents at the C₄ position, by analyzing teniposide and TOP-53.¹⁰³ On the basis of STD ¹H NMR data, it appeared that the glycosidic moiety of etoposide, which is attached to the C-ring at the C₄

position, does not interact with yeast topoisomerase II or human topoisomerase II α in the binary enzyme-drug complex. The first compound that was analyzed was teniposide; although teniposide is 10-fold more potent than etoposide in human cells, the two drugs were equipotent in purified systems. It seems that the effects of the thiophene moiety are primarily physiological (uptake, metabolism, etc.) in nature.^{146, 148} The second derivative that was analyzed was TOP-53. Although it is structurally identical to etoposide and teniposide, except for the substituent in C₄, the NOE signals produced by TOP-53 protons were ~2-fold stronger than those observed for the other podophyllotoxins. These findings suggested that this drug is able to bind to topoisomerase II faster or with closer geometry than does etoposide.¹⁰³

Based on these considerations, in order to decrease the off-target toxicity of etoposide and increase the solubility, Bailly and co-workers designed and synthesized a topoisomerase II poison known as F14512 (Figure 3.4).¹⁰² Its antiproliferative activity has been demonstrated in numerous human cancer cell lines such as leukaemia, breast cancer, lung cancer, melanomas and sarcomas.¹⁶³ F14512 is currently in phase II clinical trials for the treatment of acute myeloid leukaemia. This compound conserves the aglycone moiety of etoposide, but the C₄ position is substituted by a polyamine tail in order to improve the water solubility, DNA interaction, and recognition by the PTS expressed on tumor cells. The introduction of the positive charge of the spermine gives two important contributions: the drug is both able to bind more tightly to DNA than etoposide and displays improved water solubility.¹⁶⁴

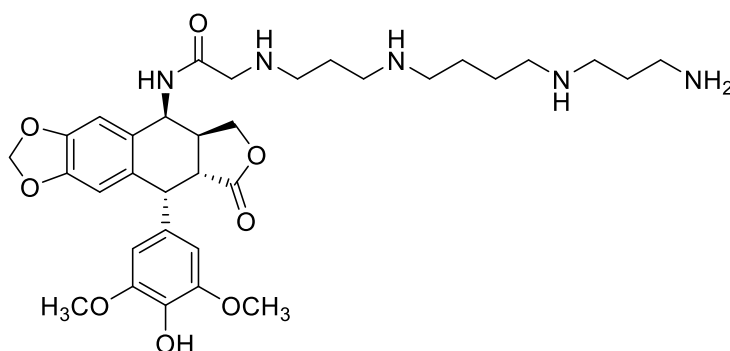


Figure 3.4. Structure of F14512.

Even though that F14512 contains an identical core to etoposide (rings A-E), the substitution of glycosidic moiety with a spermine tail not only maintain the crucial interaction with the ternary enzyme-drug-DNA complex, but it stabilizes the entire system.¹⁰² In 2011, Gentry and co-workers analyzed the effect of the C₄ spermine moiety on drug function against human topoisomerase II, by using STD ¹H NMR spectroscopy.¹⁶⁵ As discussed above, the removal of the C₄ glycosidic group had little effect on the capacity of the drug to inhibit the enzyme. This study showed that F14512 was several fold a more potent and efficacious poison than etoposide. Evidence suggested that F14512 displayed similar contacts as the parent compound with the human topoisomerase II α in the binary enzyme-drug complex but it was able to provide more interactions with the double helix in the binary DNA-drug complex.¹⁰² Thus Gentry and co-workers, on the basis of their results, suggested that F14512 formed a more stable ternary complex than etoposide, since the cleavage complex established in the presence of this drug persisted 5-10 fold longer than equivalent complexes induced by etoposide.¹⁶⁵ From these findings, it is clear that F14512 is a more potent poison than its parent compound, etoposide. The insertion of the spermine tail led to the selectivity of the drug in cancers that overexpress an active PTS. Moreover, since F14512 is able to bind the nucleic acid, it displays an increased stability of the ternary topoisomerase II-drug-DNA complex. In conclusion, while the A-, B-, and E-ring stabilized drug binding through protein interactions, it seems that the polyamine chain provides additional interactions within the ternary complex. Therefore, the linkage between the drug core and spermine plays a key role for the enhanced activity of F14512.¹⁶⁵

Furthermore, the evidence that F14512 (as well as TOP-53) displayed an enhanced topoisomerase II-poisoning activity could be explained by the finding that the glycosidic moiety was in a spacious binding pocket with relatively few interactions. Modeling analysis, by comparing the glycoside moiety with the aminoalkyl and spermine chains (TOP-53 and F14512, respectively) at C₄, showed that the substituent on this position may consolidate the interactions between the ligand-protein (for TOP-53) and ligand-DNA (for F14512) leading to closer ligand binding.⁹⁸

In the same year, Brel and co-workers¹⁶⁶ compared the action of the candidate drug F14512 to etoposide in terms of cytotoxicity, kinetic of inhibition of cell proliferation, cell cycle modulation and cell death pathways in A549 human non-small cell lung cancer

cell lines. This cell line, which expresses PTS-positivity, was used in order to validate the importance of the spermine chain. Results indicated that F14512 was 30 times more cytotoxic and its anti-proliferative activity was faster than etoposide. The values of EC_{50} were 4.6×10^{-8} M and 1.2×10^{-6} M after 48 hours and 2.6×10^{-8} M and 4.1×10^{-7} M after 72 hours for F14512 and etoposide, respectively. This study also showed that F14512 caused an irreversible anti-proliferative impact after a short time of exposition of the cells associated with a delay in their death. Its rapid effect probably was due to the presence of the PTS on the cells surface, which promoted the drug accumulation into the cells. Because of the polycationic spermine moiety, F14512 gained a higher affinity for the polyanionic structures present in the cytoplasm and in the nucleus. Thus, a change in the intracellular distribution of F14512 might be the reason for the delay of the cell death pathway. Another hypothesis is that the polyamine-conjugated drug may be sequestered into cytoplasmic vesicles. Indeed, it has been reported that polyamines linked to fluorophore bodily accumulate in acidic vesicles into the cytoplasm from which they are released into the cytosol.¹⁶⁷ Even though this last step is relatively short, both kinetic and drug target may be modified by the vectorization.

Thibault and co-workers have studied the effect of F14512 on ovarian cancer, confirming its lower toxicity and the additional ability to induce cellular senescence in A549 cells compared to etoposide.¹⁶³ The higher cytotoxicity of F14512 as compared to etoposide was not linked to its capacity to produce a great quantity of double-stranded DNA breaks. Indeed, though etoposide is responsible of a major amount of DNA damage, F14512 explicated its function at a lower level, thus supposing a different way of acting of the two drugs.¹⁰²

3.2 Drug design

As described previously, DNA is one of the main targets for the development of new antitumor agents. For the last four decades, many potential approaches have been proposed for the treatment of cancer. In this regard, topoisomerase II poisons play an important role. Many podophyllotoxin derivatives with anticancer properties have been found to be topoisomerase II poisons. Among them, etoposide is used to treat a wide spectrum of human cancer but suffers lack of selectivity. As most anticancer drugs are not able to

distinguish cancer cells from healthy ones, numerous side effects arise. As previously described, polyamines are naturally compounds protonated at physiological pH and are able to interact with the phosphate residue of the backbone of the DNA. The importance of the polyamine chain for targeting anticancer drug into the cell, was confirmed by the improved biological profile of the polyamine-conjugate F14512.

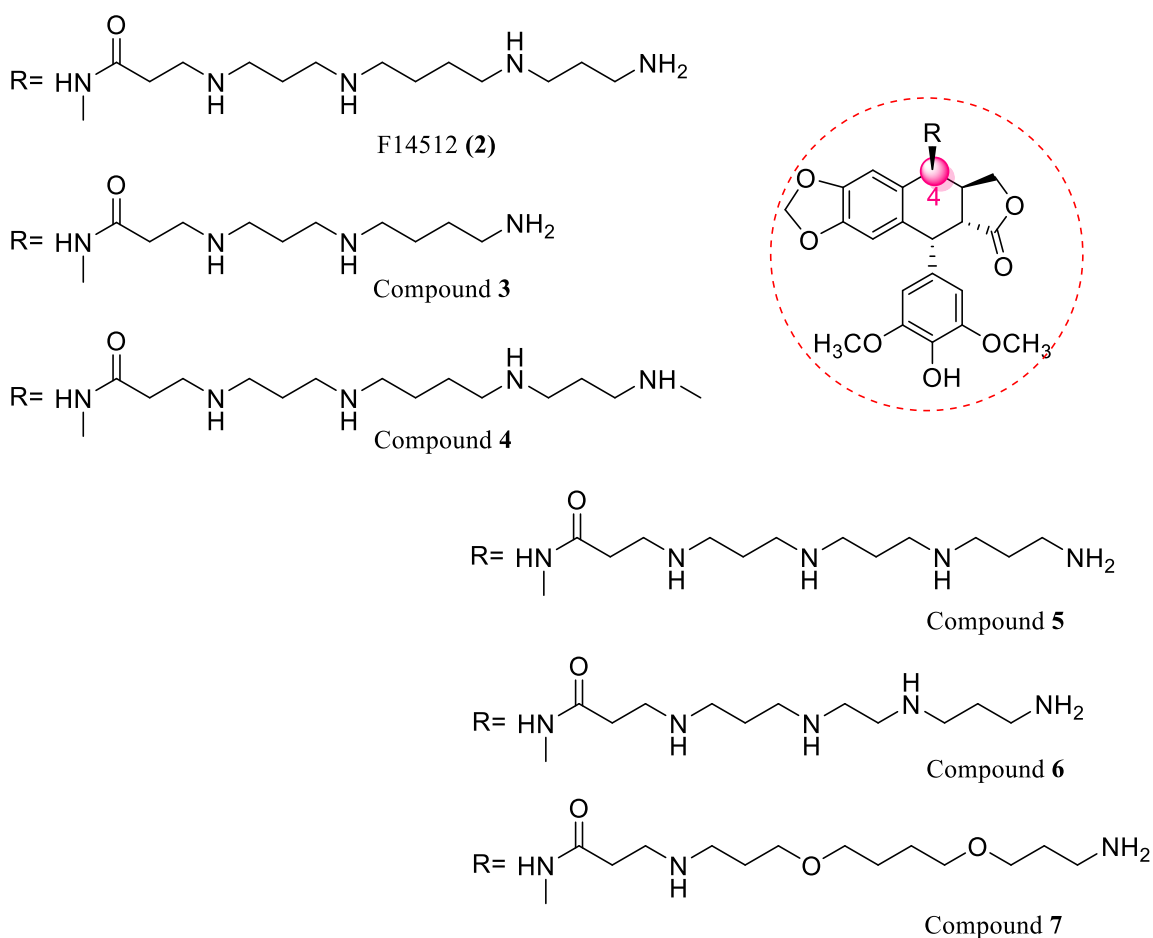


Figure 3.5. Structures of compounds 2-7.

On the basis of the studies with F14512, in order to obtain derivatives that are more potent than etoposide, we designed and synthesized five new polyamine-conjugates **3-7** (Figure 3.5). Particularly, this project centred on modifying the side chain of F14512 by exchanging the spermine moiety with different polyamine chains. Thus, we synthesized the spermidine derivative **3**, the methyl spermine derivative **4**, in which primary amine is monomethylated to a secondary amine. This latter modification was done in order to clarify the role of the

terminal primary amine function for the biological profile toward topoisomerase II activity. The compounds **5** and **6**, both bearing a spermine analogue chain with a shorter methylene spacer (two and three methylenes, respectively) between the two inner nitrogen atoms. In **7**, the inner nitrogen atoms of the spermine portion of F14512 were replaced with oxygens to explore the importance of the secondary amine function for the cell internalization through the PTS and for the increase of topoisomerase II inhibition.

3.3 Methods

3.3.1 Chemistry

The new compounds **3-7** were synthesized as hydrochloride salts as reported in Scheme 3.1 by coupling the common intermediate 4-chloroacetamido-4-deoxy-4-demethylepipodophyllotoxin (**8**) with the appropriate *N*-Boc protected polyamine (**14-18**), followed by acidic deprotection of the resulting intermediate **9-13**.

The synthesis of the key intermediate 4'-demethylepipodophyllotoxin was performed according to the literature.¹⁶⁸ A demethylation of podophyllotoxin was set out by using methanesulfonic acid and methionine as reagent, this latter was in excess for a nearly complete reaction. Furthermore, trifluoroacetic acid was used both as a co-solvent and as an entity protecting the carbocation immediately after its formation. During this reaction step, inversion of the chiral centre in C₄ was observed, confirmed by the coupling value in the NMR spectrum. The intermediate obtained was then treated with H₂SO₄ and chloroacetonitrile as solvent at r.t., leading to the intermediate **8**.

The *N*-Boc-protected polyamines **16-18** were synthesized according to literature procedures.^{169, 170} The protected polyamine **14** was prepared following the procedure reported in Scheme 3.2. 1,4-diaminobutane was selectively protected at one of the two amino functions by using di-tert-butyl dicarbonate (Boc₂O) to obtain the intermediate **21**. 3-amino-1-propanol was protected at the amino group with ethyl trifluoroacetate to give the intermediate **19**. After the activation of the hydroxyl group to the corresponding tosylate **20**, this was coupled with **21** to provide the derivative **22**. This latter compound was further reacted with Boc₂O to obtain the protected intermediate **23**. Finally, the trifluoroacetate protecting group was removed through the basic hydrolysis to give the compound **14**.

Spermine was protected on the secondary basic groups to obtain the intermediate **24**, that was treated with benzaldehyde to afford the corresponding Schiff base, reduced *in situ* with sodium borohydride to give **25**. This latter compound was then protected at the primary amine function with ethyl trifluoroacetate obtaining **26** that was converted to **27** through methylation of the benzyl amino group. The intermediate **27**, after basic hydrolysis of the trifluoroacetyl amide followed by removal of the benzylic protecting group through catalytic hydrogenation, afforded the compound **29**. The intermediate **29** was then protected with Boc₂O on the secondary amine groups to obtain *N*¹,*N*²,*N*³-tri-Boc-*N*¹spermine (**15**) (Scheme 3.3).

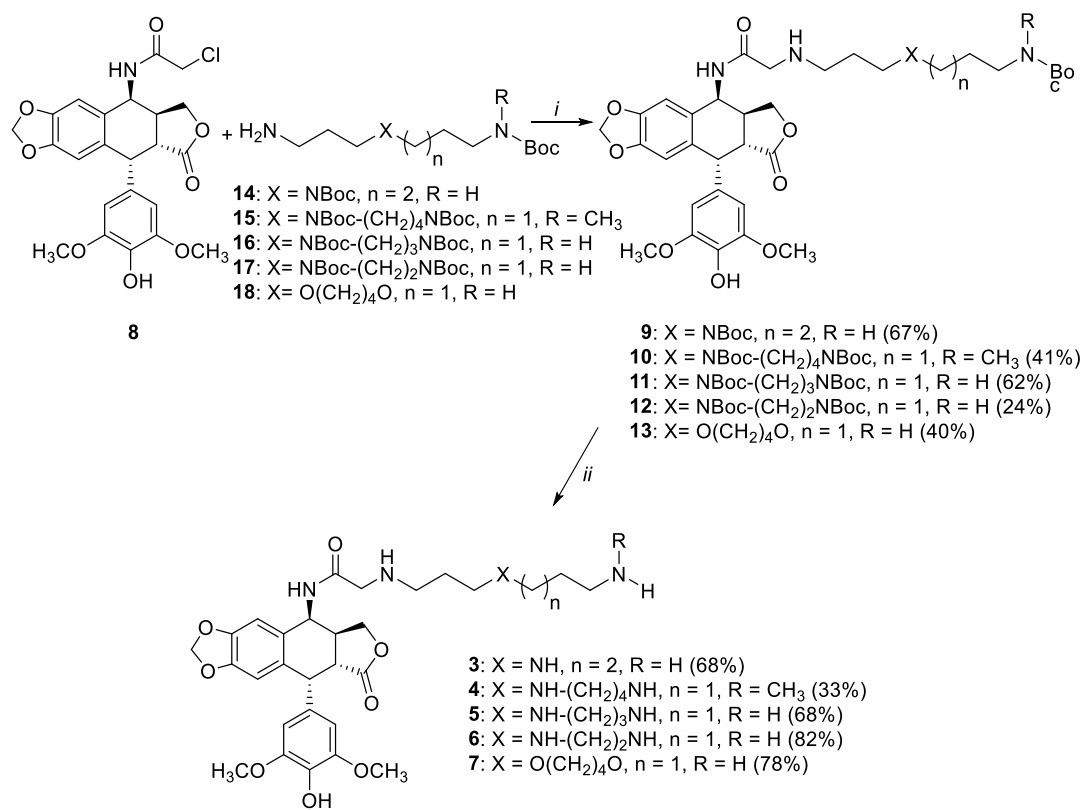
The reference compound **F14512** (**2**) was synthesized following the same synthetic procedure by coupling the intermediate **8** with *N*¹,*N*²,*N*³-tri-Boc-spermine.¹⁷¹

3.3.2 Biology

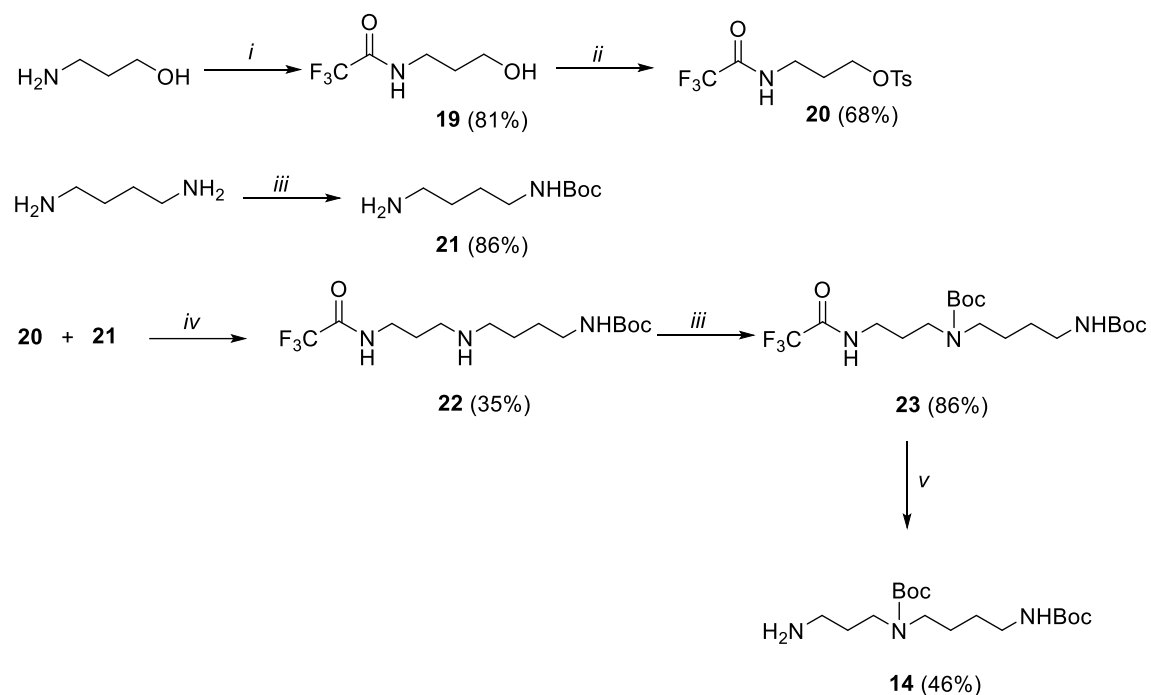
All the synthesized derivatives **2-7** were tested for their ability to inhibit the activity of topoisomerase II. Inhibition of relaxation and enhancement of cleavage were assessed. Values are showed as the concentration required to inhibit the activity of the enzyme by 50% (IC₅₀). Furthermore, was performed the interactions of these compounds with calf thymus DNA. ct-DNA is a natural DNA widely used in studies of DNA binding anticancer agents and DNA binding agents that modulate DNA structure and function.

3.3.3 Computational study

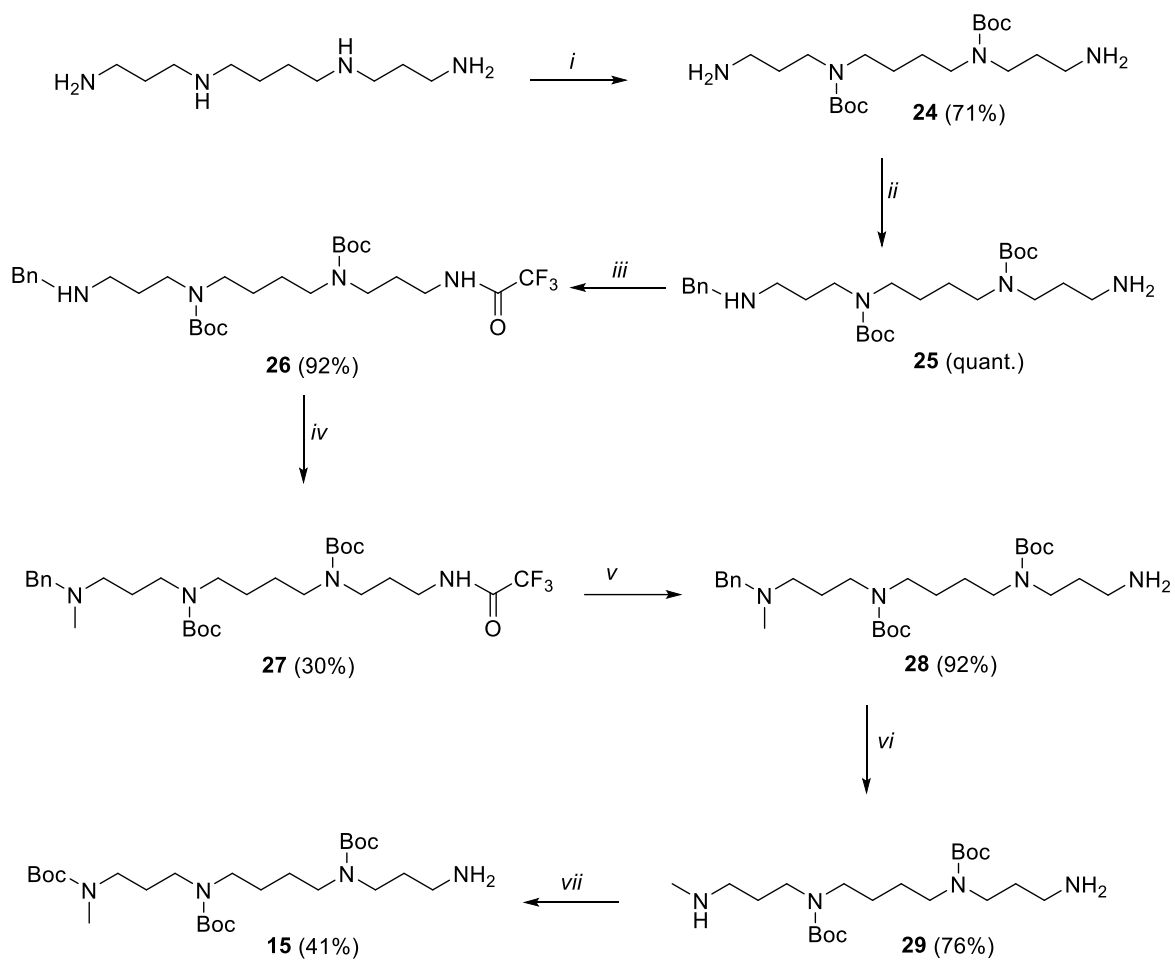
To further explore the binding mode of the synthesized compounds **2-7** for topoisomerase II-DNA cleavage complex, docking simulation were performed using the crystallographic structure of the human topoisomerase IIβ in complex with etoposide.



Scheme 3.1. Reagents and conditions: (i) DMF/CH₃CN, Et₃N, r.t., overnight; (ii) CH₂Cl₂, HCl 4M in dioxane, 0°C, 2-4 hours. Boc = (CH₃)₃COCO.



Scheme 3.2. Reagents and conditions: (i) CF_3COOEt , 4 hours, r.t.; (ii) TsCl , CH_2Cl_2 ; Et_3N , DMAP, 45 minutes, r.t.; (iii) Boc_2O , CH_2Cl_2 , 16 hours, r.t.; (iv) THF, Et_3N , 5 days, r.t.; (v) NaOH 40% p/p, MeOH, 16 hours, r.t.



Scheme 3.3. Reagents and conditions: (i) a) CF_3COOEt , MeOH, r.t., 1 hours; b) Boc_2O , MeOH, r.t., 16 hours; c) K_2CO_3 , pH = 11, reflux, 4 hours; (ii) a) benzaldehyde, toluene, reflux, 5 hours; b) NaBH_4 , EtOH, r.t., 12 hours; (iii) CF_3COOEt , r.t., 16 hours; (iv) MeI, Et_3N , THF, r.t., 24 hours; (v) NaOH 40% p/p, MeOH, r.t., 16 hours; (vi) H_2/Pd , MeOH, r.t., 5 hours; (vii) a) CF_3COOEt , MeOH, -78°C , 30 minutes; b) Boc_2O , MeOH, r.t., 16 hours; c) NaOH 40% p/p, r.t., 16 hours.

3.4 Results and discussion

F14512 is reported to be ~10-fold more potent than its parent compound etoposide in inhibiting cell proliferation.¹⁰² As mentioned above, this is partly attributed to the spermine-mediated F14512 uptake by the PTS. However, the conserved epipodophyllotoxin core and the mechanism of action suggest that the enhanced efficacy of F14512 in comparison to that of etoposide might also come from favourable interactions of its spermine moiety within the topoisomerase II-DNA cleavage complex. Despite that, the precise mechanism of action is still uncertain, since nobody has yet reported an atomic-level description and evaluation of the interaction between F14512 and the cleavage complex.

Our study started with the docking of F14512 to the binary cleavage complex using a positional restraint grounded on the underlying assumption of an etoposide-like binding mode for the conserved epipodophyllotoxin core. The long polyamine chain extends toward the major groove and interacts with the backbone phosphates of both DNA strands (Figure 3.6).

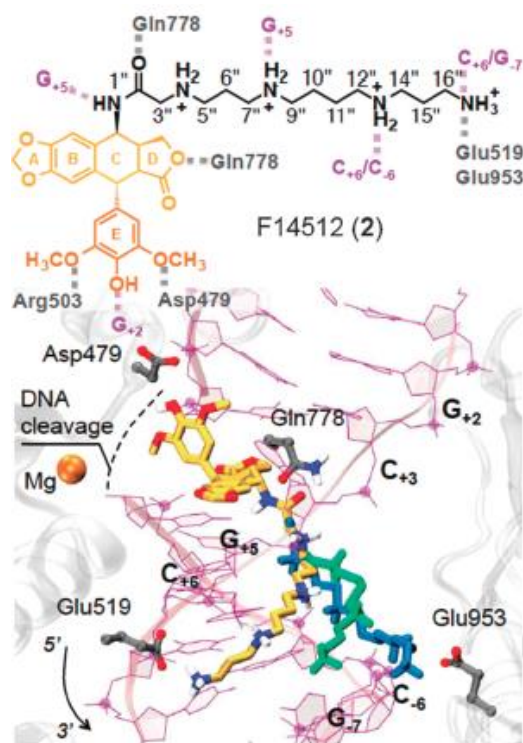


Figure 3.6. Key interactions between F14512 and the cleavage complex shown schematically (Top). Three representative binding modes of F14512 from molecular dynamics (MD) simulation are shown with different colours of the spermine moiety (Bottom).

These results indicate that the amine nitrogen atoms in positions 13'' and 17'' (N_{13''} and N_{17''}) of the spermine tail act as key anchors for binding. The N_{13''} atom interacts mainly with the DNA phosphates of C₊₆ and G₋₇. The spermine nitrogen N_{17''} alternatively H-bonds the protein residues Glu953 and Glu519, which are located close to the substrate DNA. These transient interactions occur at both DNA strands with comparable statistical distributions. The amines nitrogen in position 8'' (N_{8''}) and 4'' (N_{4''}) provides additional DNA anchoring and contributes only marginally to stabilizing the drug to the cleavage complex, respectively. In conclusion, this complex H-bond network reflects a favourable complementarity of F14512 and the cleavage complex. Etoposide, in contrast, cannot form such an H-bond network since its glycosidic moiety at C₄ is more stable and protrudes toward the DNA major groove, remaining stably located near Gln778 and Met782. Thus, the stronger drug binding of F14512 seems to be mainly due to the spermine chain, which forms, through the major groove, extensive favourable drug-target interactions with both DNA and topoisomerase II. This conclusion is also confirmed through steered MD simulations (Figure 3.6).

More studies have to be performed in order to validate this computational evidence and to better understand how our derivatives can inhibit the enzyme. Compounds **2-7** were tested against human topoisomerase II in comparison to the activity of etoposide (**1**). The IC₅₀ values obtained in a relaxation inhibition assay (Table 1) confirm that F14512 is the most potent derivative in the series, with an IC₅₀ of ~30 μM, which is ~4-fold better than etoposide in the same experimental assay. Furthermore, all the derivatives stabilized the cleavage complex, indicating that all of them act as topoisomerase II poisons. The amount of cleaved DNA produced by the enzyme in the presence of each polyamine derivative was quantified and compared to the one produced in the presence of the parent compound at the same concentration (5-50 μM concentration range). The ratio of these values provides the “relative efficiency” reported in Table 1. Although only indicative, an excellent linear correlation ($R^2 = 0.81$, Figure 3.7) was found between the observed relaxation activity of the enzyme and the extent of cleavage complex formation. This result indicates that the impairment of the enzymatic activity generated by all the examined compounds occurs according to an overall share mechanism of action. Interestingly, the relative potency of these inhibitors strictly depends on the structural features of the polyamine chain. The

activity is reduced by ~2-fold by the replacement of the tetramine spermine with the triamine spermidine (**3**) and with the transformation of the terminal primary amine into a secondary amine by methylation of the terminal nitrogen atom in compound **4**.

Table 1. Data on compound potency and properties.

Compound	IC ₅₀ ^a [μM]	Relative efficiency ^b	% Abs change ^c
Etoposide	120 ± 10	1	nd
F14512	30 ± 5	2.12 ± 0.22	17.7 ± 1.0
3	60 ± 8	1.13 ± 0.19	7.7 ± 0.7
4	70 ± 19	1.30 ± 0.03	9.5 ± 1.7
5	35 ± 4	1.39 ± 0.01	11.5 ± 4.0
6	90 ± 5	1.09 ± 0.26	6.7 ± 5.0
7	170 ± 20	0.22 ± 0.01	13.0 ± 2.4

^a Compound concentration required to inhibit the relaxation activity of topoII (IC₅₀). ^b Extent of cleavage product formation in comparison to etoposide (relative efficiency). ^c Variation of the absorbance signal at 290 nm induced by the addition of four equivalent of ctDNA (% Abs change).

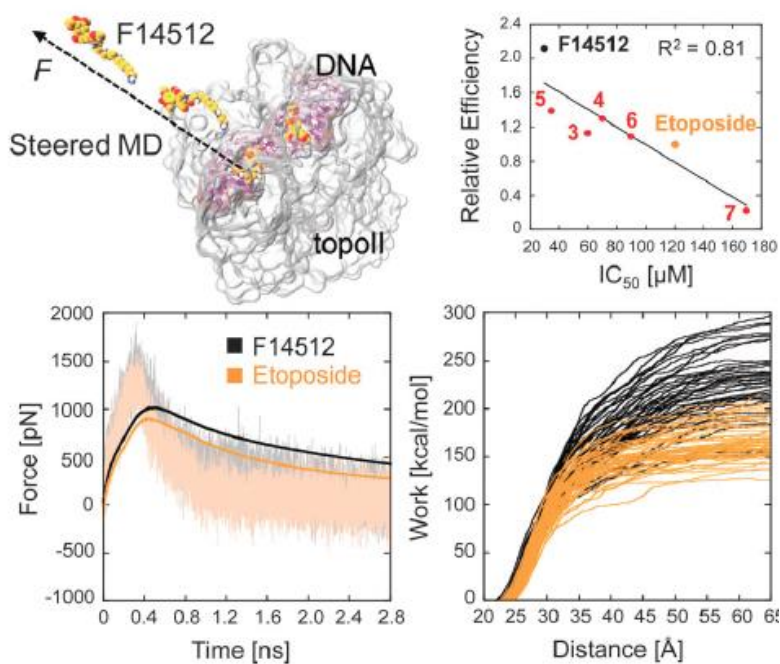


Figure 3.7. Low row: Average unbinding force profiles (left) and external work (right) for the undocking of F14512 and etoposide from the cleavage complex, as calculated from multiple steered MD simulations (top-left).

This finding suggested that the presence of an additional cationic group in F14512, such as the presence of a terminal primary amine function plays an essential role for the inhibition of the enzyme. The low inhibition can be explained by the fact that a shorter polyamine chain, as in **3** and in **6**, does not allow engagement of distant topoisomerase II residues such as Glu519 and Glu953. Compound **4**, with a methyl spermine tail, is unable to form an optimal interaction between its terminal secondary amine and the carboxylate groups of Glu519 and Glu953, due to the steric hindrance of the methyl group (Figure 3.8).

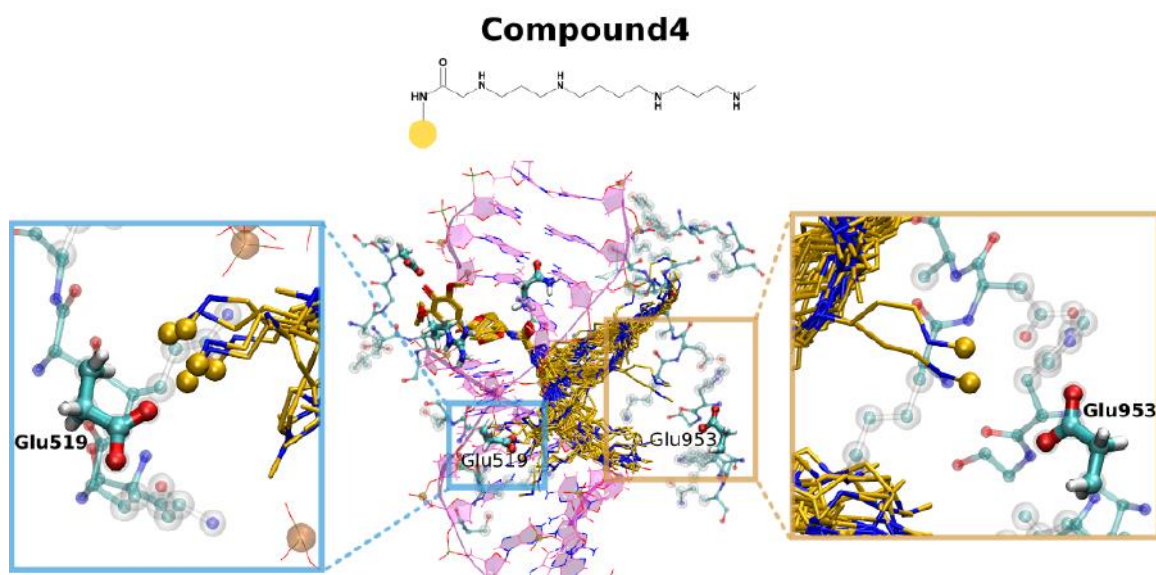


Figure 3.8. Docking of compound **4** into the cleavage complex. Compound **4** differs from F14512 for the presence of a secondary amine at position N₁₇. The methyl group of compound **4** (shown as a gold sphere) lies between N₁₇ and the oxygens of either Glu519 or Glu953.

Compound **7**, in which the inner nitrogen atoms of spermine have been substituted with oxygen atoms in order to investigate their influence in the PTS-mediated internalization, resulted the weakest and least efficient topoisomerase II poison (~170 μ M) of the series. This finding proved the key role of the polycationic character of the chain in drug activity. As mentioned above, the glycosidic moiety of etoposide is able to provide few contacts with the binary topoisomerase II-DNA complex. Furthermore, in the absence of DNA the drug showed a few interactions with the topoisomerase II, alone.^{84, 165} Thus, these results demonstrated that the drug has limited, if any, interaction with topoisomerase II, alone, while it binds tightly to the topoisomerase II-DNA cleavage complex. Different results were found with F14512, in which the insertion of the polyamine chain lead to a derivative

able to give interactions with both, enzyme and DNA alone. Therefore, to validate the key role of the polyamine chain, we also quantified the efficiency of our ligands in binding the DNA alone (*i.e.*, in the absence of enzyme), by using UV measurements. In Table 1 is reported the variation of the absorbance signal induced by DNA, which reflects the extent of the bound ligand to the DNA. These results indicate that all polyamine conjugates were able to bind DNA, as previously reported for F14512¹⁰², which here emerges as the strongest DNA binder. Compound **7** resulted also a good DNA binder, which suggests that the central amines of the polyamine chain are critical for drug binding to the topoisomerase II-DNA cleavage complex, rather than to the DNA alone.¹⁷¹

Docking calculations further support the evidence that the most active topoisomerase II poisons are those that, through the polyamine chain, form an extended network of H-bonds within the cleavage complex. In fact, the score distribution of the obtained poses for F14512 and compounds **3-7** docked to the cleavage complex reproduces well the IC₅₀ and relative efficiency trend values. Furthermore, this study shows the spermine, which extends into the major groove, interacting with both DNA strands, as in MD simulations, whereas the tail of **7**, although of the same length, is mostly located far from the DNA backbone, assuming curved conformations that cannot form stable and favourable interactions with the targeted complex.

3.5 Conclusion

This work has validated the idea that the substitution of the glycosidic moiety at C₄ of etoposide with a polyamine chain produces enhancement in topoisomerase II inhibition. F14512 displayed an IC₅₀ value ~4-fold better than the parent compound etoposide. All of synthesized compounds displayed a topoisomerase II inhibition with activity in the micromolar range. The cleavage complex assay with these molecules indicated that all the derivatives stabilized the topoisomerase II-DNA cleavage complex. Among them, F14512 was still the most potent derivative in the series with an IC₅₀ of ~30 μM. The polyamine moiety's favourable contribution is not simply connected to the efficiency of DNA recognition but is due to the stabilization of the topoisomerase II-DNA cleavage complex. These data reveal the possible drug-target configurations of the still structurally uncharacterized F14512-topoisomerase II-DNA complex. Furthermore, our computational

evidence demonstrates that an optimized polyamine moiety boosts drug binding to the cleavage complex, rather than to the DNA alone. Result of the present study suggest that the by varying the length of the polyamine side chain and the number of nitrogen groups, such as their methylation, is observed a decrease of drug activity in comparison to the parent compound F14512.

3.6 Experimental section

3.6.1 Biology

3.6.1.1 Topoisomerase inhibition

0.125 µg of pBR322 (*Inspiralis*) were incubated with increasing concentrations (0.5-200 µM) of tested compounds for 1 hour at 37 °C in the presence/absence of 1 U of human topoisomerase II α (*Inspiralis*) in the required buffer (1X). Reaction products were resolved on a 1% agarose gel prepared in 1x TAE (10 mM Tris 1mM EDTA, 0.1% acetic acid, pH 8.0). After the electrophoretic run (5 V/cm for about 90 minutes) the DNA bands were visualized by ethidium bromide staining, photographed and quantified using a Geliance 2000 apparatus.

3.6.1.2 Topoisomerase poisoning

0.125 µg of pBR322 (*Inspiralis*) were incubated with increasing concentrations (0.5-200 µM) of tested compounds for 6 minutes at 37 °C in the presence/absence of 5 U of human topoisomerase II α (*Inspiralis*). Then, the reaction was stopped with 0.1% SDS (Sodium Dodecyl Sulphate, *Sigma*), and finally the enzyme was digested with 1.6 µg of proteinase K (*Sigma*) in 10 mM Na-EDTA for 30 minutes at 45 °C. Reaction products were resolved on a 1% agarose gel in 1X TAE (10 mM Tris 1mM EDTA, 0.1% acetic acid, pH 8.0). the electrophoretic run was performed at 5 V/cm for 90 minutes and then bands were stained with ethidium bromide (0.5 µg/mL in 1X TAE) photographed and quantified using a Geliance 2000 apparatus.

3.6.1.3 ctDNA binding assay

The UV spectrum (250-350 nm) of the selected compounds was recorded (*Perkin Elmer* spectrophotometer) at 50 μ M in 10 mM Tris 50 mM KCl buffer. Then, each compound was titrated with ctDNA (*Sigma*). The UV absorbance contribution of ctDNA in the selected range was compensated by adding the same amount of DNA in the sample and reference cells. The spectra were recorded and the variation of the absorbance at 290 nm caused by a four-fold excess of ctDNA was considered for DNA binding evaluation.

3.6.2 Molecular modeling

Molecular dynamic simulations were used to equilibrate the complexed at physiological conditions and for the production runs. They have been based on the crystallographic structure of the human topoisomerase II β in complex with DNA and etoposide (*i.e.* ternary complex), solved at 2.16 Å resolution (PDB code 3QX3).⁹⁸ During the docking procedure, a positional restraint has been applied on the epipodophyllotoxin moiety of F14512 to reproduce the binding of the same core characterizing the drug etoposide.⁹⁸ All the amine groups of F14512 have been considered as protonated at physiological pH (7.4). Protonation states have been predicted at a target pKa of $10^{-7.4}$, using the Epik software for predicting pKa values for drug-like molecules.

Chapter 4- Inhibition of human topoisomerase II α by xanthone derivatives

4.1 Xanthone derivatives

Several different classes of natural products or secondary metabolites have been isolated that efficiently target topoisomerase II α and, among them, xanthone derivatives became popular. They are secondary metabolites, originally isolated from a few higher plant families, and in fungi and lichens. They are well-known compounds in medicinal chemistry because they display a wide range of biological activities, including anti-hypertensive, anti-oxidative, anti-thrombotic, and anti-cancer activity based on their diverse structure.¹⁷²⁻¹⁷⁵ The xanthen-9-one is the basic skeleton of this oxygenated heterocycles (Figure 4.1). In the recent years, several synthetic molecules or natural products with anticancer activity were identified.

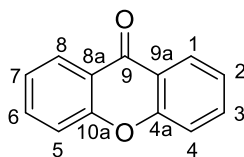


Figure 4.1. Structure of xanthen-9-one.

Mangosteen is a tropical tree from the family *Clusiaceae*, which has been cultivated for centuries in Southeast Asia rainforests and can be found in many countries worldwide.¹⁷⁶ α -mangostin is one of the xanthone present in *Mangosteen* pericarp. In 2013, Mizushina designed and synthesized six α -mangostin-related compounds. Inhibitory activity of these compounds against topoisomerase I and topoisomerase II was evaluated. In this series the most interesting compound is α -mangostin (Figure 4.2). They revealed that it inhibited the activity of both enzymes with IC₅₀ values of 15.0 μ M for topoisomerase I and 7.5 μ M for topoisomerase II. The comparison with topotecan (IC₅₀ ~45 μ M for topoisomerase I) and doxorubicin (IC₅₀ ~60 μ M for topoisomerase II) showed that the inhibitory effect on both enzymes of α -mangostin was higher. Furthermore, the inhibition of human topoisomerase II activity by this compound was > 2-fold better than that of mammalian DNA-dependent DNA polymerase activities. Moreover, Mizushina indicated

that α -mangostin bound directly to the enzyme and inhibited its activity, rather than as a DNA intercalating agent or as a template-primer substrate.¹⁷⁷

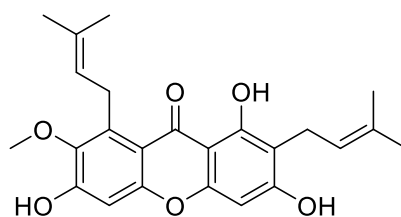


Figure 4.2. Structure of α -mangostin.

Gambogic acid (GA) is another xanthone derivative in human phase II clinical trials as an anticancer drug. It is a natural product isolated from the gamboge resin of *Garcinia Hanburyi tree* in Southeast Asia (Figure 4.3a). The resin is used as a traditional Chinese medicine for detox treatments, haemostasis, and parasiticide. Originally, GA was thought to be able to induce apoptosis¹⁷⁸, and it seems that both activation of caspases and mitochondrial pathway are involved in GA-induced apoptosis.¹⁷⁹ Recent studies have demonstrated that GA has potent cytotoxicity against different human cancers, such as hepatoma, gastric carcinoma, and lung cancer. Furthermore, Qin and co-workers, examined the effect of GA on topoisomerase I.¹⁸⁰ The results indicated that this compound caused a dose-dependent inhibition of enzyme with an IC_{50} ~ 50 μ M. They also tried to evaluate the effect of GA on the catalytic activity of human topoisomerase II α . This study demonstrated that the compound was not able to increase levels of the cleavage complex and did not induce DNA damage in a neutral comet assay. This result suggested that the effect of GA on topoisomerase II was due to the ability of the drug to interfere with the overall catalytic activity of the enzyme. The authors further suggested that GA inhibited human topoisomerase II α by binding to the ATPase active site of the enzyme and blocking interactions between the enzyme and ATP (Figure 4.3b). This hypothesis was based on molecular docking that predicted some potential binding sites for the drug within ATPase domain, revealing a possibility that GA might compete with ATP for binding to human topoisomerase II α . Results indicated that GA showed a high binding affinity for ATPase domain, with the equilibrium dissociation constant (K_D) of $3.23 \times 10^{-6} \pm 0.23 \times 10^{-6}$ mol/L, which compared to that of etoposide ($4.16 \times 10^{-5} \pm 0.46 \times 10^{-5}$ mol/L) was much smaller. These data suggested that GA specially targeted to topoisomerase II α in cells, even if the

mechanism behind the selectivity remains unknown.¹⁸⁰ In light of the low water solubility of GA, its clinical application is limited. The research is focusing on design and development of new compounds, to obtain more potent and water-soluble derivatives of this compound.

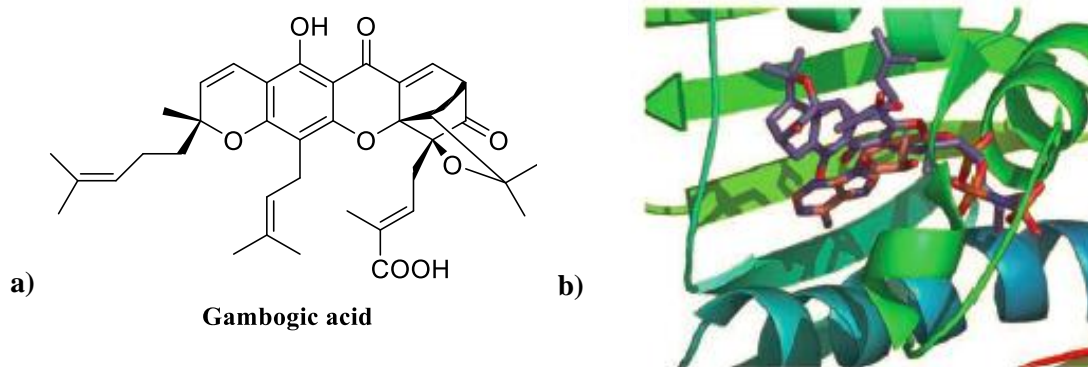


Figure 4.3. a) Structure of gambogic acid. b) Molecular docking predicts that GA might bind the ATP binding sites of human topoisomerase II α .¹⁸⁰

Xanthone derivatives, as mentioned above, are characterized by an interesting structural scaffold and biological efficacy. Thus, the study of these compounds is interesting not only from a chemosystematic viewpoint, but also from a pharmacological one. Findings have suggested that among synthetic and natural compounds, poly-oxygenated xanthenes showed effective inhibitory activity against several cancer cell lines.¹⁸¹⁻¹⁸³ In particular compound **A**, which bears two 2,3-epoxypropoxy groups at 3 and 5 positions, displayed strong anticancer activity (Figure 4.4).^{173, 184} Thus far, the exact mechanism of these compounds has not been reported yet.

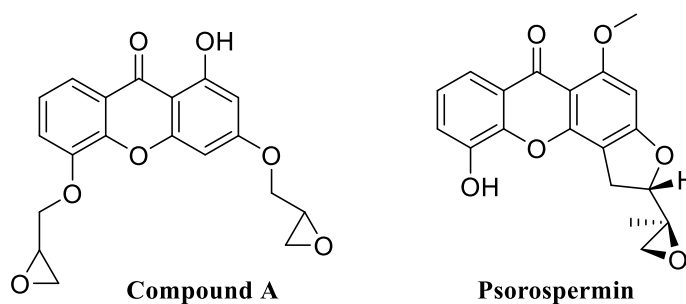


Figure 4.4. Structures of compound **A** and Psorospermin.

Psorospermin is a natural product that has been shown to have activity against drug-resistant leukaemia lines and AIDS-related lymphoma (Figure 4.4). According to the literature, psorospermin was able to intercalate into the DNA helix and covalently modify guanine at the N₇ position in the major groove through an epoxide-mediated electrophilic attack.¹⁸⁵ Furthermore, it seemed that the presence of topoisomerase II increased DNA alkylation. Kwok and co-workers showed that this enhanced DNA alkylation was dependent on pH but was independent of Mg²⁺ or ATP, which suggested that topoisomerase II-mediated psorospermin alkylation arose in the initial noncovalent binding step in the catalytic cycle of the enzyme.¹⁸⁶

In 2007, Woo and co-workers synthesized and studied anticancer activities of some epoxypropoxy xanthenes **B-D** and their epoxy ring opened halohydrin compounds **E-H** (Figure 4.5).

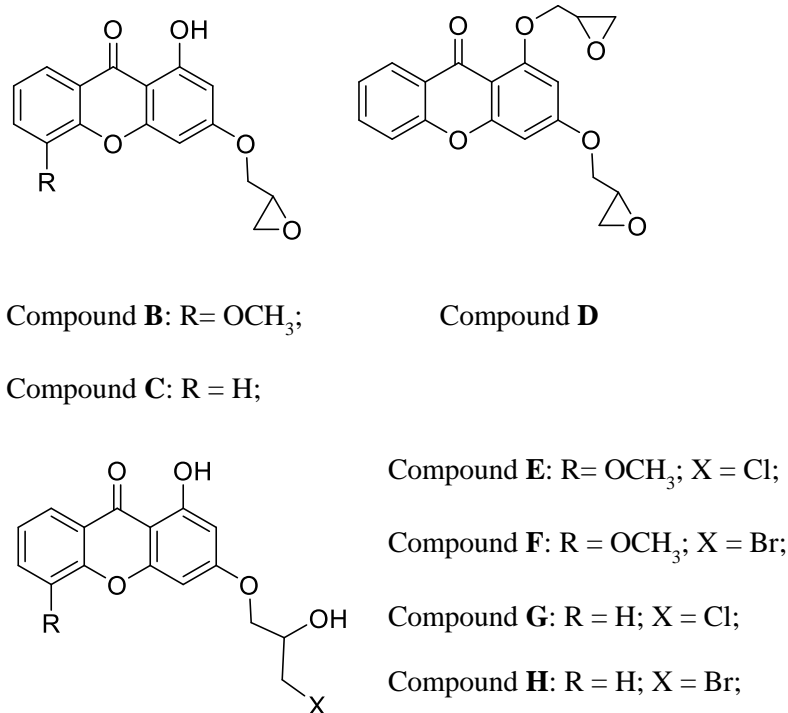


Figure 4.5. Structures of xanthone derivatives **B-H**.

These compounds were tested for their ability to inhibit topoisomerase II, by using etoposide as a positive control. The data obtained from the relaxation assay showed that the compound **D**, which bears two 2,3-epoxypropoxy groups at the C₁ and C₃, showed best biological activity of the series, displaying good cytotoxic and topoisomerase II inhibition.

Furthermore, this compound was tested for DNA cross-linking property, showing a concentration dependent DNA cross-linking activity.¹⁸¹ In 2010, Cho and co-workers synthesized a series of benzoxanthone derivatives with the goal to develop anticancer drug candidates that target topoisomerases and DNA. These derivatives were classified in three different groups based on the tetracyclic ring shapes (Figure 4.6).¹⁸⁷ Their activity toward topoisomerase I and topoisomerase II was evaluated through the relaxation assay.

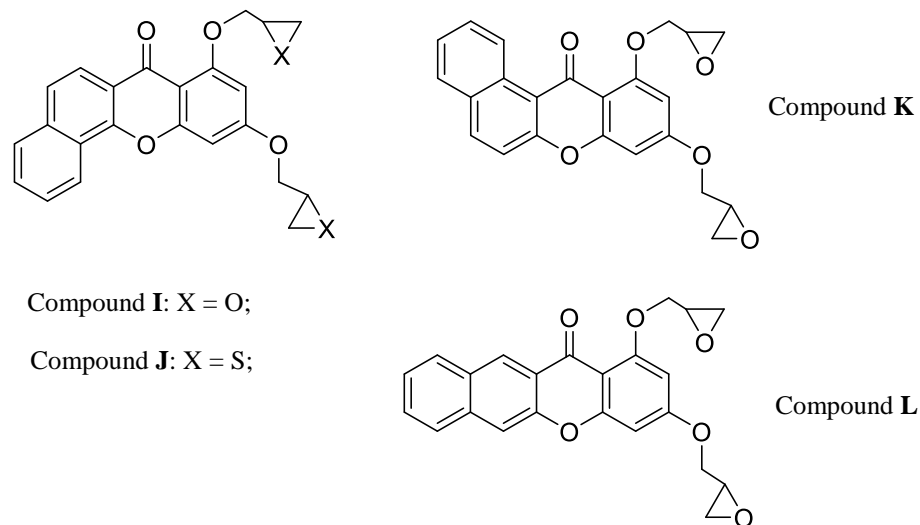


Figure 4.6. Structures of compounds I-L.

Among the compounds, compound **J** showed inhibition toward both the enzymes. Its % inhibitory values on topoisomerase I were compared to those of camptothecin for topoisomerase I, while for type II topoisomerase to those of etoposide. A significant increase of topoisomerase II inhibition was reported for compound **J**, which was ~3-fold better than that of etoposide at 20 μM (72.7% and 27.9%, for **J** and etoposide respectively).¹⁸⁷ Additionally, the DNA cross-linking test was assessed for all the compounds of the series. Results showed that among the compounds with epoxy groups, only compounds **I** and **L** cross-linked DNA duplex, but **K** did not. These data suggested that DNA cross-linking appeared after intercalation of the tetracyclic ring into DNA base pairs and this process might be dependent on the structure of the tetracyclic ring system of benzoxanthone derivatives. Consequently, they proposed that compound **L** inhibited cancer growth by binding the DNA duplex itself and/or DNA-topoisomerase II complex.

In the same year, Woo and co-workers¹⁸⁸ designed a series of new xanthone analogues possessing methyloxiranyl-methoxy groups (Figure 4.7).

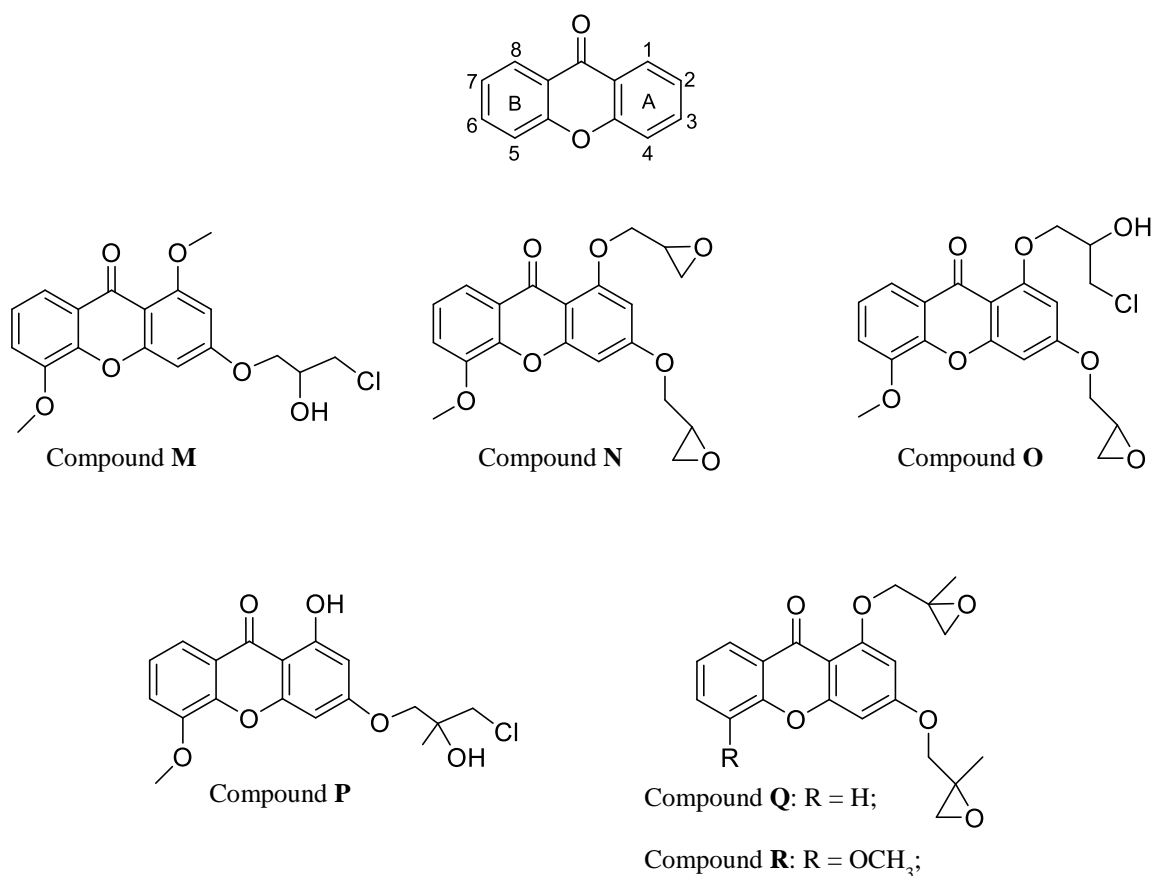


Figure 4.7. Structures of compounds **M-R**.

The first group of this series was characterized by the presence of a methoxy group at the C₅ position on the B ring, the second one by a methoxy group at the C₁ position instead of a hydroxyl group on the A ring, and the last one by a [2-(methyl)oxiranyl]methoxy group at the C₃ position in the xanthone core.¹⁸⁸ They hypothesized that the introduction of methoxy groups in the xanthone core could affect the mechanism of action of these compounds, such as intercalation and/or binding to DNA and enzymes. The data indicated that compounds that held a halohydrin group at the C₁ or C₃ positions, such as compounds **M**, **O** and **P** showed good inhibitory activity compared to etoposide at 100 μM concentration. However, the bis-epoxy substituted compounds, **Q** and **R**, showed moderate inhibitory activity at 100 μM concentration. Furthermore, compounds bearing an epoxide ring were tested for DNA cross-linking property. Among them compound **Q** was the strongest DNA cross-linker.

This result suggests that the C₅-methoxy group in compounds **N** and **R** decrease the DNA cross-linking ability of the xanthone derivatives. In particular it might block the intercalation of the planar structure of the xanthone ring into the DNA base pair which makes the compound unfavourable for electrophilic interaction with DNA.¹⁸⁸ The presence of the methyl group in the epoxide ring might also have a negative contribution during compound-DNA interaction; it might sterically alter the position of the epoxide ring or the hydrophobic interaction. Even if the correlation between DNA cross-linking and topoisomerase II inhibition is not well identified, it seems that the inhibition of the enzyme might occur through formation of compound-enzyme binary complex or compound-enzyme-DNA ternary complex by the Van der Waals interaction and/or hydrogen bond. Notwithstanding, the inhibition of topoisomerase II might also be due to DNA alkylation in an indirect manner and the cross-linked double helix DNA can be relaxed by the enzyme.¹⁸⁸ To improve the activity of xanthone derivatives inhibitors, in 2011 Su and co-workers developed a series of compounds that shared some similarity in nucleus structure with doxorubicin.¹⁸⁹

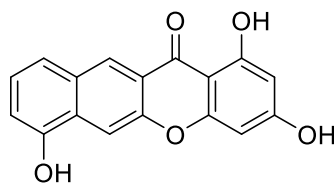


Figure 4.8. Structure of compound **S**.

In this group, compound **S** (Figure 4.8) was further tested in order to explore its effect on topoisomerase II. They founded that compound **S** strongly inhibited the activity of the enzyme by using different concentrations of the drug (from 1 to 16 μ M). It was also found that this compound, in addition to inhibit activity of the enzyme, was able to downregulate the expression of topoisomerase II protein and the level of topoisomerase II α mRNA in HepG2 cells. This finding suggested that topoisomerase II is the target of compound **S** and that this aspect plays an essential role in its antitumor activity.¹⁸⁹ These results could be useful to develop other potential inhibitors of topoisomerase II.

In the same year, Jun and co-workers synthesized a series of xanthone derivatives conjugating the nucleophile-attached alkoxy chains to the epoxide ring opened with the aim to obtain new topoisomerase II α inhibitors (Figure 4.9).¹⁹⁰

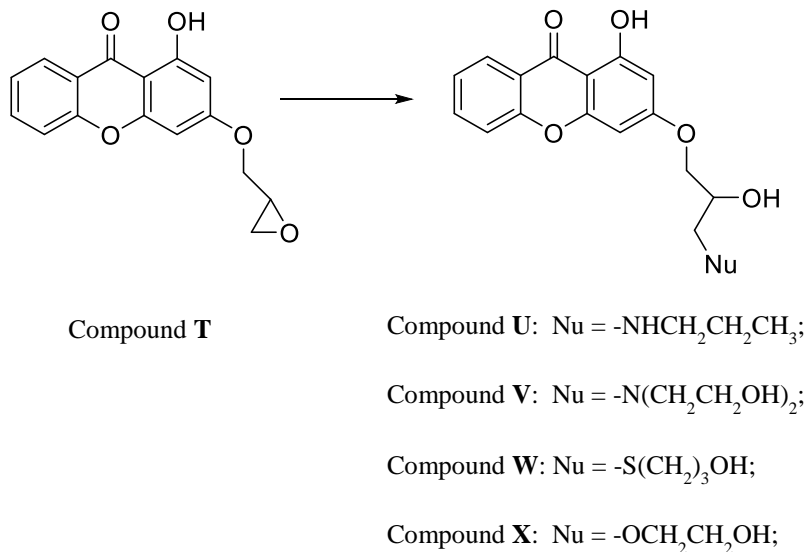


Figure 4.9. Structures of compounds **T-X**.

All the synthesized compounds displayed an enhanced inhibitory activity in comparison to the parent compound **T**, even when they were present in low concentrations (10 and 20 μ M). Compound **U**, which possessed a secondary amine on the side chain of the xanthone core, inhibited the activity of the enzyme more efficiently than compounds **V-X**, which contain a tertiary amine, S and O, respectively, in the same position. During this study they suggested that the inhibitory activities of these compounds could be attributed to the substituent on the side chain. Additionally, they suggested that the presence of a secondary amine group in the side chain, thanks to its hydrogen donor group, may play an important role for the activity of the xanthone core. This compound was also demonstrated to have higher cytotoxicity against the DU145 cell line than adriamycin, etoposide, or camptothecin. To further investigate the mechanism of action of these compounds, docking studies to the ATP-binding domain of topoisomerase II α were carried out for **U** (Figure 4.10).¹⁹⁰

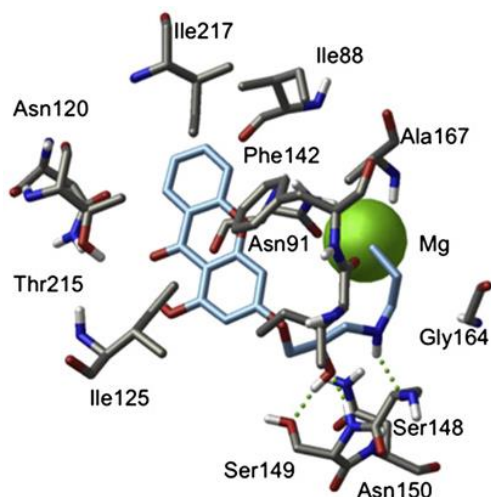


Figure 4.10. Molecular docking between compound **U** and ATP-binding of human topoisomerase II α . The ATP-binding domain topoisomerase II α is shown as a ribbon diagram in which the green sphere is the Mg²⁺ in the ATP-binding site.¹⁹⁰

According to this result, the compound seems to bind to the ATP-binding site, since the xanthone ring overlapped well with that of the purine ring of the ATP. Furthermore, in this way the compound could form hydrophobic interactions with Asn91, Asn95, Asn120, Phe142, Thr215, and Ile217. In addition, the functional groups in the side chain showed other interactions: the secondary amine group formed a hydrogen bond with Ser148, while the hydroxyl group with Ser149. To confirm these results, the ATP hydrolysis assay was used. Compound **U** did not show strong inhibition of the ATPase activity. These revealed that other mechanisms may be involved in addition to binding the ATPase domain.¹⁹⁰

On the basis of the molecular docking study of compound **U** with human topoisomerase II α ATP-binding domain, in 2013 Park and co-workers designed and synthesized a series of xanthone derivatives.¹⁰⁸ In particular, they introduced in position 3 of the xanthone core different alkyl chains with the aim to study the hydrophobic interaction effect of compounds with ATP binding site of the enzyme. All the synthesized compounds showed strong human topoisomerase II α inhibitor activity and weak topoisomerase I inhibitory activity. Among them, compound **Y** (Figure 4.11) resulted the most potent derivative of the series, showing a stronger inhibition in comparison to compound **U** (Figure 4.9).

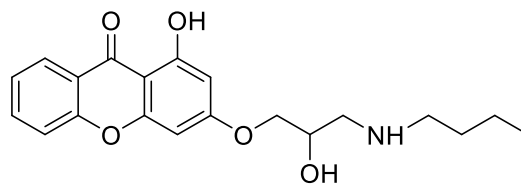


Figure 4.11. Structure of compound **Y**.

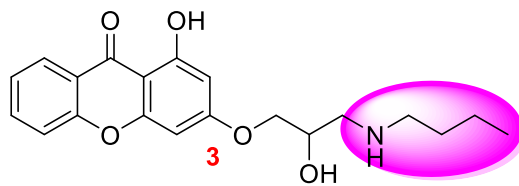
In terms of IC_{50} they found for compound **Y** an IC_{50} value of $9.0 \pm 0.08 \mu\text{M}$. This finding suggests that enhancing of the topoisomerase II inhibition is related to the length of the side chain by adding a methylene group from compound **U**.¹⁰⁸ During this study, compound **Y** was further examined to inhibit human topoisomerase II α -mediated ATP hydrolysis. It inhibited ATP hydrolysis by $23.9 \pm 1.0\%$ at $300 \mu\text{M}$ which is 2.7 times less active than novobiocin (reported as topoisomerase II α catalytic inhibitor through preventing ATP from binding to ATP-binding site of the enzyme.^{85, 108} Data collected from DNA intercalation and ATP competition assays confirmed that compound **Y** was a potent DNA intercalator and an ATP-competitive human topoisomerase II catalytic inhibitor at low concentration.¹⁰⁸

4.2 Drug design

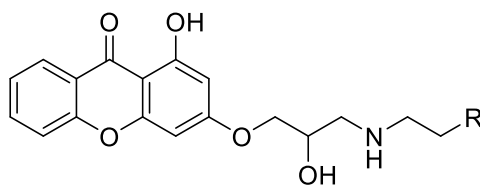
The design and synthesis of new anticancer agents is one of the most active areas in medicinal chemistry. Topoisomerase II is widely studied for cancer treatment. Unfortunately, the therapeutic activity of most anticancer drugs in clinical use is limited by their general toxicity to proliferating cells, including some normal cells. Targeted strategies that have now been developed, specifically disrupt a biological pathway by inducing the neoplastic transformation in the cells. As mentioned above, many are the strategies on the development of small molecule anticancer drugs for targeted therapy. Among them, conjugation of drugs with polyamine can be used as delivery tools to transport these polyamine analogues. Thus far, F14512 is the most promising anticancer drug currently in clinical trials.

In the search of new antitumor compounds more selective towards cancer cells, we designed, synthesised and characterized novel xanthone-polyamine conjugate derivatives. Recent studies suggested that the inhibition of topoisomerase II α by xanthone derivatives

may be more complex. First, all the ATPase studies reported for xanthone-based compound were carried out in the presence of DNA.^{108, 180, 190} Because the ATPase activity of type II topoisomerases is stimulated by DNA binding and strand passage, interference with DNA interactions could manifest itself as an indirect inhibition of ATP hydrolysis. Second, many xanthone-based compounds bind to DNA.^{108, 181} Thus, they may be able to interact with the DNA cleavage/ligation active site of type II topoisomerases. Third, some previously described xanthone derivatives display an IC₅₀ for inhibition of ATP hydrolysis that is >10-fold higher than observed for the inhibition of relaxation.^{108, 190} This makes it unlikely that the loss of overall catalytic activity could have resulted from interference with ATP interactions. Fourth, some xanthone-based compounds inhibit the DNA relaxation reaction of topoisomerase I. This is despite the fact that the type I enzyme has no binding site for ATP.¹⁹¹ Starting from the results obtained from Park¹⁰⁸ and co-workers, based on the structure activity relationship (SAR) studies, we synthesized a series of new xanthone polyamine conjugates, **2-7**. The aim of this project was to further examine the mechanism by which xanthenes inhibit topoisomerase II α . The *N*-butylamine linked in position 3 of the xanthone core of compound **1**, described above as compound **Y**, has been substituted with different polyamine moieties, including propanediamine (compound **2**), butanediamine (compound **3**), spermidine (compound **4**), spermine (compound **5**), and compound **6** and **7** where the number of the methylene groups between the two inner nitrogens has been changed (Figure 4.12). These polyamines were chosen because a previous study found that the presence of a secondary amine group in the side chain plays an important role in mediating topoisomerase II-drug interactions.^{102, 165, 171} Furthermore, the addition of a spermine side chain to the core of etoposide (generating F14512) greatly enhanced the ability of the drug to act as a topoisomerase II poison and to be taken up by cancer cells with active polyamine transport systems.^{102, 165, 171}



Compound 1



Compound 2: R = CH₂NH₂;

Compound 3: R = CH₂CH₂NH₂;

Compound 4: R = CH₂NHCH₂CH₂CH₂CH₂ NH₂;

Compound 5: R = CH₂NHCH₂CH₂CH₂CH₂NHCH₂CH₂CH₂ NH₂;

Compound 6: R = CH₂NHCH₂CH₂CH₂NHCH₂CH₂CH₂ NH₂;

Compound 7: R = CH₂NHCH₂CH₂NHCH₂CH₂CH₂ NH₂;

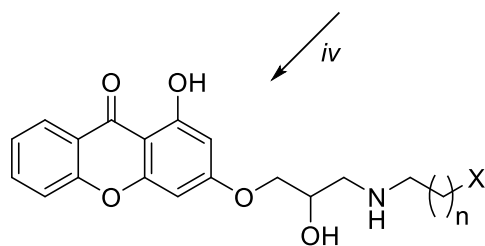
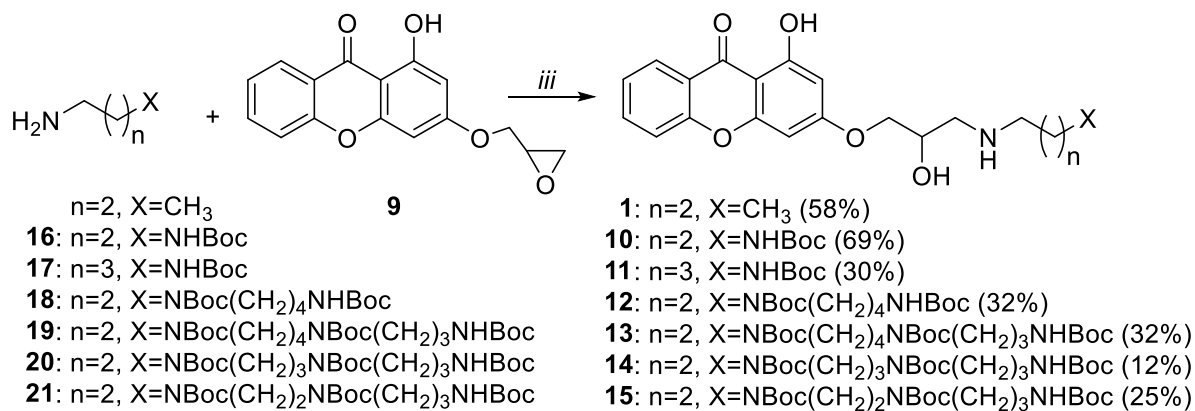
Figure 4.12. Structures of compounds 1-7.

4.3 Methods

4.3.1 Chemistry

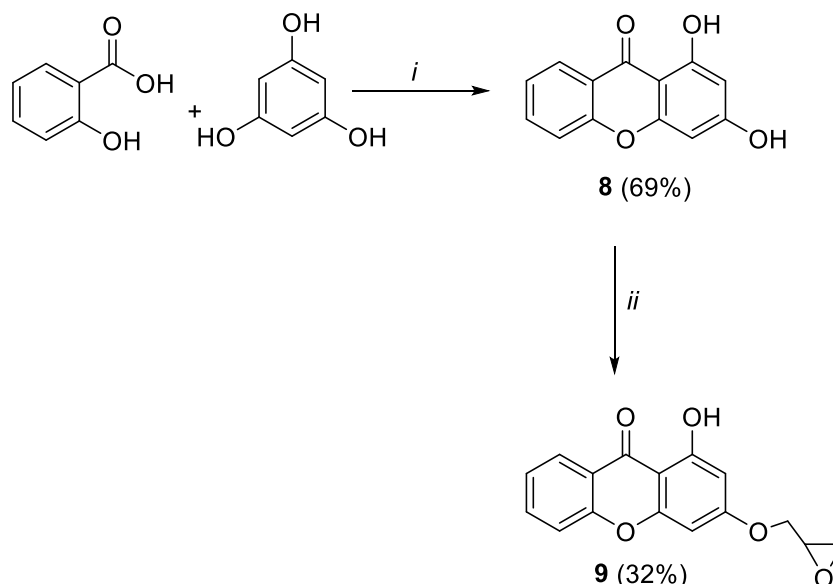
Compounds **2-7** were synthesized as hydrochloride and trifluoroacetate salts, as described in Scheme 4.1, by coupling the common intermediate 1-hydroxy-3-(oxiran-2-ylmethoxy)-9H-xanthen-9-one (**9**) with the appropriate *N*-Boc protected polyamine (**16-21**). The key intermediate **8** was obtained according to the synthetic strategy reported in literature, named Grover, Shah and Shah reaction. It required the presence of salicylic acid and phloroglucinol that were heated together with zinc chloride in phosphoryl chloride as solvent (Scheme 4.2).^{192, 193} Alkylation of **8** with commercially available epichlorohydrin in *N,N*-dimethyl formamide (DMF) was carried out and optimized by microwave assisted synthesis, shortening time reaction and leading to the epoxide chain (Scheme 4.2). The resulting oxirane derivative **9** was then conjugated with the appropriate *N*-Boc protected

polyamines. Since the ambient of reaction is basic, due the presence of the polyamine, the nucleophilic attack was at the least substituted position of the epoxide. Finally, the intermediates **10-15** were deprotected through acidic hydrolysis to give the final compounds **2-7**. The reference compound **1** was synthesized following the same synthetic procedure by coupling the intermediate **9** with butylamine. The diamine **17**, such as the polyamines **18-21** were synthesized according to reported in literature.¹⁶⁹⁻¹⁷¹ 1,3-diaminopropane was selectively protected at one of the two primary amine groups using Boc₂O to afford **16**.



- 2:** $n=2$, $\text{X}=\text{NH}_2$ (36%)*
3: $n=3$, $\text{X}=\text{NH}_2$ (45%)**
4: $n=2$, $\text{X}=\text{NH}(\text{CH}_2)_4\text{NH}_2$ (60%)**
5: $n=2$, $\text{X}=\text{NH}(\text{CH}_2)_4\text{NH}(\text{CH}_2)_3\text{NH}_2$ (33%)*
6: $n=2$, $\text{X}=\text{NH}(\text{CH}_2)_3\text{NH}(\text{CH}_2)_3\text{NH}_2$ (26%)*
7: $n=2$, $\text{X}=\text{NBoc}(\text{CH}_2)_2\text{NH}(\text{CH}_2)_3\text{NH}_2$ (38%)*

Scheme 4.1. Reagents and conditions: (iii) DMF, 50°C, 26 hours; (iv) CF_3COOH , CH_2Cl_2 , 0°C, 2 hours or HCl 4M in dioxane, 0°C, 2-5 hours. Boc=(CH_3)₃COCO. * = Hydrochloride salt; ** = Trifluoroacetate salt.



Scheme 4.2. Reagents and conditions: (i) ZnCl_2 , POCl_3 , 70°C , 3 hours; (ii) epichlorohydrin, K_2CO_3 , DMF, 80°C , 5 hours, MW.

4.3.2 Biology

Compounds **1-5** were selected to study their mechanism of action. The intermediate **8** was studied to validate the role of the side chain in position 3 of the xanthone core. Recombinant wild-type human topoisomerase II α was expressed in *Saccharomyces cerevisiae* JEL-1 Δ top1 and purified as described previously.¹⁹⁴⁻¹⁹⁶ The enzyme was stored at -80°C as a 1.5 mg/mL stock in 50 mM Tris-HCl, pH 7.9, 0.1 mM NaEDTA, 750 mM KCl, and 40% glycerol. Negatively supercoiled pBR322 DNA was prepared from *Escherichia coli* using a Plasmid Mega Kit (Qiagen) as described by the manufacturer and exonuclease treated to clean pBR322 of any chromosomal DNA contaminants. Relaxed pBR322 was prepared from supercoiled plasmid by incubation with topoisomerase I as described previously.¹⁹⁷ Kinetoplast DNA (kDNA) from *Crithidia fasciculata* was prepared as described previously.¹⁹⁸ Analytical grade etoposide was purchased from Sigma-Aldrich. [γ - ^{32}P]ATP (3000 Ci/mmol stock) was from Perkin Elmer.

4.3.3 Computational study

To obtain more details about the binding mode of these compounds, a docking study on compound **4** was assessed. The topoisomerase II DNA cleavage complex was prepared

with Protein Wizard¹⁹⁹ using the Protein Data Bank (PDB) 3QX3 (solved at 2.16 Å resolution).⁹⁸

4.4 Results and discussion

As a first step toward characterizing the activities of the xanthone derivatives against human topoisomerase II α , the effects of compounds **1-5** and **8** on enzyme-mediated DNA cleavage were determined (Figure 4.13). Consistent with previous reports^{108, 180, 190}, none of them displayed a significant ability to enhance DNA cleavage. Furthermore, was analysed the effect of compound **5** against human topoisomerase II β , *Mycobacterium tuberculosis* gyrase, *Bacillus anthracis* topoisomerase IV, and on *Escherichia coli* topoisomerase IV (data not shown). In all cases, the drug did not increase the concentration of cleavage complex with human and bacterial enzymes. Thus, these xanthone derivatives do not appear to act primarily as topoisomerase II poisons.

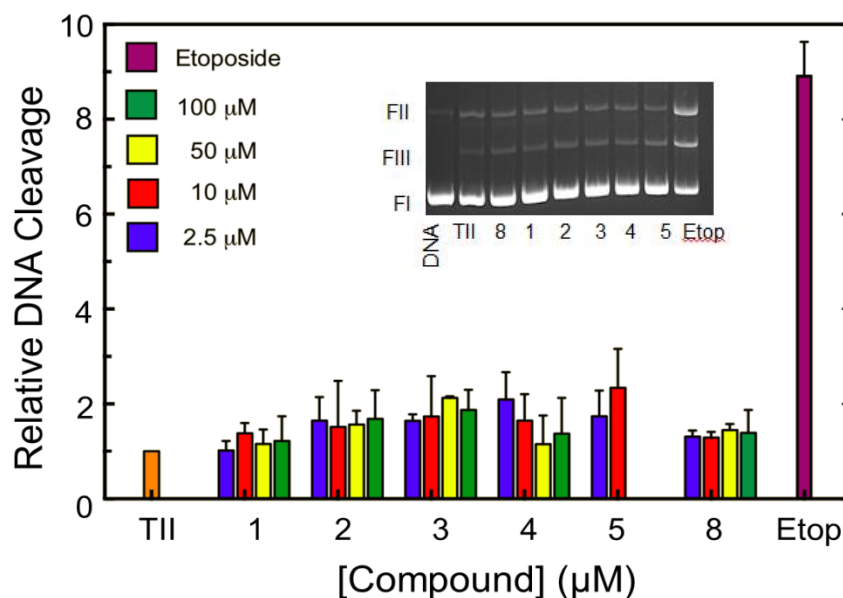


Figure 4.13. Effects of xanthone derivatives on DNA cleavage mediated by topoisomerase II α . Results for compounds **1-5** and **8** (2.5 µM, blue; 10 µM, red; 50 µM, yellow; 100 µM, green) on the generation of enzyme-mediated double-stranded DNA breaks are shown. Due to solubility issues, compound **5** was only used up to 10 µM. DNA cleavage in the presence of 100 µM etoposide (purple) is shown for comparison. DNA cleavage levels were calculated relative to control reactions that contained no drug (TII, orange) and were set to 1. Error bars represent standard deviations for 2-3 independent experiments. The inset shows an ethidium bromide-stained gel of a typical DNA cleavage experiment carried out in the presence of 10 µM compounds **1-5** and **8** and 100 µM etoposide. The positions of negatively supercoiled (form I, FI), nicked (form II, FII) and linear (form III, FIII) DNA are indicated.

Next, we examined the abilities of compounds **1-5** and **8** to inhibit the overall catalytic activity of topoisomerase II α using a DNA relaxation assay (Figure 4.14). All the compounds inhibited DNA relaxation and fell into three groups regarding potency: compounds **2** and **5** displayed an IC₅₀ \approx 1 μ M, compounds **3** and **4** displayed an IC₅₀ \approx 2.5-5 μ M, and compounds **1** and **8** displayed an IC₅₀ \approx 100 μ M. These results notwithstanding, it should be noted that a previous study reported that compound **1** displayed an IC₅₀ \approx 9 μ M for the inhibition of DNA relaxation catalyzed by topoisomerase II α .¹⁰⁸ We could not recapitulate this finding in the present study.

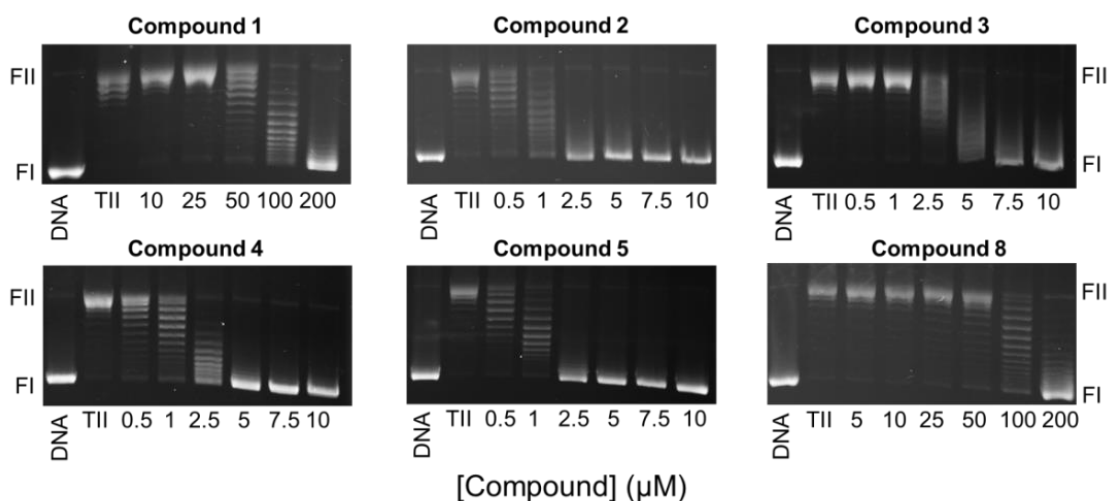


Figure 4.14. Effects of xanthone derivatives on DNA relaxation catalyzed by topoisomerase II α . Results for compounds **1-5** and **8** are shown. Assays containing intact negatively supercoiled DNA in the absence of topoisomerase II α (DNA) or negatively supercoiled DNA treated with topoisomerase II α in the absence of xanthone derivatives (TII) are shown as controls. The positions of negatively supercoiled (form I, FI) and nicked (form II, FII) DNA are indicated. Gels are representative of 2-4 independent experiments.

Given the low activity of compound **1** in our hands and the fact that the activity of compound **3** was similar to other derivatives we tested, we focused on compounds **2** and **4**, **5** and **8** for more detailed studies. The ability of xanthone derivatives to inhibit the catalytic activity of topoisomerase II α was confirmed using a decatenation assay (Figure 4.15). Although IC₅₀ values were \sim 2- to 3- fold higher than observed in the relaxation assay, the order of potency remained similar, with compounds **2**, **4**, **5** being much more potent than compound **8**. Polyamines have the potential to bind to the double helix and alter topoisomerase II-DNA interactions in the absence of a specific interaction with the

enzyme.²⁰⁰⁻²⁰² Consequently, it is possible that the xanthone derivatives inhibit the activity of topoisomerase II α in a bimodal fashion with the aromatic core of one molecule binding to the protein and the polyamine tail of another acting through a general effect on the DNA. Therefore, the importance of the linkage between the spermidine/spermine polyamine tails and the xanthone core (compound **8**) in a single molecule was examined.

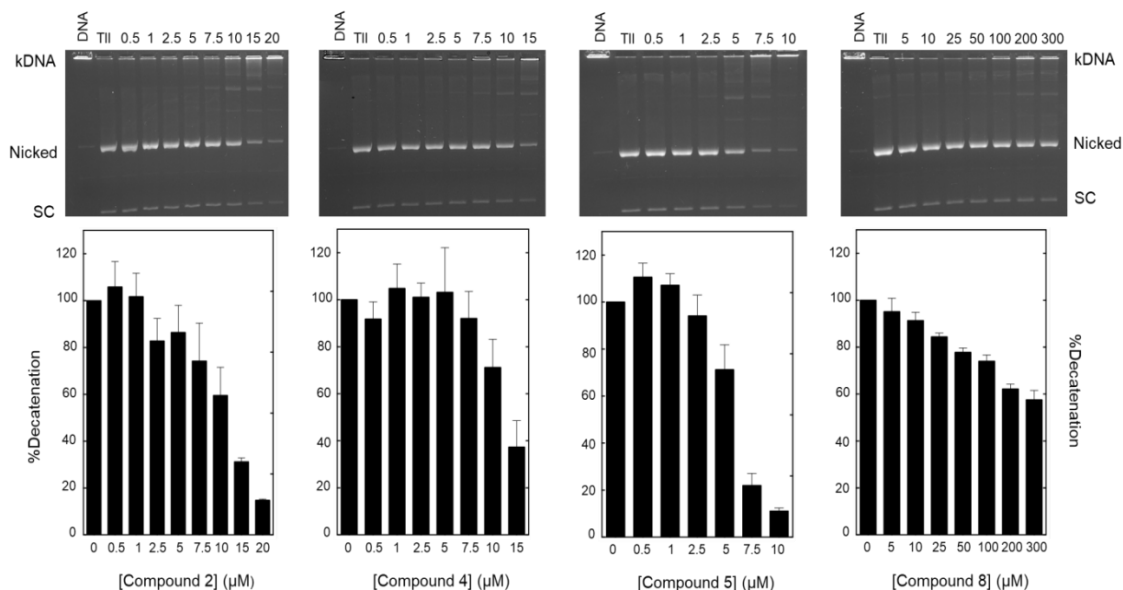


Figure 4.15. Effects of xanthone derivatives on DNA decatenation catalyzed by topoisomerase II α . Results for compounds **2**, **4**, **5** and **8** are shown. Assays containing intact kDNA in the absence of topoisomerase II α (DNA) or kDNA treated with topoisomerase II α in the absence of xanthone derivatives (TII) are shown as controls. The positions of intact kDNA at the origin (kDNA), decatenated nicked kDNA minicircles, and decatenated supercoiled (SC) kDNA minicircles are indicated. Gels are representative of 3 independent experiments. Quantification of results is shown in the bar graphs at the bottom. Levels of decatenation in the absence of xanthone derivatives was set to 100%. Error bars represent standard deviations for 3 independent experiments.

Independently, the IC₅₀ values for the inhibition of DNA relaxation by topoisomerase II α for spermidine and spermine were > 1 mM (data not shown) and that of compound **8** was >100 μM. As seen in Figure 4.16, a 1:1 mixture of compound **8** and spermidine or spermine showed no ability to inhibit DNA relaxation at 10 μM. This is compared to compounds **4** and **5** (which are essentially compound **8** coupled to spermidine and spermine, respectively), that displayed IC₅₀ values < 5 μM. Thus, the linkage between the xanthone core and the polyamine tails is critical for the potent inhibitory activity of these compounds.

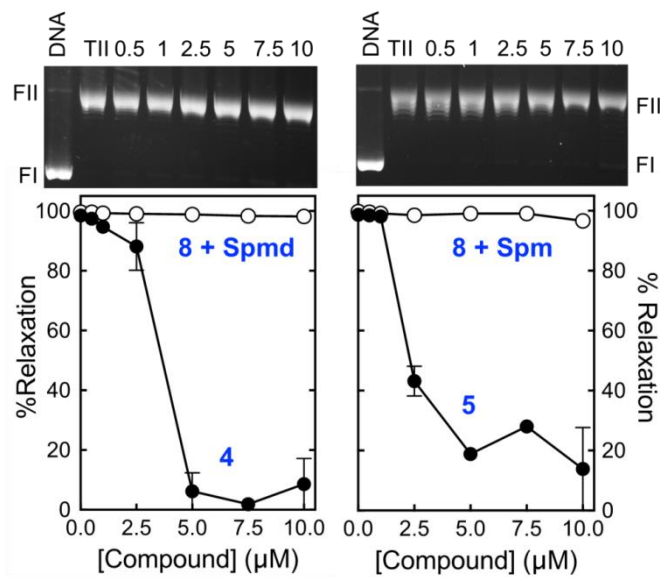


Figure 4.16. Covalent linkage of the C₃ polyamine moiety to the 1,3-dihydroxy-9h-xanthen-9-one core is necessary for the inhibition of DNA relaxation catalyzed by topoisomerase II α . The effects of a 1:1 mixture of 1,3-dihydroxy-9h-xanthen-9-one (compound **8**) + spermidine (left panel) or + spermine (right panel) on the DNA relaxation activity of human topoisomerase II α is shown. Assays containing intact negatively supercoiled DNA in the absence of topoisomerase II α (DNA) or negatively supercoiled DNA treated with topoisomerase II α in the absence of xanthone derivatives (TII) are shown as controls. The positions of DNA markers are as shown in Figure 4.14. Gels are representative of 2 independent experiments. Quantification of results is shown in the graphs at the bottom. Data for compound **8** + spermidine (Spmd, left) and compound **8** + spermine (Spm, right) are shown as open circles. Control reactions in the presence of compound **4** (left) and **5** (right) are shown as closed circles. Error bars represent standard error of the means for 2 independent experiments.

As discussed above, the mechanism by which a compound inhibits the activity of topoisomerase II can have profound cellular consequences. Thus, it is important to understand which step of the topoisomerase II catalytic cycle is affected by xanthenes. This catalytic cycle can be divided into six discrete steps: 1) DNA binding, 2) DNA bending, 3) DNA cleavage, 4) strand passage, 5) DNA religation, 6) release of the DNA substrate and enzyme turnover.^{12, 13, 60} ATP binding drives the strand passage step and ATP hydrolysis is required for enzyme turnover and the completion of the catalytic cycle.^{12, 13, 47, 74}

To determine whether the xanthone derivatives affect topoisomerase II activity at steps up to and including DNA scission, we reassessed the effects of the compounds **2**, **4**, **5** and **8** on enzyme-mediated DNA cleavage (Figure 4.17). Normally, topoisomerase II α maintains very low levels of cleavage complexes in the presence of Mg²⁺, its physiological divalent cation.⁶⁴ This makes it difficult to determine the ability of the drug to inhibit this reaction

step. Consequently, the experiments shown in Figure 4.16 were carried out in the presence of Ca^{2+} , which raises baseline levels of DNA cleavage ~10- to 15-fold.⁶⁴ No substantial inhibition was observed for xanthone concentrations up to 10 μM , the range in which compounds inhibited overall catalytic activity. This finding strongly suggests that these compounds do not impair the overall catalytic activity (DNA relaxation or decatenation) of topoisomerase II α by inhibiting any of the reaction steps through DNA cleavage. However, this conclusion comes with the caveat that the DNA cleavage assay utilizes 150 nM enzyme as compared to the relaxation assay, which uses 3 nM. Thus, it could take higher concentrations of xanthone derivatives to inhibit the catalytic activity of topoisomerase II α under conditions of the cleavage assay.

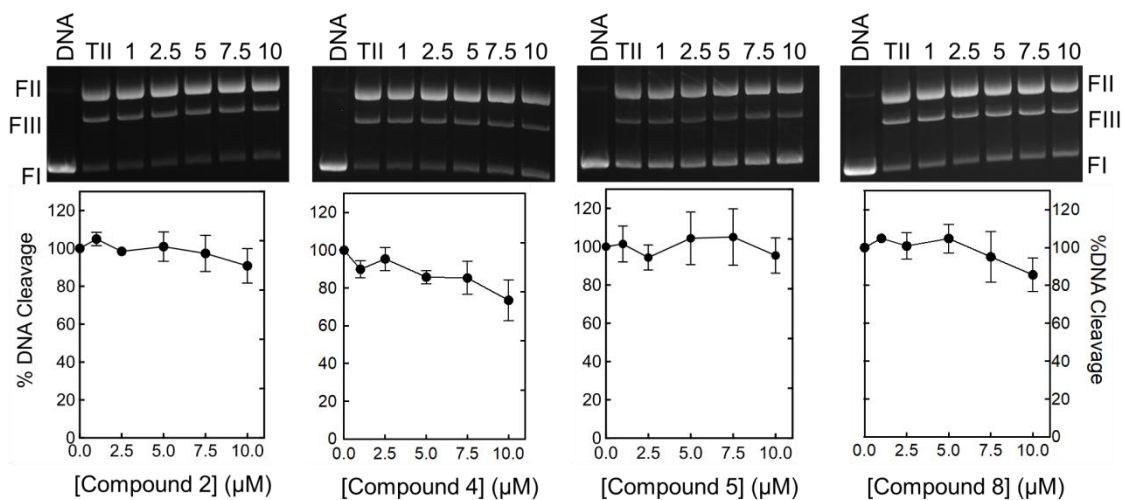


Figure 4.17. Inhibition of topoisomerase II α -mediated DNA cleavage by xanthone derivatives. Results for compounds **2**, **4**, **5** and **8** are shown. Reactions were carried out in the presence of CaCl_2 to enhance baseline levels of DNA cleavage by the enzyme. Assays containing negatively supercoiled DNA in the absence of topoisomerase II α (DNA) or negatively supercoiled DNA treated with topoisomerase II α in the absence of xanthone derivatives (TII) are shown as controls. The positions of DNA markers are as shown in Figure 4.13 inset. Gels are representative of 3 independent experiments. Quantification of results is shown in the graphs at the bottom. Levels of DNA cleavage in the absence of xanthone derivatives was set to 100%. Error bars represent standard deviations for 2-3 independent experiments.

Therefore, as a control, the effects of compounds **2**, **4**, **5** and **8** on DNA relaxation catalyzed by 150 nM topoisomerase II α were determined (Figure 4.18). Similar to the results of Figure 4.14, compounds **2**, **4**, and **5** displayed complete (or near complete) inhibition of enzyme activity by 10 μ M. (Note that 10 μ M compound **8** displayed no ability to inhibit DNA relaxation under either assay condition). Taken together, the results shown in Figures 4.17 and 4.18 indicate that the xanthone derivatives act by inhibiting topoisomerase II α in a reaction step that follows DNA cleavage.

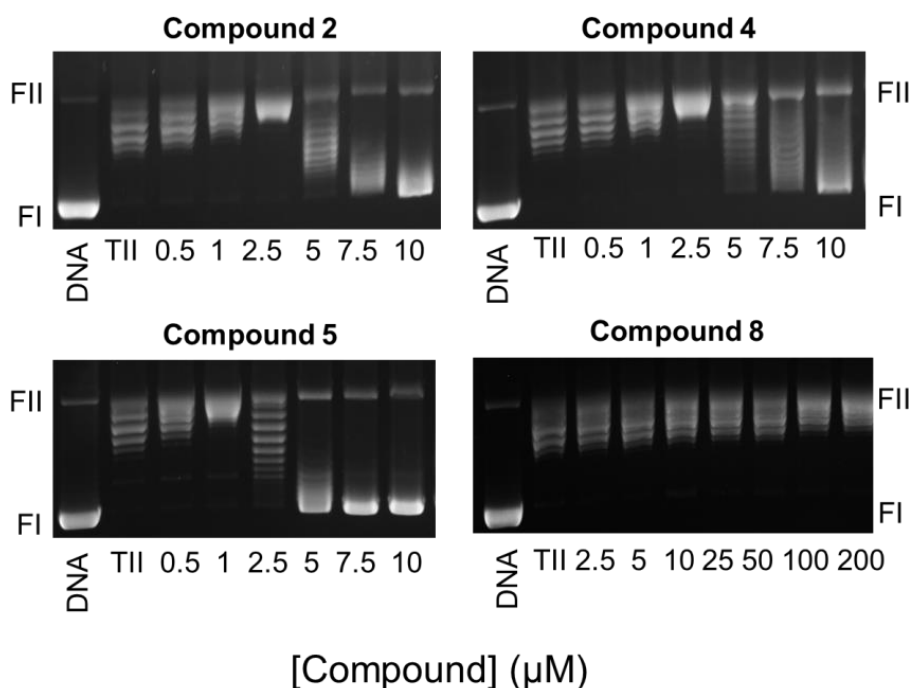


Figure 4.18. Effects of xanthone derivatives on DNA relaxation catalyzed by high concentrations of topoisomerase II α . Results for compounds **2**, **4**, **5** and **8** are shown. Assays containing intact negatively supercoiled DNA in the absence of topoisomerase II α (DNA) or negatively supercoiled DNA treated with topoisomerase II α in the absence of xanthone derivatives (TII) are shown as controls. The positions of DNA markers are as in Figure 4.14. Gels are representative of 2-4 independent experiments.

Consequently, we examined the effects of compounds **4**, and **5** on DNA strand passage mediated by the enzyme (Figure 4.19). A DNA catenation assay was employed that utilizes a high concentration (150 nM) of topoisomerase II α and replaces the ATP cofactor with the non-hydrolyzable analogue, APP(NH)P. Because APP(NH)P cannot be hydrolyzed by topoisomerase II α , this assay monitors enzyme activity through the strand passage step.⁶⁰

By using a DNA catenation assay, a single catalytic event moves the DNA substrate away from the bands of relaxed DNA. Relaxed, rather than negatively supercoiled, DNA was used for this assay because it is a preferred substrate for catenation. Similar to the results in Figure 4.18, compounds **4** and **5** all displayed IC₅₀ values < 10 μM. Because these compounds showed little ability to inhibit DNA cleavage (Figure 4.17), the step that immediately precedes the strand passage step, we conclude that the xanthone derivatives decrease the overall catalytic activity of topoisomerase II α by inhibiting the ability of the enzyme to carry out DNA strand passage.

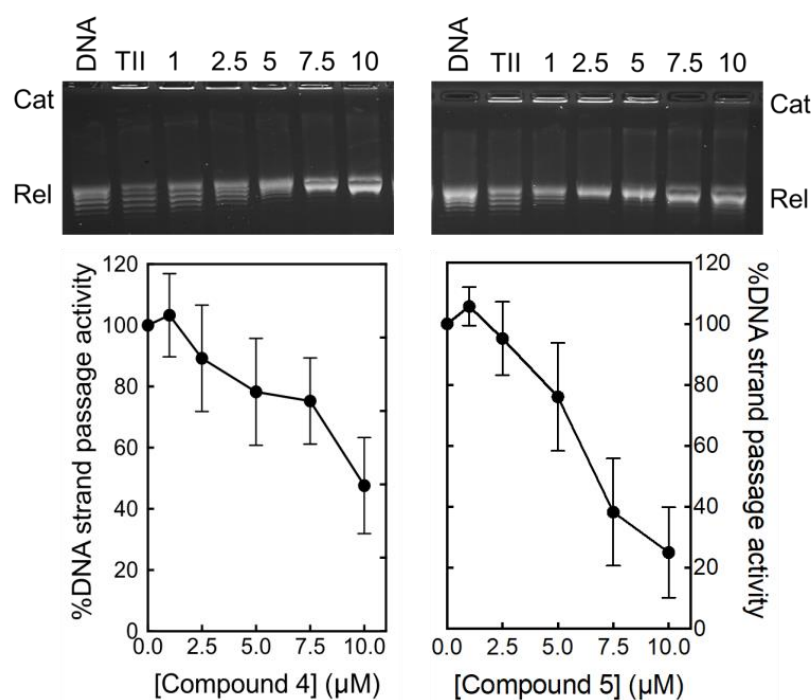


Figure 4.19. Effects of xanthone derivatives on DNA strand passage mediated by topoisomerase II α . Results for compounds **4**, and **5** are shown. Assays monitored the catenation of relaxed DNA in the presence of the non-hydrolysable ATP analogue APP(NH)P so that the enzyme could only carry out one round of DNA strand passage. Assays containing relaxed DNA in the absence of topoisomerase II α (DNA) or relaxed DNA treated with topoisomerase II α in the absence of xanthone derivatives (TII) are shown as controls. The positions of relaxed DNA (Rel) and catenated DNA at the origin (Cat) are indicated. Gels are representative of at least 3 independent experiments. Quantification of results is shown in the graphs at the bottom. Levels of catenation in the absence of xanthone derivatives was set to 100%. Error bars represent standard deviations for at least 3 independent experiments.

Xanthenes can inhibit the strand passage step in three different ways: they can bind at the ATP active site and interfere with topoisomerase II α -ATP interactions, they can bind at the DNA cleavage/ligation active site and interfere directly with DNA movement, or they may

bind outside of either active site and cause deleterious conformational changes in the enzyme. On the basis of modeling studies and the ability of compounds to inhibit enzyme-catalyzed ATP hydrolysis, previous studies suggested that xanthone derivatives acted by inhibiting topoisomerase II α -ATP interactions.^{108, 180, 190} Therefore, we assessed the effects of compound **4** on ATP hydrolysis catalyzed by topoisomerase II α . As seen in Figure 4.20, compound **4** inhibited ATP hydrolysis with an IC₅₀ \approx 10 μ M. However, as with earlier studies, ATPase assay mixtures contained DNA. As discussed above (and shown in Figure 4.20), rates of ATP hydrolysis are stimulated \sim 5-fold by the presence of DNA.

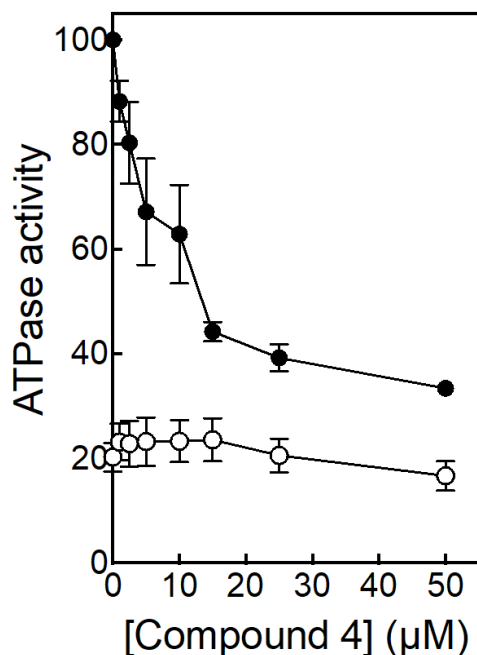


Figure 4.20. Effects of compound **4** on ATP hydrolysis catalyzed by topoisomerase II α . Assays carried out in the presence or absence of negatively supercoiled DNA are shown as closed or open circles, respectively. ATPase activity in the presence of DNA and in the absence of compound **4** was set to 100%. Error bars represent standard error of the means for 2 independent experiments.

Thus, decreased rates of ATP hydrolysis observed in the presence of compound **4** could be due to interactions of the xanthone derivative at either the DNA or ATP sites. In order to distinguish between these two possibilities, the effects of compound **4** on ATP hydrolysis were examined in the absence of DNA (Figure 4.20).

Under this condition, no inhibition was observed up to 50 μM xanthone. Thus, we conclude that the xanthone-induced decrease in the rate of ATP hydrolysis in the presence of DNA is not due to a direct inhibition of ATP binding. Rather, it is observed because xanthone derivatives inhibit the ability of DNA to stimulate the rate of ATP hydrolysis. Consistent with this conclusion, ATPase rates generated in the presence of supercoiled plasmid asymptotically approached those seen in the absence of DNA as the concentration of compound **4** increased (Figure 4.20).

To further define the site of interaction of xanthone derivatives on topoisomerase II α , we used a competition assay to determine whether these compounds could be inhibiting DNA strand passage (and ATP hydrolysis) by acting at the DNA cleavage/ligation active site. The competition assay determined the ability of compounds **2**, **4** and **5** (which do not inhibit the DNA cleavage step) to block DNA cleavage enhancement by etoposide. This drug has been shown to bind at the DNA cleavage/ligation active site of human type II topoisomerases.⁹⁸ As seen in Figure 4.21, all three compounds competed with etoposide, diminishing the ability of the anticancer drug to induce topoisomerase II α -mediated DNA scission.²⁰⁴

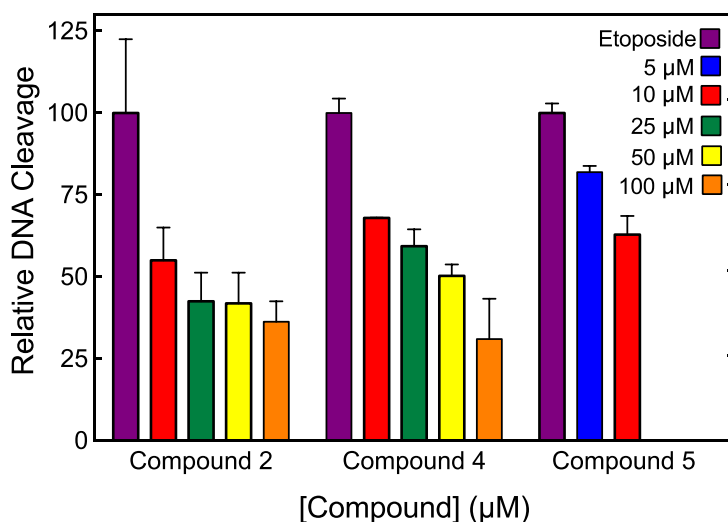


Figure 4.21. Ability of xanthone derivatives to inhibit the enhancement of topoisomerase II α -mediated DNA cleavage by 100 μM etoposide. Results for compounds **2**, **4**, and **5** (5 μM , blue; 10 μM , red; 25 μM , green; 50 μM , yellow; 100 μM , orange) on the generation of enzyme-mediated double-stranded DNA breaks are shown. Due to solubility issues, compound **5** was only used up to 10 μM . DNA cleavage in the presence of 100 μM etoposide (purple) in the absence of xanthone derivatives set to 100%. Error bars represent standard deviations for 2-3 independent experiments.

These data strongly suggest that the xanthone derivatives interact near the DNA cleavage/ligation active site of the human type II enzyme, even though they have little effect on the cleavage reaction. A similar conclusion has been drawn for the binding of some quinolone-derivatives that do not enhance DNA cleavage to eukaryotic or prokaryotic type II topoisomerases.^{205, 206} Finally, to determine the feasibility of xanthone binding at the cleavage/ligation active site of topoisomerase II α , compound **4** was docked into the topoisomerase II cleavage complex by molecular modeling (Figure 4.22). Results suggest that the heterocyclic moiety of the xanthone derivative preferentially locates in a region similar to that of the 4'-demethylepipodophyllotoxin core of etoposide.⁹⁸ The polyamine chain extends toward the DNA major groove, as was observed in previous computations of F14512 and other polyamine-conjugates.¹⁷¹ Compound **4** has the potential to form several favorable interactions with both the enzyme and the DNA. The hydroxyl group along the polyamine chain points toward Gln778, while the central nitrogen atom is in close enough proximity to form hydrogen bonds with the backbone of either Lys814 or Ala816. The terminal amine is stabilized by the DNA, as it lays in between the phosphates of DNA bases C₊₃ and A₊₄.²⁰⁴

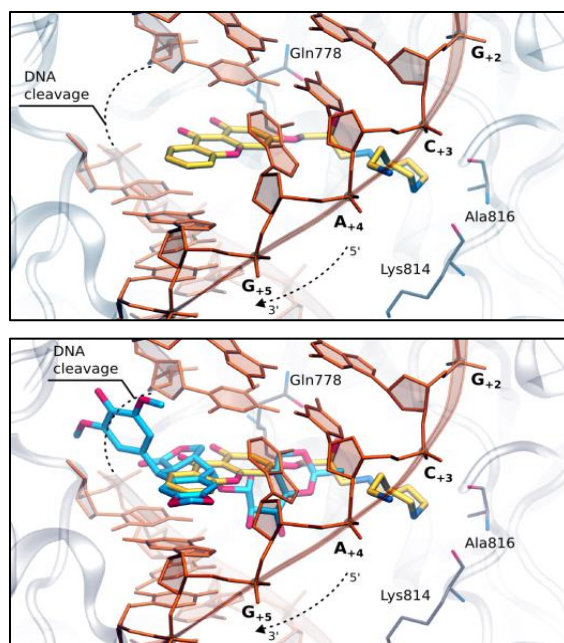


Figure 4.22. Molecular modeling of compound **4**. Docking of compound **4** (yellow) into the DNA cleavage/ligation active site of topoisomerase II α (Top). Superposition between etoposide (blue; PDB 3QX3) and the docking pose of compound **4** into the topoisomerase II DNA cleavage complex (Bottom).

4.5 Conclusion

Results of the present study indicate that xanthone derivatives represent a potent class of topoisomerase II inhibitors with anticancer potential. Previously, these compounds were believed to inhibit enzyme activity by interfering with the binding of the high-energy ATP cofactor. Compounds **2-5** showed a high inhibitory activity in the submicromolar range against topoisomerase II α , resulting more potent than their parent compound **1**. From these results, it appears that the presence of the side chain containing a primary and secondary amine is critical. However, the number of secondary amines in the chain and their distance from the primary amine appear to be less important. Also, important proof of its significance is that they all showed very similar values of IC₅₀. However, these evidences strongly suggest that xanthone-polyamine conjugates act at the DNA cleavage/ligation active site of human topoisomerase II α and impair catalytic activity by blocking the DNA strand passage step of the topoisomerase II catalytic cycle.

4.6 Experimental section

4.6.1 Chemistry

Chemical reagents were purchased from Sigma Aldrich. All reactions were performed with dry glassware under a nitrogen atmosphere unless otherwise noted. Nuclear magnetic resonance spectra (NMR) were recorded at 400 MHz for ¹H and 100 MHz for ¹³C on Varian VXR 400 spectrometer in CDCl₃, DMSO or CD₃OD as solvents. Chemical shifts (δ) are given in ppm from tetramethylsilane (TMS) with the solvent resonance as internal standard (CDCl₃: δ 7.26, DMSO: δ 2.50, CD₃OD: δ 3.31 for ¹H-NMR and CDCl₃: δ 77.16, DMSO: δ 39.52, CD₃OD: δ 49.00 for ¹³C-NMR). For ¹H-NMR, data are reported as follows: chemical shift, multiplicity (s = singlet, d = doublet, dd = double of doublets, t = triplet, q = quartet, m = multiplet, br s = broad singlet), coupling constants (Hz) and integration. Microwave assisted synthesis was performed by using CEM Discover® SP apparatus (2.45 GHz, maximum power of 300W). Electron spray ionization (ESI) mass spectra were recorded on Varian VG 7070E instrument. Chromatographic separations were

performed on silica gel columns by flash or gravity column (Kieselgel 40, 0.040-0.063 mm; Merck) chromatography. Reactions were followed by thin-layer chromatography (TLC) on Merck (0.25 mm) glass-packed pre-coated silica gel plates (60 F254) that were visualized in an iodine chamber, or with a UV lamp, KMnO₄, or bromocresol green. All the names were attributed by Chem BioDraw Ultra 16.0.

1-hydroxy-3-(oxiran-2-ylmethoxy)-9H-xanthen-9-one (9)

Epichlorohydrin (0.14 mL, 1.751 mmol) was added to a suspension of 1,3-dihydroxy-9H-xanthen-9-one (**8**) (200 mg, 0.876 mmol) and K₂CO₃ (151 mg, 1.093 mmol) in dry DMF (10 mL). The mixture was stirred under microwave irradiation at 80 °C for 5 hours. After evaporating the solvent under reduced pressure, the crude compound was purified by gravity chromatography on silica gel column, eluting with CH₂Cl₂:MeOH (9.9:0.1) to yield the desired compound **9** as yellow solid (32%).

¹H NMR (400 MHz, DMSO-*d*₆): δ 2.72 (q, *J* = 2.4 Hz, 1H), 2.85-2.88 (m, 1H), 3.35-3.37 (m, 1H), 3.96-4.10 (m, 1H), 4.53 (dd, *J*₁ = 11.2 Hz, *J*₂ = 2.4 Hz, 1H), 6.46 (d, *J* = 2 Hz, 1H), 6.70 (d, *J* = 2 Hz, 1H), 7.50 (t, *J* = 7.6, 1H), 7.63 (d, *J* = 8.4 Hz, 1H), 7.87-7.89 (m, 1H), 8.15-8.17 (m, 1H), 12.80 (br s, 1H exchangeable with D₂O).

General procedure for the synthesis of intermediates 10-15 and final compound 1

Intermediates (**16-21**) and butylamine (2.5-5 eq) were added to a solution of compound **9** (1 eq) in dry DMF (10 mL). Reaction mixtures were stirred for 26 hours at 50 °C, and the solvent was evaporated to yield the crude products **10-15** and **1**, respectively. These compounds were purified further by gravity column chromatography.

Tert-butyl (3-((2-hydroxy-3-((1-hydroxy-9-oxo-9H-xanthen-3-yl)oxy)propyl)amino)propyl)carbamate (10)

Compound **10** was synthesized from **9** (100 mg, 0.352 mmol) and **16** (306 mg, 1.759 mmol). The compound was eluted with CH₂Cl₂:MeOH: aq 33% NH₄OH (9:1:0.1), which afforded **10** as a yellow oil: 100 mg (69 %).

¹H NMR (400 MHz, DMSO-*d*₆): δ 1.36 (s, 9H), 1.51-1.54 (m, 2H), 2.53-2.55 (m, 1H), 2.59-2.67 (m, 2H), 2.91-2.98 (m, 2H), 3.05-3.07 (m, 1H), 3.84-3.94 (m, 1H), 4.00-4.04 (m,

1H), 4.11-4.16 (m, 1H), 6.40 (d, $J = 2\text{Hz}$, 1H), 6.45 (d, $J = 2\text{Hz}$, 1H), 6.78 (br s, 1H exchangeable with D_2O), 7.47-7.51 (t, $J = 7.2\text{Hz}$, 1H), 7.57-7.61 (m, 1H), 7.86-7.90 (m, 1H), 8.14-8.16 (m, 1H). $^{13}\text{C NMR}$ (100 MHz, CDCl_3): δ 212.61, 179.85, 165.95, 162.34, 157.05, 155.23, 135.64, 125.03, 124.29, 119.62, 117.49, 103.07, 97.33, 93.06, 79.50, 71.51, 67.63, 51.86, 46.68, 37.40, 29.56, 27.99 (3C).

Tert-butyl(4-((2-hydroxy-3-((1-hydroxy-9-oxo-9H-xanthen-3-yl)oxy)propyl)amino)butyl)carbamate (11)

Compound **11** was synthesized from **9** (100 mg, 0.352 mmol) and **17** (265 mg, 1.410 mmol). The compound was eluted with CH_2Cl_2 :MeOH: aq 33% NH_4OH (9:1:0.1), which afforded **11** as a yellow oil: 50 mg (30 %).

$^1\text{H NMR}$ (400 MHz, $\text{DMSO}-d_6$): δ 1.36 (s, 9H+2H), 1.40-1.44 (m, 2H), 2.50-2.54 (m, 1H), 2.58-2.62 (m, 1H), 2.65-2.69 (m, 1H), 2.81-2.96 (m, 2H), 3.04-3.06 (m, 1H), 3.91-3.92 (m, 1H), 4.01-4.05 (m, 1H), 4.13-4.15 (m, 1H), 6.41 (d, $J = 2\text{Hz}$, 1H), 6.65 (d, $J = 2\text{ Hz}$, 1H), 6.79 (br s, 1H exchangeable with D_2O), 7.49 (t, $J = 7.4\text{ Hz}$, 1H), 7.61 (d, $J = 8.4\text{ Hz}$, 1H), 7.88 (t, $J = 7.4\text{ Hz}$, 1H), 8.15 (d, $J = 7.6\text{ Hz}$, 1H). $^{13}\text{C NMR}$ (100 MHz, $\text{DMSO}-d_6$): δ 181.67, 179.85, 167.27, 163.91, 157.95, 154.50, 135.20, 125.90, 124.30, 120.57, 118.85, 101.07, 96.03, 90.41, 80.30, 69.00, 52.40, 45.38, 35.80, 29.03, 27.51 (3C), 26.79, 25.00.

Tert-butyl (4-((tert-butoxycarbonyl)amino)butyl)(3-((2-hydroxy-3-((1-hydroxy-9-oxo-9H-xanthen-3-yl)oxy)propyl)amino)propyl)carbamate (12)

Compound **12** was synthesized from **9** (100 mg, 0.352 mmol) and **18** (304 mg, 0.880 mmol). The compound was eluted with CH_2Cl_2 :MeOH: aq 33% NH_4OH (9:1:0.1), which afforded **12** as a yellow oil: 70 mg (32 %).

$^1\text{H NMR}$ (400 MHz, CDCl_3): δ 1.42 (s, 9H), 1.44 (s, 9H), 1.51-1.53 (m, 4H), 1.66-1.77 (m, 2H), 2.69-2.77 (m, 4H), 3.04-3.12 (m, 4H), 3.21-3.28 (m, 2H), 4.03-4.10 (m, 3H), 6.33 (d, $J = 2\text{ Hz}$, 1H), 6.44 (d, $J = 2\text{ Hz}$, 1H), 7.34-7.42 (m, 2H), 7.67-7.71 (m, 1H), 8.21-8.23 (m, 1H). $^{13}\text{C NMR}$ (100 MHz, CDCl_3): δ 179.96, 162.60, 162.20, 157.76, 156.09, 155.60, 154.50, 135.12, 125.91, 124.10, 120.66, 117.67, 114.90, 106.20, 101.50, 97.68, 93.31, 79.80, 79.50, 70.80, 51.69, 46.65, 46.20, 36.53, 31.49, 28.47 (6C), 27.49, 26.60.

Tert-butyl(4-((tert-butoxycarbonyl)(3-((tert-butoxycarbonyl)amino)propyl)amino)butyl)(3-((2-hydroxy-3-((1-hydroxy-9-oxo-9H-xanthen-3-yl)oxy)propyl)amino)propyl)carbamate (13)

Compound **13** was synthesized from **9** (100 mg, 0.352 mmol) and **19** (618 mg, 1.230 mmol). The compound was eluted with CH₂Cl₂:MeOH: aq 33% NH₄OH (9.2:0.8:0.1), which afforded **11** as a yellow oil: 88 mg (32 %).

¹H NMR (400 MHz, CDCl₃): δ 1.43 (s, 9H), 1.44 (s, 18H), 1.46-1.52 (m, 4H), 1.60-1.67 (m, 2H), 1.72-1.83 (m, 2H), 2.62-2.74 (m, 4H), 3.08-3.29 (m, 10H), 4.06-4.13 (m, 3H), 6.34 (d, *J* = 2 Hz, 1H), 6.44 (d, *J* = 2 Hz, 1H), 7.36 (t, *J* = 7.6 Hz, 1H), 7.41 (d, *J* = 8.8 Hz, 1H), 7.70 (t, *J* = 7.6 Hz, 1H), 8.22 (d, *J* = 7.6 Hz, 1H). **¹³C NMR** (100 MHz, CDCl₃): δ 180.87, 165.87, 163.59, 162.20, 157.76, 156.09 (2C), 154.50, 135.10, 125.92, 124.10, 120.69, 117.67, 114.90, 104.15, 101.50, 97.66, 93.35, 79.76 (3C), 70.99, 53.50, 51.77 (2C), 48.50, 46.86, 46.36, 39.90, 28.53 (9C), 26.14 (3C).

Tert-butyl (3-((tert-butoxycarbonyl)(3-((tert-butoxycarbonyl)amino)propyl)amino)propyl)(3-((2-hydroxy-3-((1-hydroxy-9-oxo-9H-xanthen-3-yl)oxy)propyl)amino)propyl)carbamate (14)

Compound **14** was synthesized from **9** (107 mg, 0.376 mmol) and **20** (644 mg, 1.318 mmol). The compound was eluted with CH₂Cl₂:MeOH: aq 33% NH₄OH (9.2:0.8:0.1), which afforded **14** as a yellow oil: 35 mg (12 %).

¹H NMR (400 MHz, CDCl₃): δ 1.41 (s, 9H), 1.44 (s, 18H), 1.70-1.75 (m, 6H), 2.63-2.68 (m, 2H), 3.06-3.34 (m, 12H), 4.04-4.17 (m, 3H), 6.32 (s, 1H), 6.42 (s, 1H), 7.32-7.38 (m, 2H), 7.68 (t, *J* = 7.6 Hz, 1H), 8.19 (d, *J* = 7.6, 1H). **¹³C NMR** (100 MHz, CDCl₃): δ 180.92, 165.87, 163.62, 157.79, 156.13, 155.90, 135.16, 125.95, 124.15, 120.71, 117.72, 104.19, 97.67, 93.38, 79.88(2C), 79.50, 71.04, 69.90, 54.92, 51.80, 48.20, 44.89, 29.80, 28.57(6C), 28.51.

Tert-butyl (2-((tert-butoxycarbonyl)(3-((2-hydroxy-3-((1-hydroxy-9-oxo-9H-xanthen-3-yl)oxy)propyl)amino)propyl)amino)ethyl)(3-((tert-butoxycarbonyl)amino)propyl)carbamate (15)

Compound **15** was synthesized from **9** (50 mg, 0.176 mmol) and **21** (292 mg, 0.616 mmol). The compound was eluted with CH₂Cl₂:MeOH: aq 33% NH₄OH (9:1:0.1), which afforded **14** as a yellow oil: 33 mg (25 %).

¹H NMR (400 MHz, CDCl₃): δ 1.42 (s, 9H), 1.45 (s, 18H), 1.60-1.90 (m, 4H), 2.61-2.77 (m, 2H), 3.02-3.16 (m, 1H), 3.25-3.29 (m, 11H), 4.05-4.13 (m, 2H), 4.14-4.26 (m, 1H), 6.33 (s, 1H), 6.43 (s, 1H), 7.35-7.41 (m, 2H), 7.65-7.77 (m, 1H), 8.21 (d, *J* = 7.6 Hz, 1H). **¹³C NMR** (400 MHz, CDCl₃): δ 209.11, 180.95, 165.79, 163.63, 157.81, 156.14, 135.21, 125.97, 124.20, 120.71, 117.72, 97.67, 93.37, 51.75, 45.33, 43.64, 29.81, 28.56, 28.49.

3-(3-(butylamino)-2-hydroxypropoxy)-1-hydroxy-9H-xanthen-9-one (1)

Compound **1** was synthesized from **9** (100 mg, 0.352 mmol) and butylamine (0.12 mL, 1.23 mmol). The compound was eluted with CH₂Cl₂:MeOH: aq 33% NH₄OH (9.7:0.3:0.1), which afforded **1** as a pale yellow solid: 70 mg (58 %).

¹H NMR (400 MHz, CDCl₃): δ 0.93 (t, *J* = 7.2 Hz, 3H), 1.36-1.39 (m, 2H), 1.48-1.52 (m, 2H), 2.66-2.67 (m, 2H), 2.69-2.76 (m, 1H), 2.86-2.87 (m, 1H), 4.03-4.10 (m, 3H), 6.35 (d, *J* = 2 Hz, 1H), 6.44 (d, *J* = 2 Hz, 1H), 7.36-7.42 (m, 2H), 7.68-7.71 (m, 1H), 8.21-8.23 (d, *J* = 7.6 Hz, 1H). **¹³C NMR** (100 MHz, CDCl₃): δ 180.93, 165.91, 163.65, 157.79, 156.14, 135.14, 125.97, 124.14, 120.74, 117.71, 105.11, 97.67, 93.40, 71.20, 67.85, 51.61, 49.64, 32.36, 20.47, 14.09. **MS (ESI⁺):** *m/z* 358 [M+H]⁺.

General procedure for the synthesis of compounds 2 and 5-7

A solution of 4M HCl in dioxane (0.8-1mL) was added dropwise to a cooled (0 °C) solution of Boc-compounds **10** and **13-15** (1 eq) in CH₂Cl₂ (0.5-0.8 mL). After being stirred at 0 °C for 2-5 hours, the solvent was removed under reduced pressure. These compounds were purified further by gravity column chromatography. The remaining residues were converted to their hydrochloride salts and washed with Et₂O to provide the final compounds **2** and **5-7** as hydrochloride salts.

3-(3-((3-aminopropyl)amino)-2-hydroxypropoxy)-1-hydroxy-9H-xanthen-9-one (2)

Compound **2** was synthesized from **10** (50 mg, 0.109 mmol) as a pale yellow solid: 12 mg (36%).

¹H NMR (400 MHz, DMSO-*d*₆) δ 1.99-2.02 (m, 2H), 2.89-2.92 (m, 2H), 2.99-3.07 (m, 4H), 4.16-4.19 (m, 2H), 4.23-4.31 (m, 1H), 5.97 (br s, 1H exchangeable with D₂O), 6.45 (d, *J* = 2Hz, 1H), 6.69 (d, *J* = 2Hz, 1H), 7.51 (t, *J* = 7.4 Hz, 1H), 7.63 (d, *J* = 8 Hz, 1H), 7.88-7.89 (m, 1H), 8.16 (d, *J* = 7.6 Hz, 1H). ¹³C NMR (100 MHz, DMSO-*d*₆): δ 180.80, 165.77, 162.31, 157.70, 155.80, 136.65, 125.59, 125.19, 119.89, 118.13, 103.59, 97.96, 93.84, 70.38, 64.92, 49.33, 44.62, 36.40, 23.61. MS (ESI⁺): *m/z* 359 [M+H]⁺.

3-(3-((3-((4-((3-aminopropyl)amino)butyl)amino)propyl)amino)-2-hydroxypropoxy)-1-hydroxy-9H-xanthen-9-one (5)

Compound **5** was synthesized from **13** (60 mg, 0.076 mmol) as a pale yellow solid: 15.8 mg (33%).

¹H NMR (400 MHz, CD₃OD): δ 1.57-1.75 (m, 4H), 1.81-1.90 (m, 4H), 2.72-2.75 (m, 2H), 2.80-2.93 (m, 12H), 4.03-4.10 (m, 2H), 4.10-4.14 (m, 1H), 6.30 (d, *J* = 1.2 Hz, 1H), 6.46 (d, *J* = 1.2 Hz, 1H), 7.37-7.42 (m, 2H), 7.71-7.78 (m, 1H), 8.11 (d, *J* = 8 Hz, 1H). ¹³C NMR (100 MHz, CD₃OD): δ 181.90, 167.52, 164.54, 159.09, 157.33, 136.58, 126.53, 125.34, 121.58, 118.74, 114.90, 104.79, 101.50, 98.57, 94.24, 72.42, 69.18, 52.68, 40.00, 46.30 (2C), 29.63, 27.80, 27.02, 26.63 (2C). MS (ESI⁺): *m/z* 244 [M+H]²⁺.

3-(3-((3-((3-((3-aminopropyl)amino)propyl)amino)propyl)amino)-2-hydroxypropoxy)-1-hydroxy-9H-xanthen-9-one(6)

Compound **6** was synthesized from **14** (45 mg, 0.058 mmol) as a white solid: 9.3 mg (26%).

¹H NMR (400 MHz, CD₃OD): δ 1.27-1.33 (m, 2H), 1.85-1.92 (m, 6H), 2.82-2.85 (m, 3H), 2.92-3.01 (m, 9H), 4.11-4.14 (m, 2H), 4.17-4.23 (m, 1H), 6.40 (s, 1H), 6.59 (s, 1H), 7.45 (t, *J* = 7.6 Hz, 1H), 7.51 (d, *J* = 8.4 Hz, 1H), 7.77-7.84 (m, 1H), 8.20 (d, *J* = 8 Hz, 1H). ¹³C NMR (100 MHz, CD₃OD): δ 180.24, 164.98, 160.78, 156.63, 154.96, 135.79, 124.48, 124.31, 118.70, 117.31, 102.60, 97.22, 92.91, 70.04, 66.30, 50.00, 48.82, 45.58 (2C), 24.67(3C), 24.36(2C), 24.03. MS (ESI⁺): *m/z* 237 [M+H]²⁺.

3-(3-((3-((2-((3-aminopropyl)amino)ethyl)amino)propyl)amino)-2-hydroxypropoxy)-1-hydroxy-9H-xanthen-9-one (7)

Compound **7** was synthesized from **15** (33 mg, 0.043 mmol) as a white solid: 10 mg (38%).

¹H NMR (400 MHz, CD₃OD): δ 1.85-1.92 (m, 4H), 2.78-2.81 (m, 2H), 2.87-2.90 (m, 2H), 3.00-3.07 (m, 10H), 4.12-4.16 (m, 2H), 4.18-4.26 (m, 1H), 6.39 (d, *J* = 2 Hz, 1H), 6.59 (d, *J* = 2 Hz, 1H), 7.41-7.47 (m, 1H), 7.50 (d, *J* = 8.8 Hz, 1H), 7.78-7.84 (m, 1H), 8.20 (d, *J* = 8 Hz, 1H). **¹³C NMR** (100 MHz, CD₃OD): δ 180.00, 169.83, 164.51, 159.18, 157.42, 136.67, 126.57, 123.80, 121.59, 118.71, 111.35, 109.93, 98.49, 71.86, 69.73, 66.95, 57.80, 52.06, 49.30(2C), 46.00, 45.70, 39.04, 27.30. **MS (ESI)**: *m/z* 459 [M+H]⁻.

General procedure for the synthesis of compounds 3 and 4

Trifluoroacetic acid (0.6-0.9 mL) was carefully added to a stirred solution of Boc-compound **11** or **12** (1 eq) in CH₂Cl₂ (0.6-0.9 mL) at 0 °C. After stirring at 0 °C for 2 hours, the solvent was removed under reduced pressure in the presence of heptane to aid the azeotropic removal of trifluoroacetic traces. Remaining residues were washed with ether to obtain **3** and **4** as trifluoroacetate salts.

3-(3-((4-aminobutyl)amino)-2-hydroxypropoxy)-1-hydroxy-9H-xanthen-9-one (3)

Compound **3** was synthesized from **11** (30 mg, 0.064 mmol) as a brown solid: 17 mg (45%).

¹H NMR (400 MHz, DMSO-*d*₆): δ 1.45-1.68 (m, 4H), 2.76-2.86 (m, 2H), 2.99-3.09 (m, 2H), 3.17-3.20 (m, 2H), 4.16-4.20 (m, 3H), 6.05 (br s, 1H exchangeable with D₂O), 6.44 (d, *J* = 2Hz, 1H), 6.69 (d, *J* = 2Hz, 1H), 7.45-7.58 (m, 1H), 7.62-7.64 (m, 1H), 7.95-8.09 (m, 1H), 8.16-8.18 (m, 1H). **¹³C NMR** (100 MHz, DMSO-*d*₆): δ 180.46, 165.68, 162.35, 157.52, 155.65, 136.41, 125.50, 125.00, 119.88, 117.98, 110.06, 103.43, 97.79, 93.66, 70.44, 64.73, 48.99, 46.64, 36.66, 25.87. **MS (ESI)**⁺: *m/z* 373 [M+H]⁺.

3-(3-((3-((4-aminobutyl)amino)propyl)amino)-2-hydroxypropoxy)-1-hydroxy-9H-xanthen-9-one (4)

Compound **4** was synthesized from **12** (56 mg, 0.089 mmol) as a pale yellow solid: 41.1 mg (60 %).

¹H NMR (400 MHz, DMSO-*d*₆): δ 1.77-1.78 (m, 4H), 1.89-1.92 (m, 2H), 2.16-2.23 (m, 2H), 2.96-3.02 (m, 4H), 3.04-3.11 (m, 4H), 4.15-4.16 (m, 2H), 4.31-4.33 (m, 1H), 6.41 (d, *J* = 2 Hz, 1H), 6.61 (d, *J* = 2 Hz, 1H), 7.45 (t, *J* = 7.4 Hz, 1H), 7.53 (d, *J* = 8.4 Hz, 1H), 7.80-7.84 (m, 1H), 8.22 (d, *J* = 8 Hz, 1H). **¹³C NMR** (100 MHz, CD₃OD): δ 180.50, 166.98, 157.40, 136.63, 126.53, 125.36, 121.57, 118.68, 98.46, 94.20, 71.37, 66.28, 63.80, 61.05, 51.02, 46.20, 45.91, 45.77, 41.77, 39.85, 35.45, 27.47, 25.44. **MS (ESI⁺)**: *m/z* 215 [M+H]⁺.

1,3-dihydroxy-9H-xanthen-9-one (8)

Compound **8** was synthesized according to the protocol reported in literature.¹⁹² All data were in agreement with those previously published.

¹H NMR (400 MHz, DMSO-*d*₆): δ 6.21 (d, *J* = 1.2 Hz, 1H), 6.40 (d, *J* = 1.6 Hz, 1H), 7.46 (t, *J* = 7.6 Hz, 1H), 7.59 (d, *J* = 8.8 Hz, 1H), 7.85 (t, *J* = 7.8 Hz, 1H), 8.12 (d, *J* = 8 Hz, 1H), 11.12 (br s, 1H exchangeable with D₂O), 12.82 (br s, 1H exchangeable with D₂O).

Tert-butyl (3-aminopropyl)carbamate (16)

Compound **16** was synthesized by reacting Boc₂O (26.18 g, 0.120 mol) in CH₂Cl₂ (30 mL) and 1,3-propanediamine (44.45 g, 0.600 mol) in CH₂Cl₂ (30 mL) as described previously.¹⁷¹ The resulting compound was a yellow oil (86% yield).

¹H NMR (400 MHz, CDCl₃) δ 1.42 (s, 9H), 1.58-1.62 (m, 2H), 2.72-2.75 (m, 2H), 3.18-3.20 (m, 2H), 4.70 (br s, 1H exchangeable with D₂O).

4.6.2 Biology

4.6.2.1 Cleavage of Plasmid DNA

DNA cleavage reactions were performed using the procedure of Fortune and Osheroff.¹⁹⁷ Reaction mixtures contained 10 nM negatively supercoiled pBR322 DNA and 150 nM human topoisomerase II α in a final volume of 20 μ L of cleavage buffer [10 mM Tris-HCl,

pH 7.9, 5 mM MgCl₂, 100 mM KCl, 0.1 mM NaEDTA, and 2.5% (v/v) glycerol]. Reactions were carried out in the presence of 0-100 μM xanthone derivatives. Reactions were incubated for 6 minutes at 37 °C and enzyme-DNA cleavage complexes were trapped by the addition of 2 μL of 4% SDS followed by 2 μL of 250 mM NaEDTA, pH 8.0. Proteinase K (2 μL of a 0.8 mg/mL solution) was added, and samples were incubated for 30 minutes at 45 °C to digest the enzyme. Samples were mixed with 2 μL of agarose loading dye [60% sucrose (w/v), 10 mM Tris-HCl, pH 7.9, 0.5% bromophenol blue, 0.5% xylene cyanol], heated for 2 minutes at 45 °C, and subjected to electrophoresis in a 1% agarose gel in 40 mM Tris-acetate, pH 8.3, and 2 mM EDTA containing 0.5 μg/mL ethidium bromide. DNA bands were visualized by UV light and quantified using an Alpha Innotech digital imaging system. DNA cleavage was monitored by the conversion of supercoiled plasmid to linear molecules.

In some experiments, the 5 mM MgCl₂ in the cleavage buffer was replaced with 5 mM CaCl₂ in order to increase baseline levels of enzyme-mediated DNA cleavage.²⁰⁷

In some experiments, the ability of xanthone derivatives to block the enhancement of enzyme-mediated DNA cleavage by 100 μM etoposide was determined. Cleavage buffer containing 5 mM MgCl₂ was utilized. In these cases, the xanthone and etoposide were added simultaneously.

4.6.2.2 DNA Relaxation

DNA relaxation reactions were carried out using the procedure of Fortune and Osheroff.¹⁹⁷ Reaction mixtures contained 5 nM negatively supercoiled pBR322 DNA, 3 nM human topoisomerase II α , 1 mM ATP and 0-200 μM xanthone derivatives in a total of 20 μL of relaxation buffer [10 mM Tris-HCl, pH 7.9, 5 mM MgCl₂, 175 mM KCl, 0.1 mM NaEDTA, and 2.5% (v/v) glycerol]. Mixtures were incubated at 37 °C for 4 minutes. Reactions were stopped by the addition of 3 μL of 0.77% SDS-77 mM NaEDTA, pH 8.0. Samples were mixed with 2 μL of agarose loading dye, heated for 2 minutes at 45 °C, and subjected to electrophoresis in a 1% agarose gel in 100 mM Tris-borate, pH 8.3, and 2 mM EDTA. Gels were stained for 30 minutes using 1.0 μg/mL ethidium bromide and rinsed in deionized water. DNA bands were visualized and quantified as described above.

4.6.2.3 Decatenation of kinetoplast DNA

Decatenation assays were carried out using the procedure of Miller *et al.*¹⁹⁸ Reaction mixtures contained 0.3 µg of kDNA, 4 nM human topoisomerase II α , 1 mM ATP and 0-300 µM xanthone derivatives in a total of 20 µL of relaxation buffer. Reaction mixtures were incubated for 15 min at 37 °C and terminated with 3 µL of 0.77% SDS-77 mM NaEDTA, pH 8.0. Samples were mixed with 2 µL of agarose loading dye, heated for 2 minutes at 45 °C, and subjected to electrophoresis in a 1% agarose gel in 100 mM Tris-borate, pH 8.3, and 2 mM EDTA containing 0.5 µg/mL ethidium bromide. DNA bands were visualized and quantified as described above.

4.6.2.4 DNA Strand passage

DNA strand passage reactions were carried out using the procedure of Osheroff.⁶⁰ Reaction mixtures contained 5 nM relaxed pBR322 DNA, 150 nM of human topoisomerase II α , 1 mM adenylyl imidodiphosphate [APP(NH)P] and 0-10 µM xanthone derivatives in a total of 20 µL of relaxation buffer. Reaction mixtures were incubated at 37 °C for 2 minutes and were stopped by the addition of 3 µL of 0.77% SDS-77 mM NaEDTA, pH 8.0. Proteinase K (2 µL of a 0.8 mg/mL solution) was added, and samples were incubated for 30 minutes at 45 °C to digest the enzyme. Samples were mixed with 2 µL of agarose loading dye, heated for 2 minutes at 45 °C, and subjected to electrophoresis in a 1% agarose gel in 100 mM Tris-borate, pH 8.3, and 2 mM EDTA. Gels were stained for 30 minutes using 1.0 µg/mL ethidium bromide, and rinsed in deionized water. DNA bands were visualized and quantified as described above.

4.6.2.5 ATP hydrolysis

ATPase assays were performed as described by Osheroff *et al.*⁶⁹ Reaction mixtures contained 30 nM human topoisomerase II α , 5 nM negatively supercoiled pB322 DNA, 1 mM [γ -³²P]ATP, and 0-50 µM compound **4** in a total of 20 µL of cleavage buffer. Reactions were initiated by the addition of topoisomerase II α and mixtures were incubated at 37 °C for 0-8 minutes. Samples (2.0 µL) were removed at various time intervals and spotted on to polyethyleneimine-impregnated thin layer cellulose chromatography plates. Plates were

developed by chromatography in freshly prepared 400 mM NH_4HCO_3 , and released ^{32}P was visualized and quantified using a Bio-Rad Molecular Imager FX.

4.6.3 Molecular modeling

The grid for the docking of compound **4** was centered at the position of etoposide in monomer A, while the maximum size of the docked ligand was set to 36 Å. The amine groups of the polyamine chain were fully protonated as predicted by the Epik software, at pH 7.4.⁽¹⁴⁾ Finally, compound **4** was docked within the topoisomerase II active site using the Glide²⁰⁸ software of the Schrodinger suite (Release 2017-1).

Chapter 5- Inhibition of human topoisomerase II α by merbarone derivatives

5.1 Merbarone derivatives

As discussed in the first chapter, topoisomerase II is the target for some of the most active anticancer drug used in the treatment of human malignancies. Among them, anthracyclines (*e.g.*, adriamycin and daunorubicin) and epipodophyllotoxins (*e.g.*, etoposide and teniposide), act as poisons.⁴⁹ Other drugs act as catalytic inhibitors of the enzyme. Thus, they may antagonise the effect of topoisomerase II poisons. Among them, merbarone, fostriecin, aclarubicin, bisdioxopiperazines and novobiocin.^{86, 104, 105, 209, 210}

Merbarone is another well-known drug that acts as a catalytic inhibitor of topoisomerase II. It is a non-sedating derivative of thiobarbituric derivative (Figure 5.1) (6-hydroxy-4-oxo-*N*-phenyl-2-thioxo-1H-pyrimidine-5-carboxamide) and shows inhibition against topoisomerase II. Since it displayed excellent activity against some murine tumors, including L1210 and P388 leukaemias, B16 melanoma, and M5076 sarcoma, it was developed to the clinical trial stage.^{104, 211} However, these trials were halted due to insufficient anticancer activity and nephrotoxicity issues.⁸⁵

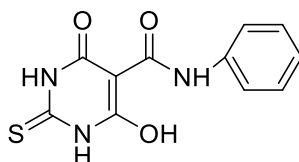


Figure 5.1. Structure of merbarone.

In 1989, Drake and co-workers, with the aim of identifying novel inhibitors of topoisomerase II, demonstrated that merbarone was a potent inhibitor of topoisomerases, showing selectivity toward the type II enzyme because the concentration required for inhibition of the type I enzyme was ~10-fold higher than that required for the type II enzyme.¹⁰⁴ It was also found that merbarone inhibited chromosome condensation and sister chromatid segregation in non-synchronized human leukemic CEM cells and induced G₂/M blockade.^{212, 213}

Ten years later, Fortune and co-workers¹⁹⁷ studied the effect of this drug on the activity of the human topoisomerase II α and the enzyme from *Drosophila* and yeast. From their data

on inhibition of relaxation of negatively supercoiled pBR322 plasmid DNA, merbarone was more potent against eukaryotic topoisomerase II with an $IC_{50} \sim 40 \mu M$. The IC_{50} values for *Drosophila* or yeast were significantly higher, ~ 350 and $\sim 700 \mu M$, respectively. During his study, Fortune and co-workers demonstrated that merbarone had no effect on topoisomerase II-DNA binding and found that the apparent K_D values calculated in the absence or presence of the drug were 43 ± 9 or 45 ± 10 nM topoisomerase II α , respectively. Furthermore, they analysed the effect of merbarone on ATP hydrolysis, showing that no inhibition was observed up to $200 \mu M$. To further investigate the mechanism of action of merbarone, the inhibition of topoisomerase II-mediated cleavage assay was assessed. Merbarone strongly inhibited this step of the catalytic cycle that follows DNA binding, with an $IC_{50} \sim 50 \mu M$. Since the IC_{50} values for inhibition of relaxation and inhibition of cleavage were similar, they suggested that the primary mechanism by which merbarone inhibited the overall catalytic activity of human topoisomerase II α was by blocking DNA cleavage.¹⁹⁷ Further investigation in cellular models of merbarone showed that it was able to reduce the number of enzyme-mediated DNA stranded breaks produced by the antitumor agents *m*-AMSA and teniposide, but not camptothecin.¹⁰⁴ This finding suggested that this compound interfered with the mechanism of action of other two poisons, *m*-AMSA and teniposide, by inhibiting the stabilization of topoisomerase II-DNA cleavage complexes induced by the last two drugs.¹⁰⁴ In particular, the attenuation of teniposide action in culture was observed only when cells were treated with merbarone prior to the addition of the poison.²¹² This result was useful to determine a possible mechanism of action of merbarone, by indicating that this drug blocked a step of the catalytic cycle prior to cleavage, DNA binding.²¹² As reported above, Fortune and co-workers found, instead, that merbarone acted by inhibiting the DNA cleavage step. Based on this finding, the effect of merbarone on the topoisomerase II poisons were re-examined. First, merbarone reduced the increase of the cleavage complex induced by etoposide. Second, merbarone decreased the stimulation of the cleavage by an apurinic site located within a topoisomerase II recognition sequence. Thus, this drug is able to affect cleavage enhancement induced both by anticancer drugs and by DNA lesions.¹⁹⁷ Since, the concentration of merbarone (100 - $400 \mu M$) required to diminish cleavage in presence of etoposide or a DNA lesion was higher, it is possible that this latter may compete with DNA cleavage-enhancing drugs for a binding

site within the topoisomerase II-DNA complex.¹⁹⁷ Furthermore, they showed that the diminution of cleavage was higher when the cleavage complex was incubated with merbarone prior to the addition of etoposide, rather than when the poison was added before. When the two drugs were added simultaneously, an intermediate level of cleavage attenuation was observed. Thus, they suggested that the actions of both these drugs on topoisomerase II α were mutually exclusive and that merbarone they may occupy an interaction domain overlapping with that of etoposide.¹⁹⁷

Due to these previous finding, in 2003 Ranise and co-workers synthesized two series of merbarone analogues that included the 2-thiobarbiturate framework. During a previous study, they described the synthesis of 5-substituted 1,3-diphenyl-2,6-dithiobarbiturates **A-C** (Figure 5.2).²¹⁴

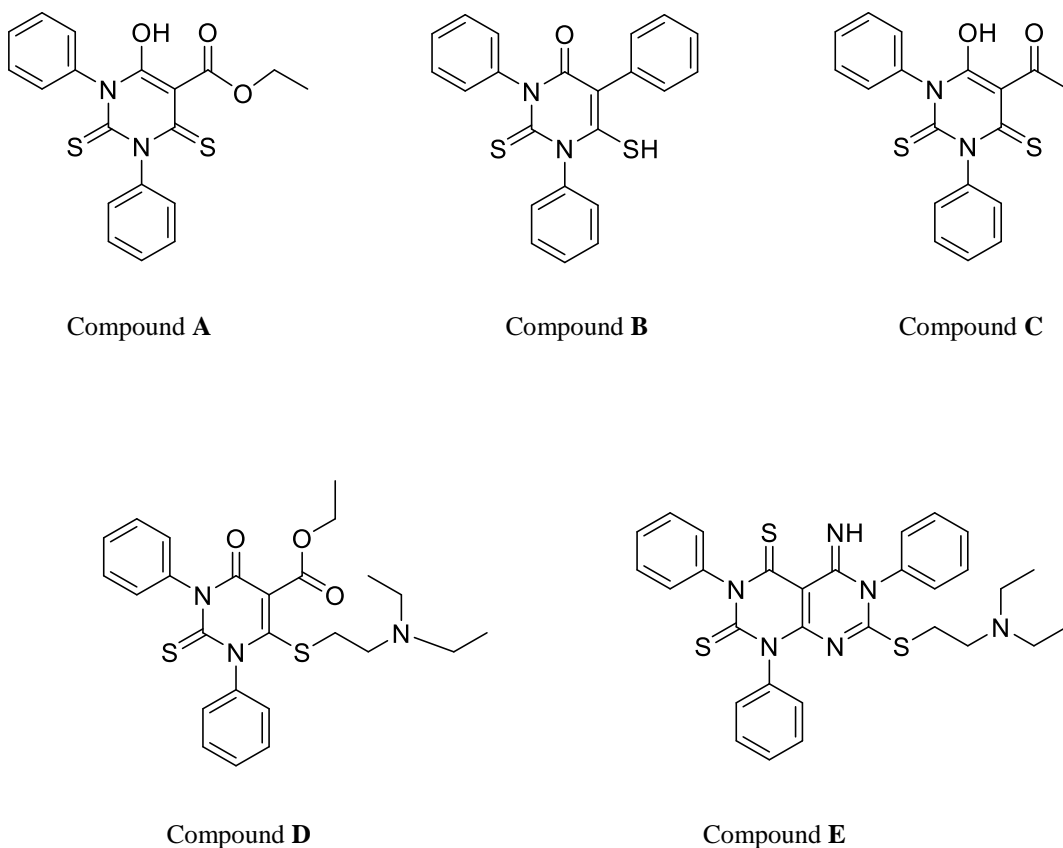


Figure 5.2. Structures of compounds **A-E**.

These compounds had phenyl rings in positions 1 and 3 of the central core, which increased the lipophilicity of the compounds in comparison to merbarone (as shown by their

calculated LogP). Despite that, compounds **A-C** did not show an increased ability to cross the CNS (or other biological membranes), in comparison to merbarone. Thus, in order to both suppress acid ionizability and improve pharmacodynamics and pharmacokinetic properties they synthesized different compounds. Among them, **D** and **E** (Figure 5.2)²¹⁵ resulted active in the low micromolar concentration range. They were able to inhibit the formation of supercoiled DNA from the relaxed form of DNA at 100 μM , indicating that they were stronger inhibitors of topoisomerase II α in comparison to merbarone. Furthermore, both monocyclic and bicyclic derivatives displayed the same potency against leukaemia cell lines and appeared to be up to 100-fold more potent than merbarone.²¹⁵ Notwithstanding, bicyclic derivatives were more potent than monocyclic against solid tumor cell lines, showing antiproliferative activity in the concentration range of 1-10 μM against NSCLC, colon, CNS, melanoma, renal, prostate and breast cancer cell lines. In light of the results obtained for compound **D**, in 2013, Spallarossa and co-workers

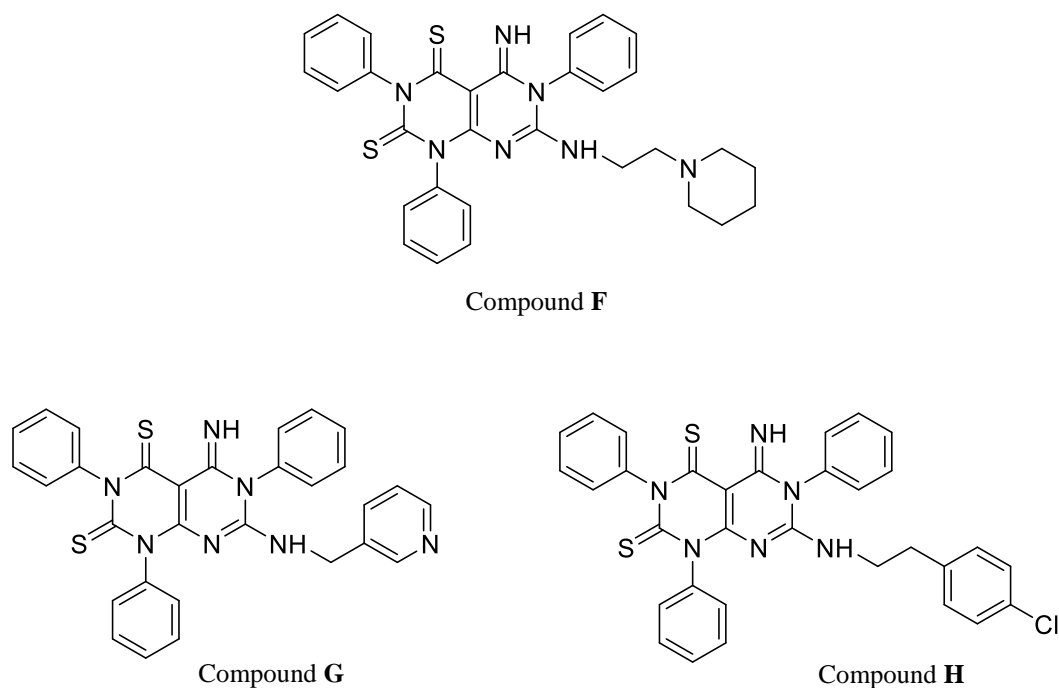


Figure 5.3. Structures of compounds **F-H**.

designed a new series of aza-isosters derivatives, in which the pyridopyrimidine substructure was functionalized at position **7** with side chains that provided different steric,

conformational, and acid/base properties.²¹⁶ Among them, derivatives **F-H** (Figure 5.3) inhibited the enzyme more efficiently than merbarone, which was used as reference drug. All of these compounds displayed IC₅₀ values in the low micromolar range. Furthermore, spectrophotometric and electrophoretic analyses showed that these compounds were not able to bind DNA or to stabilize cleavage complexes. These findings were consistent with previous data on merbarone, demonstrating that the compounds acted as inhibitors of type II topoisomerase. Compound **H** was also tested against *Escherichia coli* topoisomerase IV, *Escherichia coli* topoisomerase I, and human topoisomerase I with no positive results. In conclusion, compounds **F-H** were the most promising compounds of the series for antiproliferative potency or spectrum of action showing inhibitory activity against topoisomerase II α .

In 2015, Baviskar and co-workers, on the basis of the results from the molecular docking of merbarone in human topoisomerase II α , suggested that it established metal coordination bonds (through carbonyl oxygens) with Mg²⁺ (2.09 Å), hydrogen bonding interactions with Asp543 (3.13 Å), Asp545 (1.90 Å), and Lys614 (2.91 Å), and NH- π interactions with Lys614 (distance 3.50 Å) (Figure 5.4).

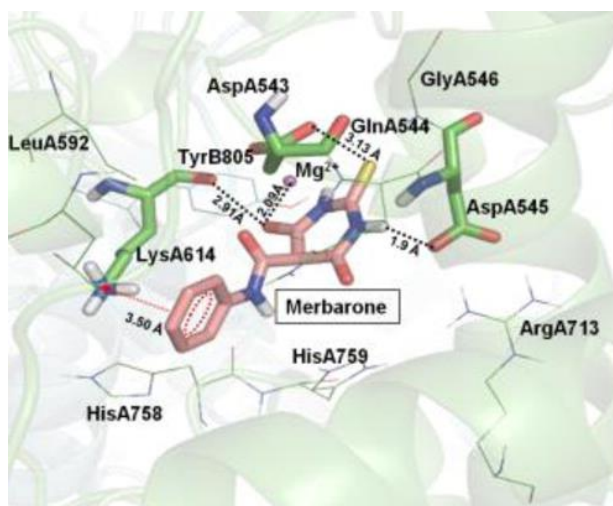


Figure 5.4. Molecular docking of merbarone in human topoisomerase II α .²¹⁷

The binding is further stabilized by interactions with polar residues (such as Gln544, Arg713, His758, and His759) and hydrophobic residues (such as Gly546, Ile577, Leu592, and Tyr805). Thus, they suggested that all of these interactions (as well as others with

additional catalytic components of the enzyme) may be considered as the molecular recognition interactions for merbarone (Figure 5.4).²¹⁷

5.2 Drug design

Topoisomerase II inhibitors are useful for many different types of cancer because of the essential role of the enzyme in faster replicating cancer cells. As described in Chapter 1, some of them act as poisons by stabilizing the cleavage complex, others as inhibitors, by acting at some step in the catalytic cycle of the enzyme. These latter compounds, even if they are able to induce chromosomal alterations in cells *in vitro* and *in vivo*, have not been scrupulously tested. The goal of research in the field of the topoisomerase II inhibition is to find new potent poisons of this enzyme. One of the possible explanation for this is that most catalytic inhibitors of topoisomerase II, unfortunately, are not specific for this enzyme except for bisdioxopiperazines. Merbarone, as mentioned above, belong to the class of the catalytic inhibitors and, unfortunately, has never reached the market because of its side effects.

Thus, in order to obtain a more potent derivative and also to direct the action toward the poisoning of the enzyme, we designed and synthesized five new compounds **1-5** via a pharmacophore hybridization strategy (Figure 5.5).^{218, 219} We introduced key pharmacophoric elements of etoposide (E-ring)⁹⁸ and merbarone (thiobarbituric core)^{197, 217} into a new hybrid scaffold (Figure 5.6). Compound **1** bearing a 3,5-dimethoxy-4-phenol ring (like the E-ring of etoposide), in compound **2** the two methoxy groups has been removed, compound **3** with only one methoxy group in position 3, compound **4** where this methoxy group has been replaced by an hydroxyl group and compound **5** that displays an aromatic ring without substituent. Thus, these new hybrid molecules were generated based on merbarone's thiobarbituric core, which was modified as follows. First, phenyl rings were introduced at each nitrogen of the thiobarbituric core. Lipophilic substituent at those nitrogen atoms have been shown to improve merbarone's cell permeability.^{215, 216, 220} Second, the phenyl ring in merbarone was functionalized to mimic the pendant aromatic ring (E-ring) of etoposide, which was demonstrated to enhance topoisomerase II-mediated DNA cleavage.⁹⁸ This modification was carried out with the aim of modulating the drug-target interactions at the topoisomerase II-DNA cleavage complex.

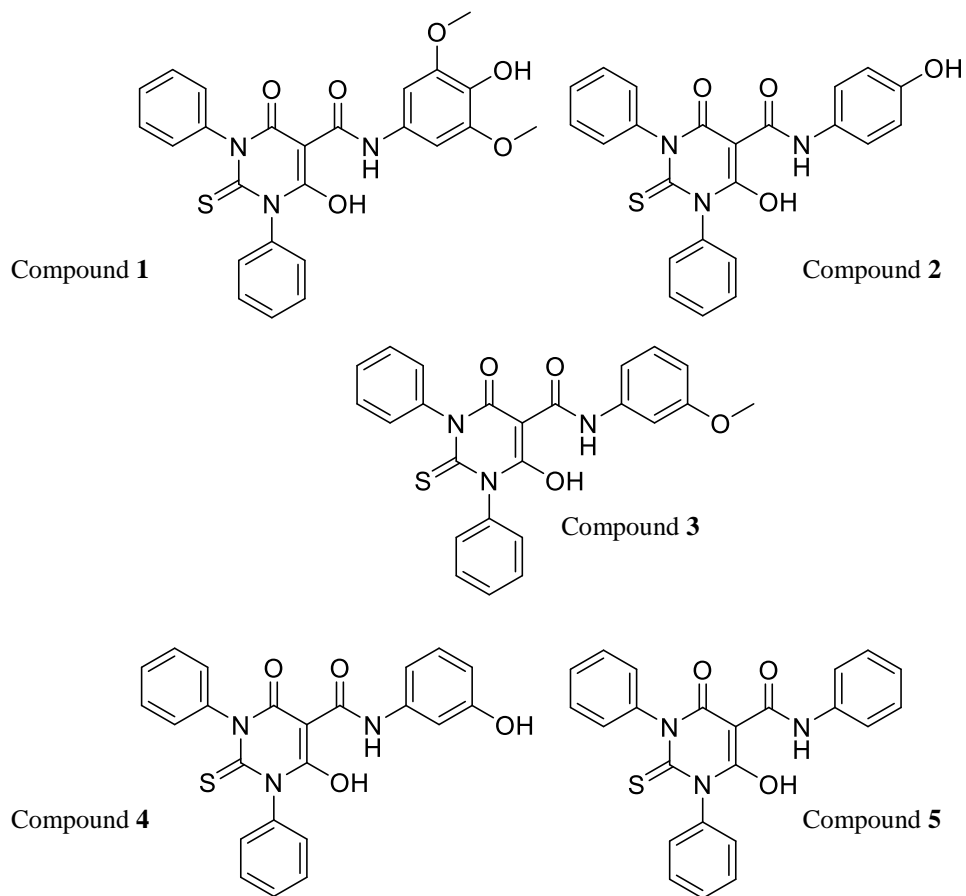


Figure 5.5. Structures of five new merbarone-derivatives 1-5.

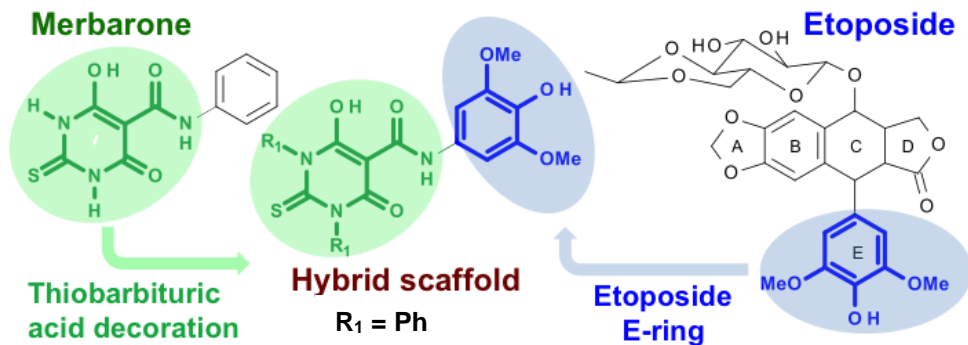


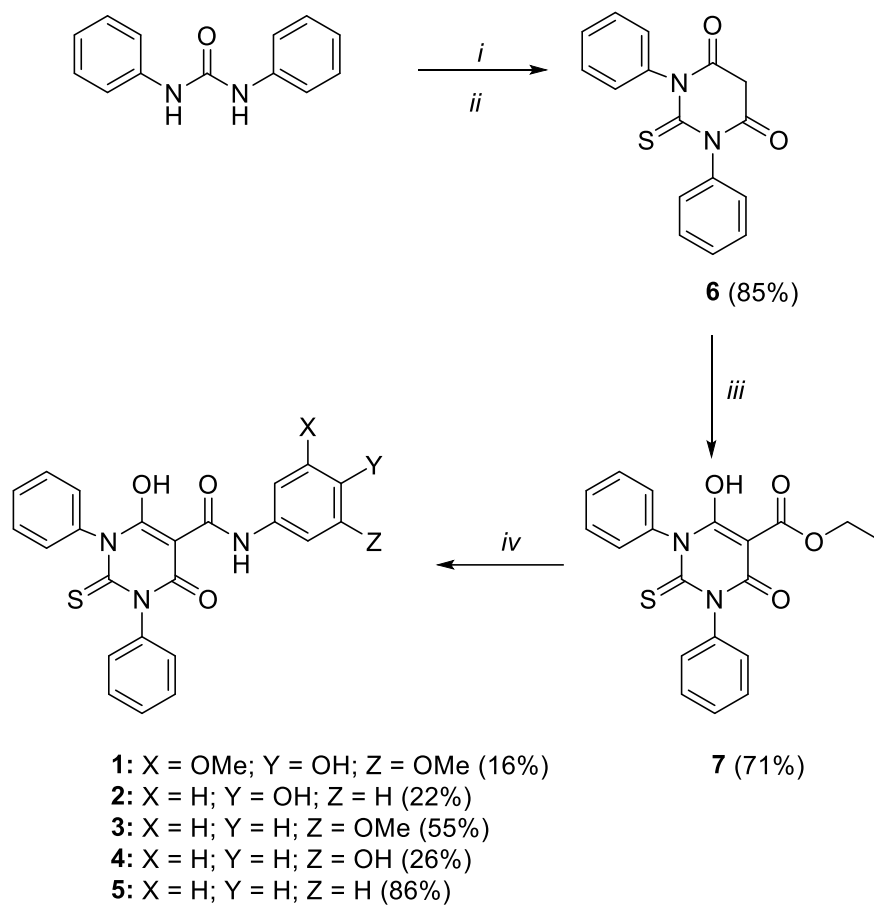
Figure 5.6. Topoisomerase II poisons designed via a pharmacophore hybridization strategy. The new hybrid functional scaffold (center) is obtained by merging merbarone's thiobarbituric core, with different decorations of the two heterocycle nitrogen atoms (left), with the E-ring of etoposide (right).

5.3 Methods

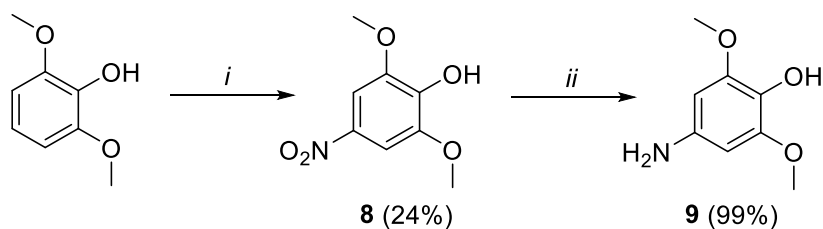
5.3.1 Chemistry

Compounds **1-5** were synthesized according to the synthetic procedure reported in Scheme 5.1. The intermediate **6** was synthesized from *N,N'*-diphenylthiourea and methyl 3-chloro-3-oxopropionate. Under reduced pressure, the HCl formed from the condensation of methyl 3-chloro-3-oxopropionate and the thiocarbanilide was thought to catalyse the cyclization to afford the desired intermediate **6**, over the course of several days. Acylation of compound **6** with ethyl chloroformate in the presence of pyridine and 4-dimethylaminopyridine (DMAP) gave the key intermediate **7**, which was conjugated with the appropriate aromatic amines by using DMF as solvent to afford the final compounds **1-5**.

Intermediate **9** was synthesized from 2,6-dimethoxyphenol by using *tert*-butyl nitrite as nitrating agent that displays chemoselectivity for phenols (Scheme 5.2).²²¹ The reaction was initiated by a rate-limiting nitrosyl exchange between the alkyl nitrite and aromatic hydroxyl group. The aromatic *O*-nitroso derivatives, through a thermal homolysis, led to resonance-stabilized phenoxy radicals and •NO. The final steps of this reaction involve rapid oxidation of •NO with O₂, prior to coupling of the resultant NO₂ with phenoxy radical, affording 2,6-dimethoxy-4-nitro-phenol (**8**). Finally, the reduction of the nitro group to an amine, by using palladium on activated carbon, afforded the 4-amino-2,6-dimethoxyphenol (**9**) in good yield.



Scheme 5.1. Reagents and conditions: (i) methyl 3-chloro-3-oxopropionate, CH_2Cl_2 , N_2 , r.t., 16 hours; (ii) Low pressure, r.t., 72 hours; (iii) ethyl chloroformate, DMAP, pyridine, CH_2Cl_2 , N_2 , 0°C to r.t.; (iv) Ar-NH_2 , DMF, N_2 , 100°C , 30 minutes.



Scheme 5.2. Reagents and conditions: (i) *tert*-butyl nitrite, THF, r.t., 30 minutes; (ii) 1,4-cyclohexadiene, Pd-C, CH₃CH₂OH, N₂, r.t., 16 hours.

5.3.2 Biology

Initially, compounds **1-5** were tested to assess their ability to inhibit the activity of topoisomerase II. Their effects on the overall catalytic activity of the enzyme were monitored using the relaxation assay. To determine whether these derivatives were able to increase levels of the cleavage complexes, a DNA cleavage assay was utilized. Values are shown as the concentration required to the activity of the enzyme by 50% (IC₅₀). For all the derivatives, the circular dichroism (CD) titration of ctDNA was evaluated.

In parallel, the cytotoxic effects of these new compounds on the viability of different tumour cellular lines were evaluated.

5.3.3 Computational study

To investigate the binding mode of compounds **1-5** for topoisomerase II, docking simulations were performed using the available crystallographic structures from the PDB code 3QX3, solved at 2.16 Å resolution.⁹⁸

5.4 Results and discussion

Initially, all the compounds were tested against human topoisomerase II in a relaxation inhibition assay. Table 1 reports the IC₅₀ values for *N,N'*-diphenyl derivatives **1-5** (Figure 5.5).

Table 1. ^aIC₅₀ values. ^bCompound concentration necessary to observe the same amount of topoisomerase II-DNA cleavage complex generated by etoposide at 20 μM. ^cInteraction with DNA in absence of topoisomerase II enzyme. ^dExtension of the functionalized group of the hybrid compound to the DNA minor groove, compared to the E-ring of etoposide. ^eAntiproliferative activity for each cellular line.

Compound	TopoII inhibition ^a (μM)	Cleavage complex ^b (μM)	DNA Interaction ^c	Minor groove ^d	HeLa ^e (μM)	MCF7 ^e (μM)	A549 ^e (μM)	DU145 ^e (μM)
Etoposide	120 ± 10	20	no	yes	2.4 ± 0.9	10.5 ± 4.0	1.3 ± 0.1	1.0 ± 0.4
Merbarone	120 ± 12	no	no	no	62.3 ± 6.4	83.9 ± 3.0	40.0 ± 2.7	18.9 ± 2.0
1	120 ± 15	200	no	yes	18.1 ± 0.8	53.5 ± 1.9	17.5 ± 1.1	26.7 ± 0.1
2	150 ± 19	200	no	yes	42.9 ± 6.1	66.1 ± 7.5	37.1 ± 3.7	42.5 ± 7.7
3	30 ± 6	100	no	yes	8.5 ± 0.5	14.0 ± 0.9	6.9 ± 0.2	12.5 ± 1.5
4	200 ± 22	no	no	no	39.1 ± 1.3	94.2 ± 0.7	59.4 ± 6.1	49.6 ± 2.7
5	5 ± 1.0	200	no	yes	10.8 ± 0.2	13.6 ± 0.8	9.2 ± 0.3	16.8 ± 0.8

Molecular modelling and docking showed that these derivatives formed good contacts with topoisomerase II residues located in front of both DNA grooves (Asp479 and Arg503 - more on this below).²²² Thus, *N,N'*-diphenyl derivatives likely act as good linkers between distal topoisomerase II-DNA structural elements, mimicking etoposide's binding mode. Compound **1** was equipotent to merbarone (Table 1), with an IC₅₀ of 120 μM. Compound **2** was slightly worse than **1**, with an IC₅₀ of 150 μM. These results are in agreement with previous studies that demonstrate the crucial role of the etoposide E-ring substituents for topoisomerase II inhibition.^{84, 103} Interestingly, conserving only one methoxy group in the meta-position, as in **3**, returned an IC₅₀ of 30 μM, with a 4-fold increase of potency compared to both merbarone and etoposide. Replacing this methoxy in **3** with a hydroxyl group, as in **4**, significantly decreased topoisomerase II inhibitory activity (IC₅₀ 200 μM). Finally, a naked phenyl ring, as in **5**, showed an IC₅₀ of 5 μM, which is 24-fold better than merbarone and etoposide, although the topoisomerase II-DNA cleavage complex formation was reduced (Table 1). The molecular mechanisms leading to the topoisomerase II inhibition by the five compounds, **1-5**, were further characterized (see Table 1). UV measurements showed that DNA alone does not produce variations of the ligand absorbance induced by DNA. This suggests a lack of relevant binding of all our new derivatives to the DNA alone. Consistently, as already observed with merbarone^{197, 217}, CD titration of ctDNA with the compounds **1-5** showed their inability to alter DNA structural arrangement in the absence of topoisomerase II.

Therefore, this excludes an interference in the DNA-topoisomerase II binding step as a mechanism of inhibition. Intriguingly, these derivatives seemed to act differently than merbarone, while behaving similarly to etoposide. In fact, while merbarone is not a poison^{197, 217}, compounds **1-3** and **5** showed the ability to stabilize the topoisomerase II-DNA cleavage complex (Figure 5.7). These compounds induced the presence of linear DNA, although to a lesser extent than etoposide. Notably, this evidence sustains our docking calculations at the etoposide binding site.⁹⁸ In contrast, **4**'s poor potency in blocking topoisomerase II activity was reflected in its inability to generate the topoisomerase II-DNA cleavage complex. These findings suggested that compounds **1-3** and **5** act by poisoning the topoisomerase II, similarly to etoposide. In addition, our docking calculations further support the hypothesis that these hybrid topoisomerase II poisons may favor the formation of a stable topoisomerase II-DNA cleavage complex.

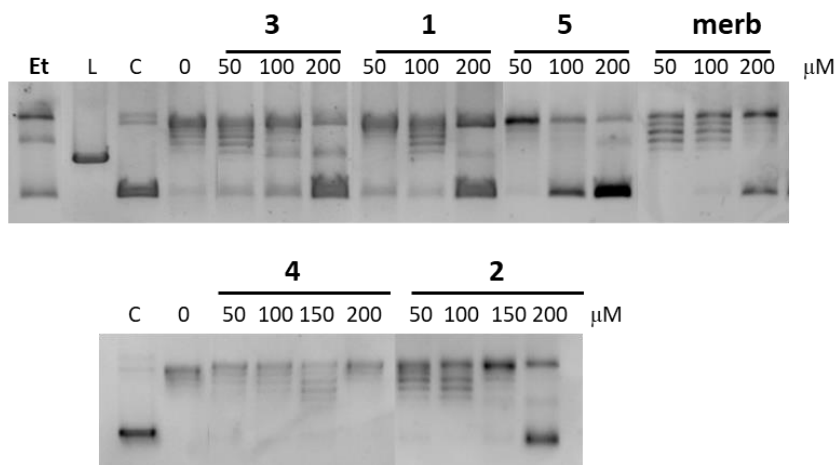


Figure 5.7. Cleavage reactions of compounds **1-5**, Merbarone and Etoposide (Et).

Indeed, our docking results suggest key interactions between the *N,N'*-diphenyl derivatives and the cleavage complex. In particular, **1** is predicted to have a binding mode very similar to that of etoposide (Figure 5.8), with its 3,5-dimethoxy-4-phenol ring forming an H-bond with Asp479. Also, one of the two unsubstituted phenyl rings of **1** was extended toward the binding site that is occupied by the glycosidic moiety of etoposide (Figure 5.8).⁹⁸ The other phenyl ring, instead, overlapped with the D-ring of etoposide, thus closer to the scissile phosphate of the T₊₁ nucleotide along the cleaved DNA strand (Figure 5.8).

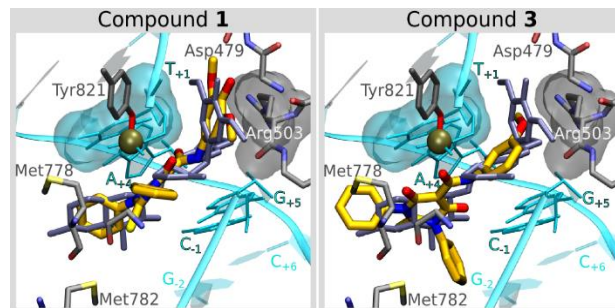


Figure 5.8. Docking of compounds **1** and **3** (yellow) in the topoisomerase II (gray) /DNA (cyan) cleavage complex, and their superposition to the crystal pose of etoposide (PDB 3QX3).⁹⁸

Interestingly, this binding mode of the two naked phenyl rings was conserved in **4** and **5**, too. However, the 3-phenol ring of **4** interacted with the side chain of Arg503, pointing its hydroxyl group toward the DNA backbone. For this reason, the binding pose of **4** did not allow an extension of the 3-phenol ring into the DNA minor groove, as shown for compounds **1-3** and **5**. This may explain **4**'s inability to stabilize the topoisomerase II-DNA cleavage complex. Moreover, the two naked phenyl rings of **3** protruded into the DNA major groove, in front of the T₊₁/A₊₄ and C₋₁/G₊₅ base pairs, interacting with the side chains of Met782 and Met778. In this way, the methoxy group of **3** was between the side chain of Arg503 and the deoxyribose of the T₊₁ nucleotide (Figure 5.8). Thus, the methoxy group forms key topoisomerase II-DNA interactions in **3**, likely explaining its slightly higher ability to stabilize cleavage complexes (100 μM for **3** vs 200 μM for all the other new compounds). The relevance of this methoxy group is well-known for etoposide, where its removal leads to a significant loss of activity.^{84, 98, 103} For these five new derivatives, we evaluated the antiproliferative activity of these compounds in human endometrial (HeLa), breast (MCF7), lung (A549), and androgen-independent prostate (DU145) cancer cell lines. Overall, we found a general improvement of the antiproliferative activity of these new compounds compared to merbarone, with an increase in potency, up to 6-fold in HeLa, MCF7, and A549 cell lines. These compounds were also slightly more potent than merbarone in DU145 cells (Table 1). Compared to etoposide, they were equipotent (MCF7) or slightly less active (HeLa, A549 and DU145). Notably, we also observed an increase in H2AX phosphorylation after treatment of HeLa cells with compound **5**²²³, which indicates that the cytotoxicity observed is likely caused by cellular inhibition of topoisomerase II (Figure 5.9).²²⁴

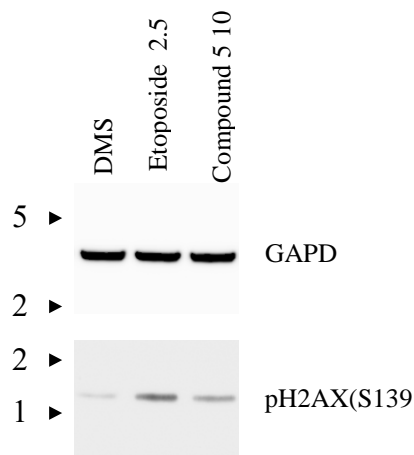


Figure 5.9. HeLa cells treated with the compound **5** at their IC_{50} concentration or with DMSO (control vehicle). After exposure, assessment of H2AX phosphorylation as a reporter of DNA damage (Huang et al., 2003) was performed by immunodetection using anti-phospho-H2AX antibody (Ser139). GAPDH was used as control for equal protein loading. Numbers on the left indicate MW (kDa). A clear induction of the phosphorylation of H2AX is visible after treatment with topoII inhibitors

5.5 Conclusion

Here, we present the characterization of the five new human topoisomerase II poisons obtained by combining key pharmacophoric elements of etoposide and merbarone into a single new hybrid functional scaffold. We obtained new merbarone derivatives that displayed significant activity toward in blocking topoisomerase II, including when compared to the two template structures. These new hybrid molecules show promising antiproliferative activity against human cancer cells. Thus, taken together, these results endorse a further exploration of this first set of new hybrid compounds to better characterize their mechanism of action and their overall potential as novel anticancer therapeutics.

5.6 Experimental section

5.6.1 Chemistry

Chemical reagents were purchased from Sigma Aldrich. All reactions were performed with dry glassware under a nitrogen atmosphere unless otherwise noted. Nuclear magnetic resonance spectra (NMR) were recorded at 400 MHz for ^1H and 100 MHz for ^{13}C on Varian VXR 400 spectrometer in CDCl_3 , DMSO or CD_3OD as solvents. Chemical shifts (δ) are given in ppm from tetramethylsilane (TMS) with the solvent resonance as internal standard (CDCl_3 : δ 7.26, DMSO: δ 2.50, CD_3OD : δ 3.31 for ^1H -NMR and CDCl_3 : δ 77.16, DMSO: δ 39.52, CD_3OD : δ 49.00 for ^{13}C -NMR). For ^1H -NMR, data are reported as follows: chemical shift, multiplicity (s = singlet, d = doublet, dd = double of doublets, t = triplet, q = quartet, m = multiplet, br s = broad singlet), coupling constants (Hz) and integration. Microwave assisted synthesis was performed by using CEM Discover® SP apparatus (2.45 GHz, maximum power of 300W). Electron spray ionization (ESI) mass spectra were recorded on Varian VG 7070E instrument. Chromatographic separations were performed on silica gel columns by flash or gravity column (Kieselgel 40, 0.040-0.063 mm; Merck) chromatography. Reactions were followed by thin-layer chromatography (TLC) on Merck (0.25 mm) glass-packed pre-coated silica gel plates (60 F254) that were visualized in an iodine chamber, or with a UV lamp, KMnO_4 , or bromocresol green. All the names were attributed by Chem BioDraw Ultra 16.0.

Synthesis of ethyl 4-hydroxy-6-oxo-1,3-diphenyl-2-thioxo-pyrimidine-5-carboxylate (7)

Under N_2 atmosphere, ethyl chloroformate (5.81 mmol) was dropwise added to a 0 °C solution of compound **6** (1.64 g, 5.53 mmol), DMAP (0.44 mmol) and pyridine (6.91 mmol) in dry CH_2Cl_2 (4 mL). The reaction crude was allowed warming to r.t., stirred for 16 hours, diluted with CH_2Cl_2 (20.7 mL), washed with water (27.7 mL). The combined organic layers were dried over Na_2SO_4 and concentrated under reduced pressure. The residue was triturated in CH_2Cl_2 (5.5 mL) to give the desired compound **7** as yellowish solid: 1.45 g (71 %).

^1H NMR (400 MHz, $\text{DMSO}-d_6$) δ 1.14 (t, $J = 7.1$ Hz, 3H), 4.00 (q, $J = 7.1$ Hz, 2H), 7.10 (d, $J = 7.7$ Hz, 4H), 7.25 (t, $J = 7.3$ Hz, 2H), 7.35 (t, $J = 7.6$ Hz, 4H).

General procedure for the synthesis of compounds 1-5

A mixture of **7** (1 mmol) and an appropriate aniline (1 mmol) in dry DMF (1 mL) was stirred at 100 °C for 30 minutes, then cooled to r.t. and poured into water (10 mL). The resulting solid was filtered, rinsed twice with water (2 x 10 mL) and MeOH (2 x 5 mL) to provide the final compounds **1-5**.

4-hydroxy-N-(4-hydroxy-3,5-dimethoxy-phenyl)-6-oxo-1,3-diphenyl-2-thioxo-pyrimidine-5-carboxamide (1)

Compound **1** was synthesized from **9** (63.8 mg, 0.51 mmol) as white solid: 15.7 mg (16 %). ¹H NMR (400 MHz, CDCl₃): δ 3.86 (s, 6H), 5.47 (s, 1H), 6.76 (s, 2H), 7.31 (dd, $J_1 = 7.4$ Hz, $J_2 = 3.1$ Hz, 4H), 7.47–7.58 (m, 6H), 11.82 (s, 1H). ¹³C NMR (100 MHz, CDCl₃): δ 178.59, 168.63, 162.39, 147.22, 139.26, 138.16, 137.04, 133.42, 129.87, 129.76, 129.36, 129.15, 128.77, 128.63, 127.34, 99.60, 56.59. MS (ESI⁺): m/z 492 [M+H]⁺.

4-hydroxy-N-(4-hydroxyphenyl)-6-oxo-1,3-diphenyl-2-thioxo-pyrimidine-5-carboxamide (2)

Compound **2** was synthesized from 4-aminophenol (30.0 mg, 0.27 mmol) as white solid: 25.1 mg (22 %).

¹H NMR (400 MHz, DMSO-*d*₆): δ 6.78 (d, $J = 8.8$ Hz, 2H), 7.32-7.34 (m, 6H), 7.40 (t, $J = 7.3$ Hz, 2H), 7.48 (t, $J = 7.5$ Hz, 4H), 9.64 (s, 1H), 11.49 (s, 1H). ¹³C NMR (100 MHz, DMSO-*d*₆): δ 178.40, 168.12, 155.76, 139.19, 129.16, 128.98, 128.39, 124.02, 115.69, 83.59. MS (ESI⁺): m/z 432 [M+H]⁺.

4-hydroxy-N-(3-methoxyphenyl)-6-oxo-1,3-diphenyl-2-thioxo-pyrimidine-5-carboxamide (3)

Compound **3** was synthesized from *m*-aniside (0.031 mL, 0.27 mmol) as white solid: 66.1 mg (55 %).

¹H NMR (400 MHz, CDCl₃): δ 3.79 (s, 3H), 6.78 (dd, $J_1 = 8.2$ Hz, $J_2 = 2.4$ Hz, 1H), 7.01-7.13 (m, 2H), 7.27 (d, $J = 4.4$ Hz, 2H), 7.28-7.40 (m, 4H), 7.45–7.52 (m, 2H), 7.52-7.62 (m, 4H), 11.85 (s, 1H). ¹³C NMR (100 MHz, CDCl₃): δ 169.33, 167.83, 160.36,

139.22, 136.31, 130.26, 129.87, 129.77, 129.38, 129.14, 128.75, 128.63, 114.25, 112.31, 107.77, 83.65, 55.57. **MS (ESI⁺):** m/z 446 [M+H]⁺.

4-hydroxy-N-(3-hydroxyphenyl)-6-oxo-1,3-diphenyl-2-thioxo-pyrimidine-5-carboxamide
(4)

Compound **4** was synthesized from 3-aminophenol (30 mg, 0.27 mmol) as white solid: 29.6 mg (26 %).

¹H NMR (400 MHz, CDCl₃): δ 5.08 (s, 1H), 6.76-6.68 (m, 1H), 6.98 (d, J = 8.0 Hz, 1H), 7.13 (s, 1H), 7.24 (t, J = 8.1 Hz, 1H), 7.33 (t, J = 6.9 Hz, 4H), 7.43-7.68 (m, 6H), 11.84 (s, 1H). **¹³C NMR** (100 MHz, CDCl₃): δ 178.29, 169.02, 167.55, 161.96, 156.07, 138.87, 137.76, 136.13, 130.15, 129.56, 129.47, 129.09, 128.84, 128.43, 128.31, 113.96, 113.24, 108.90, 83.38. **MS (ESI⁺):** m/z 432 [M+H]⁺.

4-hydroxy-6-oxo-N,1,3-triphenyl-2-thioxo-pyrimidine-5-carboxamide (5)

Compound **5** was synthesized from aniline (25 μ L, 0.37 mmol) as white solid: 118.4 mg (86 %).

¹H NMR (400 MHz, DMSO-*d*₆): δ 7.24 (t, J = 7.4 Hz, 1H), 7.31-7.36 (m, 4H), 7.37-7.43 (m, 4H), 7.46-7.50 (m, 3H), 7.51-7.57 (m, 2H), 11.65 (s, 1H). **¹³C NMR** (100 MHz, CDCl₃): δ 178.67, 169.32, 167.82, 162.32, 139.22, 138.14, 135.21, 129.88, 129.79, 129.51, 129.39, 129.15, 128.75, 128.63, 126.58, 122.08, 83.61. **MS (ESI⁻):** m/z 414 [M-H]⁻.

Synthesis of 1,3-Diphenyl-2-thiobarbituric acid (6)

Under N₂ atmosphere, methyl 3-chloro-3-oxopropionate (2.1 mL, 18.9 mmol) was dropwise added to a solution of *N,N'*-diphenylthiourea (2.0 g, 8.6 mmol) in dry CH₂Cl₂ (100 mL) and the reaction crude stirred at r.t. for 16 hours. Afterwards, the reaction crude was concentrated to dryness under reduced pressure and the resulting oil stored under vacuum at r.t. until converted into a solid, total time 72 hours. Finally, resulting solid was solved in the minimum CH₂Cl₂ (10 mL) and slowly poured into cold cyclohexane (100 mL). The yellowish precipitate was collected via suction filtration to give **7** as yellow solid: 2.16 g (85 %).

¹H NMR (400 MHz, CDCl₃): δ 4.11 (s, 2H), 7.18-7.25 (m, 4H), 7.39-7.57 (m, 6H). **MS (ESI⁺)**: *m/z* 295 [M-H]⁺.

2,6-dimethoxy-4-nitro-phenol (8)

tert-Butyl nitrite (12.6 mL, 95.36 mmol) was added to a solution of 2,6-dimethoxyphenol (5 g, 31.79 mmol) in THF (160 mL). The reaction was stirred for 30 minutes at r.t. and concentrated to dryness under reduced pressure. The crude compound was purified by gravity chromatography on silica gel column, eluting with cyclohexane:ethyl acetate (from 9:1 to 7:3) afforded the compound **8** as white solid: 1.5 g (24 %).

¹H NMR (400 MHz, CDCl₃): δ 3.98 (s, 6H), 6.08 (s, 1H), 7.57 (s, 2H). **MS (ESI⁺)**: *m/z* 198.1 [M-H]⁺.

4-amino-2,6-dimethoxy-phenol (9)

Under N₂ atmosphere, 1,4-cyclohexadiene (1 mL, 10.04 mmol) was added to the intermediate **8** (100 mg, 0.50 mmol) and palladium on activated carbon (100 mg) suspension in ethanol (10 mL). The mixture was stirred at r.t. for 16 hours, then the catalyst was filtered off through a celite coarse patch. The filtrate was concentrated to dryness at reduced pressure to obtain the compound **9** as white solid: 85 mg (99 %).

¹H NMR (400 MHz, DMSO-*d*₆): δ 3.65 (s, 6H), 4.52 (s, 2H), 5.88 (s, 2H), 7.15 (s, 1H). **MS (ESI⁺)**: *m/z* 168 [M-H]⁺.

5.6.2 Biology

5.6.2.1 Topoisomerase inhibition

0.125 μg of pBR322 (*Inspiralis*) was incubated with increasing concentrations (0.5-200 μM) of tested compounds for 1 hour at 37 °C in the presence/absence of 1 U of human topoisomerase IIα (*Inspiralis*) in the required buffer (1X). Reaction products were resolved on a 1 % agarose gel prepared in 1X TAE (10 mM Tris 1 mM EDTA, 0.1 % acetic acid, pH 8.0). After the electrophoretic run (5 V/cm for about 90 minutes) the DNA bands were visualized by ethidium bromide staining, photographed and quantified using a Geliance 2000 apparatus.

5.6.2.2 Topoisomerase II α poisoning

0.125 μ g of pBR322 (*Inspiralis*) was incubated with increasing concentrations (0.5-200 μ M) of tested compounds for 6 minutes at 37 °C in the presence/absence of 5 U of topoisomerase II α . Then, the reaction was stopped with 0.1 % SDS (Sodium Dodecyl Sulphate, *Sigma*), and finally the enzyme was digested with 1.6 μ g of proteinase K (*Sigma*) in 10 mM Na-EDTA for 30 minutes at 45 °C. Reaction products were resolved on a 1 % agarose gel in 1X TAE (10 mM Tris 1 mM EDTA, 0.1 % acetic acid pH 8.0). The electrophoretic run was performed at 5 V/cm for 90 minutes and then bands were stained with ethidium bromide (0.5 μ g/mL in 1X TAE) photographed and quantified using a Geliance 2000 apparatus.

5.6.2.3 ctDNA binding assay

The UV spectrum (250-350 nm) of the selected compounds was recorded (*Perkin Elmer* spectrophotometer) at 50 μ M in 10 mM Tris 50 mM KCl buffer. Then, each compound was titrated with ctDNA (*Sigma*). The UV absorbance contribution of ctDNA in the selected range was compensated by adding the same amount of DNA in the sample and reference cells. The spectra were recorded and the variation of the absorbance at 290 nm caused by a 4-fold excess of ctDNA was considered for DNA binding evaluation.

5.6.2.4 Circular Dichroism titration of ctDNA binding assay

The CD spectrum (230-330 nm) of 88 μ M ctDNA (residue concentration) was acquired in a on a JASCO J-810 spectropolarimeter in 10 mM Tris, 50 mM KCl buffer. Then, increasing concentrations of each compound were added and the corresponding spectrum was acquired. Observed ellipticities were converted to molar ellipticity (Mol. Ellip.)

5.6.2.5 Cell viability assay

To measure the antiproliferative activity of the compounds, cell viability was measured using the MTT assay. Cells were seeded in 96 well plates at a density of 5000 cells/well (A549 and DU-145), 10000 cells/well (MCF7) or 2500 cells/well (HeLa) and after 24 hours were treated with compounds or vehicle (DMSO, final concentration 0.5 %) as control. After 72 hours of treatment, MTT solution was added to a final concentration of 0.5 mg/mL

and cells were further incubated for 2 hours. Insoluble formazan crystals were solubilized by the addition of a 10 % SDS/0.01 N HCl solution and absorbance measured at 570 nm (reference 690 nm) in a plate reader (Infinite M200, Tecan). Inhibition curves consisted of 9 serial dilutions in triplicate in each case, and results were analyzed as sigmoidal dose–response curves using GraphPad Prism software (version 5.03). Values are reported as the mean \pm SD of two independent experiments.

5.6.2.6 Immunodetection of H2AX phosphorylation

HeLa cells were seeded in 6 well plates at a density of 0.5×10^6 cells/well and the following day were treated with etoposide, compound **5** or DMSO as control (final concentration 0.3 %) for 90 minutes. The concentration of etoposide and compound **5** were 2.5 and 10 μ M, respectively (IC₅₀ concentration). After exposure to the compounds, media was removed, and the cells were quickly washed with cold PBS, detached, pelleted by centrifugation, frozen immediately and stored at -80 °C. Proteins were extracted using RIPA buffer including protease and phosphatases inhibitors and protein concentration was measured using the Bradford assay (*BioRad*). Thirty mg protein were then separated by electrophoresis using NuPAGE 4-12 % precast gels (*Invitrogen*) and transferred into nitrocellulose membranes. After blocking for 1 hour with 5 % milk in 20 mM Tris HCl pH 7.6 buffer containing 150 mM NaCl and 0.1 % Tween 20 (TBST), primary antibodies (anti-phospho-H2AX antibody (Ser139) at 1:1000 dilution; Cell Signaling Technology, #9718S; anti-GAPDH at 1:2500 dilution; *Sigma*) were applied and incubated overnight at 4 °C. Membranes were then washed several times in TBST and incubated with secondary antibodies conjugated to HRP for 1 hour at r.t. *LightBlot*® Extend chemiluminescent substrate (*Euroclone*) was applied and images were obtained using an ImageQuant LAS-4000 (*Fujitsu*) apparatus.

5.6.3 Molecular modeling

The grid for docking the compounds was centered at the centroid of nucleotides T₊₁ (PDB ChainD) and G₊₅ (PDB ChainF), whose bases enclose the aglycone core of etoposide (PDB Chain A). Docking calculations were performed with Glide software of the Schrodinger suite 9.3, using the extra precision (XP) scoring function.²⁰⁸ The maximum size of the

docked ligands was set to 24 Å. At first, the docking protocol was tested on etoposide, which is the co-crystallized ligand in 3QX3. Then, compounds **1-5** were docked and the resulting poses analyzed.

Chapter 6 - Inhibition of human topoisomerase II α by 4-

Amino-2-pyrido-bicyclic pyrimidines derivatives

6.1 4-Amino-2-pyrido-bicyclic pyrimidines derivatives

N-heterocycles are compounds largely used in medicinal chemistry. They are found in pharmaceuticals, natural products, dyes, organic materials, and in biologically active molecules.²²⁵ Over the years, there was a strong interest in the development and pharmacology of heteroaromatic organic compounds, such as benzimidazole, benzothiazoles, indole, acridine, oxadiazole, imidazole, quinolones and quinazolines for their diverse activities.²²⁵ Regarding anticancer activity, they have effects in different types of cancer by inhibiting cell growth and induction of cell differentiation and apoptosis. Some *N*-heterocycles compounds have been approved by the US FDA, such as alectinib, lenvatinib, palbociclib, olaparib, vandetanib.²²⁶ Quinazolines display a large spectrum of biological activities, including antibacterial, antifungal, anticonvulsant, anti-inflammatory, anti-HIV, anticancer and analgesic.²²⁵ These compounds have attracted the attention of the pharmaceutical research for their action against the epidermal growth factor receptor (EGFR) tyrosine kinase. Inhibition of this receptor kinase has been identified as a tactical strategy in controlling tumor proliferation, and intensive research in this field has led to the discovery and subsequent approvals of two important drugs for the treatment of non-small cell lung cancer, gefitinib and erlotinib (Figure 6.1).^{227, 228}

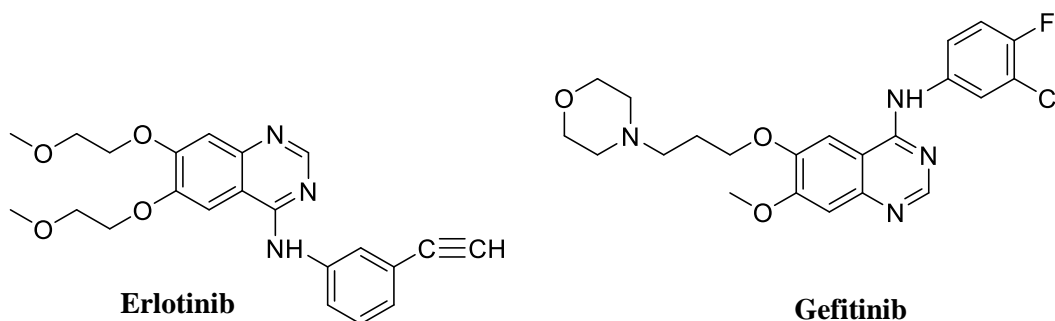


Figure 6.1. Structures of erlotinib and gefitinib.

In 2005, Katiyar and co-workers designed and synthesized a series of 2,4,6-trisubstituted pyrimidine derivatives as a new class of antifilarial topoisomerase II inhibitors.²²⁹ All synthesized compounds were tested for their inhibitory activity against topoisomerase II.

Compounds **A-G** (Figure 6.2) showed 60-80% inhibition at 40 $\mu\text{g/mL}$ and 20 $\mu\text{g/mL}$ concentration. Among them, five compounds (**C-E** and **F, G**) exhibited 70-80% inhibition at 10 $\mu\text{g/mL}$, and three compounds (**D, E** and **G**) have shown 40-60% inhibition at 5 $\mu\text{g/mL}$ concentration. These values were then compared to those of the standard antifilarial drug (diethylcarbamazine) and topoisomerase II inhibitors (novobiocin, nalidixic acid), showing that they were better inhibitors of the enzyme. In the light of the above, they suggested that amino groups such as the 4-aminophenyl group at position 2 play a key role for the inhibitory activity against the topoisomerase II.²²⁹

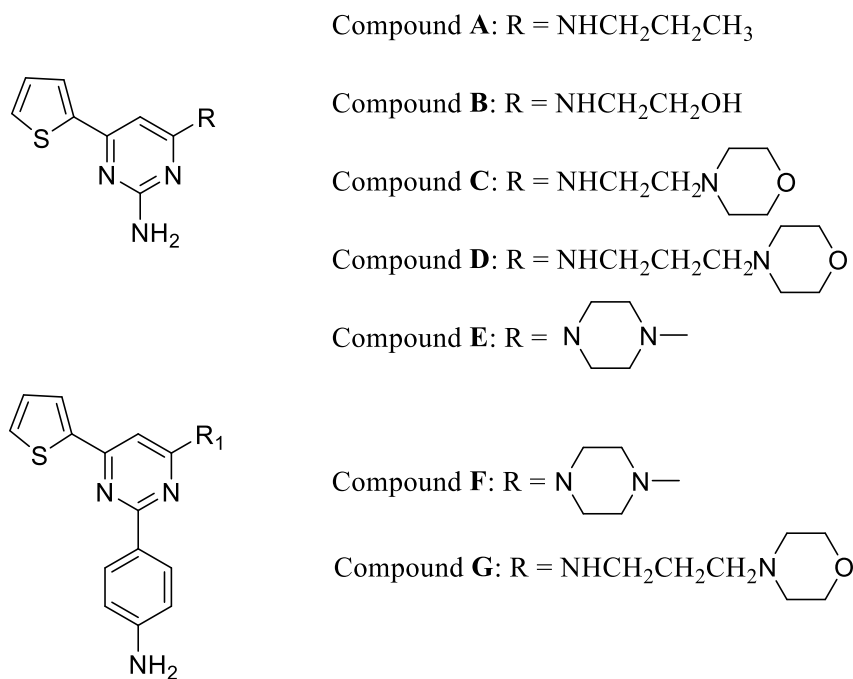


Figure 6.2. Structures of compounds **A-G**.

In 2011, Marzaro and co-workers synthesized a new series of benzo[*h*]quinazoline and benzo[*f*]quinazoline derivatives bearing the dimethylaminoethyl substituent. Compounds **H** and **I** (Figure 6.3) inhibited the relaxation ability of topoisomerase II in a concentration-dependent manner. Since they are not able to stabilise the formation of double strand breaks, they were defined as possible topoisomerase II catalytic inhibitors. Furthermore, both benzoquinazoline nuclei intercalate between DNA base pairs, by forming a complex with the nucleic acid.²³⁰

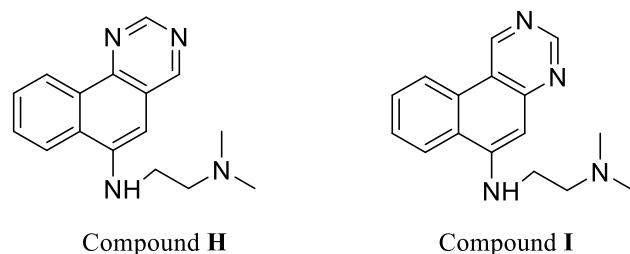


Figure 6.3. Structures of compounds **H** and **I**.

In the same year, Le and co-workers designed the 4-amino-2-phenylquinazolines as the bioisosteres of 3-arylisoquinolines, demonstrating their activity against topoisomerase I. Compounds **L** and **M** (Figure 6.4) showed potent cytotoxicities as well as a good topoisomerase I inhibitory activity. Docking of compound **M** suggested the probable interaction mode of the compound in the binding site of the complex between topoisomerase I and DNA. Furthermore, since the 2-phenyl ring of the 4-amino-2-phenylquinazolines was parallel to the quinazolinone ring, it was able to improve the DNA intercalation ability in the DNA-topoisomerase I complex.²³¹

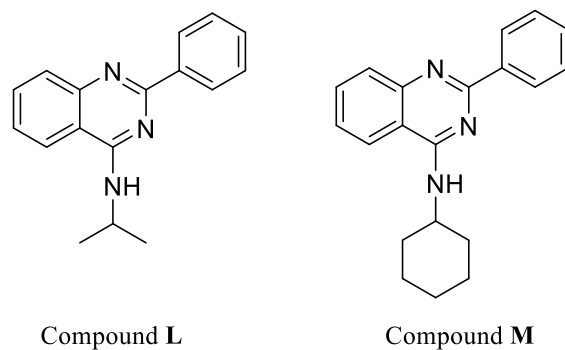


Figure 6.4. Structures of compounds **L** and **M**.

Based on this work, in 2015 Khadka and co-workers designed and synthesized 2-arylquinazolinone derivatives with the aim of obtaining new compounds to evaluate the inhibitory effects on topoisomerases.²³² They monitored the inhibition of these compounds at two different concentrations, 100 μM and 20 μM .

In particular, they found that an amino group in position 6 improved solubility and affected other pharmacological properties. Compounds **N** and **O** (Figure 6.5) are an example of these compounds that showed cytotoxicity and topoisomerase I inhibition.²³²

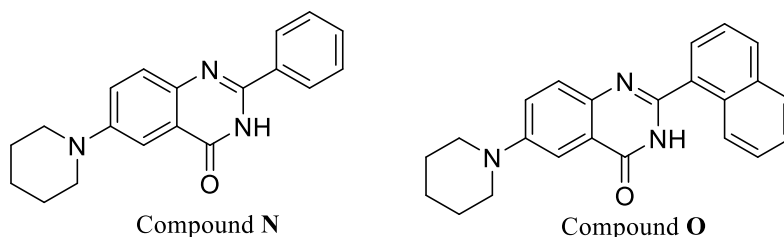


Figure 6.5. Structures of compounds **N** and **O**.

6.2 Drug design

An important goal of my present and future work is to find new potent topoisomerase II-targeting inhibitors with α isoform selectivity in order to reduce the risks of secondary malignancy and other toxicities. Thus, strong topoisomerase II inhibition, regardless the molecular mechanism implicated, is the primary aim of the research in this field of the anticancer therapy. In this regard, the design of compounds with molecular and cellular selectivities is more important than to have higher cytotoxicity. As described above, the quinazoline moiety represents an important core in medicinal chemistry. In recent years, the FDA has approved several quinazoline derivatives as anticancer drugs, such as lapatinib, gefitinib and erlotinib. Based on these considerations, we designed a series of 4-amino-2-pyrido-bicyclic pyrimidines with the aim of obtaining more potent entities active against topoisomerase II α . We focused attention on seven selected compounds of this series (Figure 6.6). In order to investigate the role of the amine function in position 6 of the bicyclic core, we synthesized tetrahydrobenzo-pyrimidine (compounds **1** and **5**), tetrahydropirido-pyrimidine (compound **3**), quinazoline (compound **2**), and 6-amino-quinazoline (compounds **4**, **6** and **7**) derivatives functionalised in position 4 with aliphatic or aromatic amines. In particular, in this position we inserted a *m*-fluoroaniline (compounds **1-4**), a 4-amino-*N,N*-dimethylaniline (compound **5**), a morpholine (compound **6**) and piperidine (compound **7**) rings.

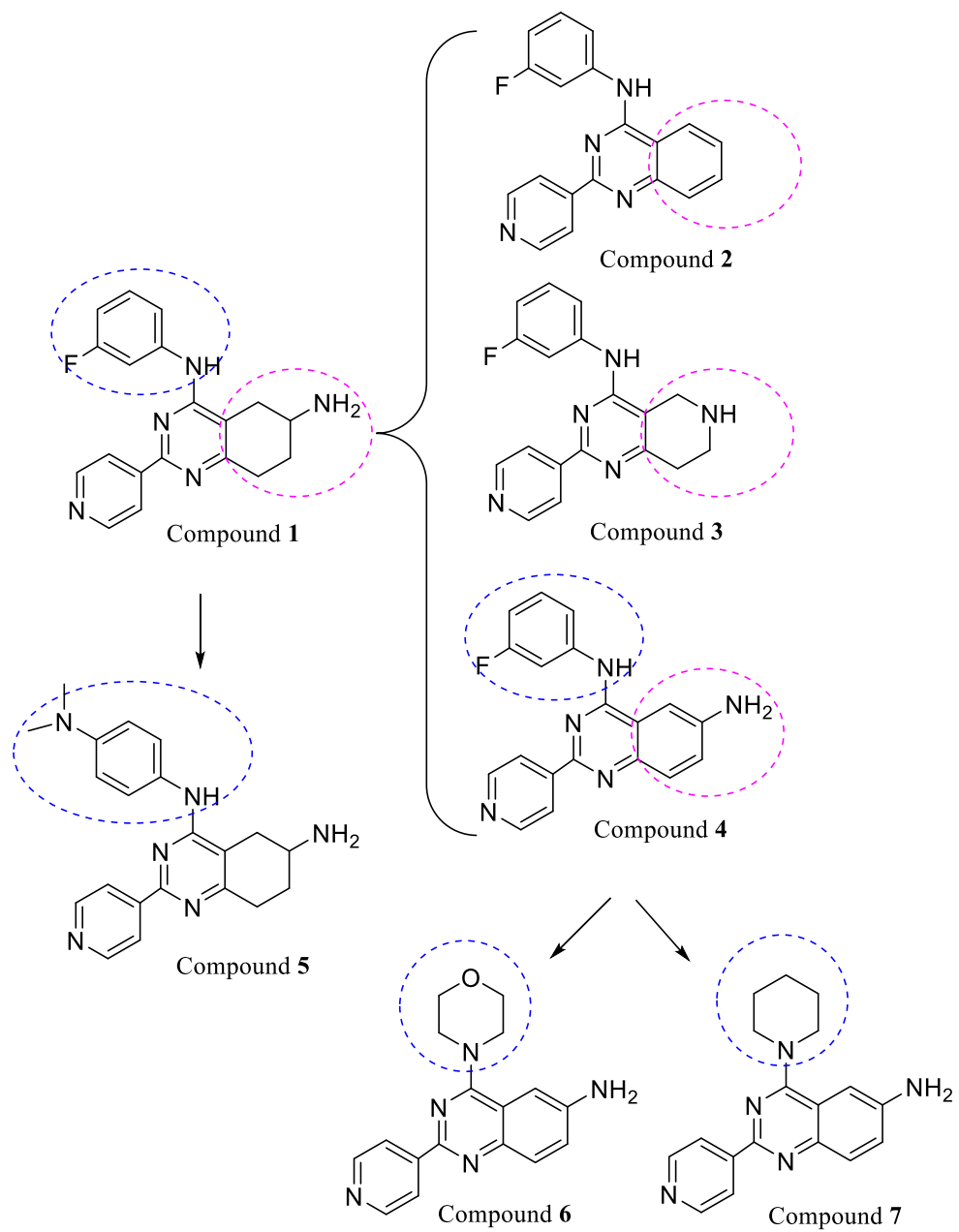


Figure 6.6. Structures of 4-amino-2-pyrido-bicyclic pyrimidine conjugates **1-7**.

6.3 Methods

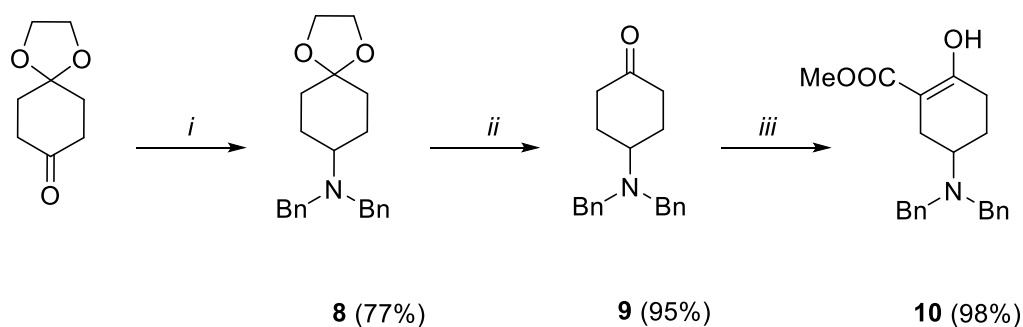
6.3.1 Chemistry

The final compound **5** was synthesized according to the Schemes 6.1 and 6.2.

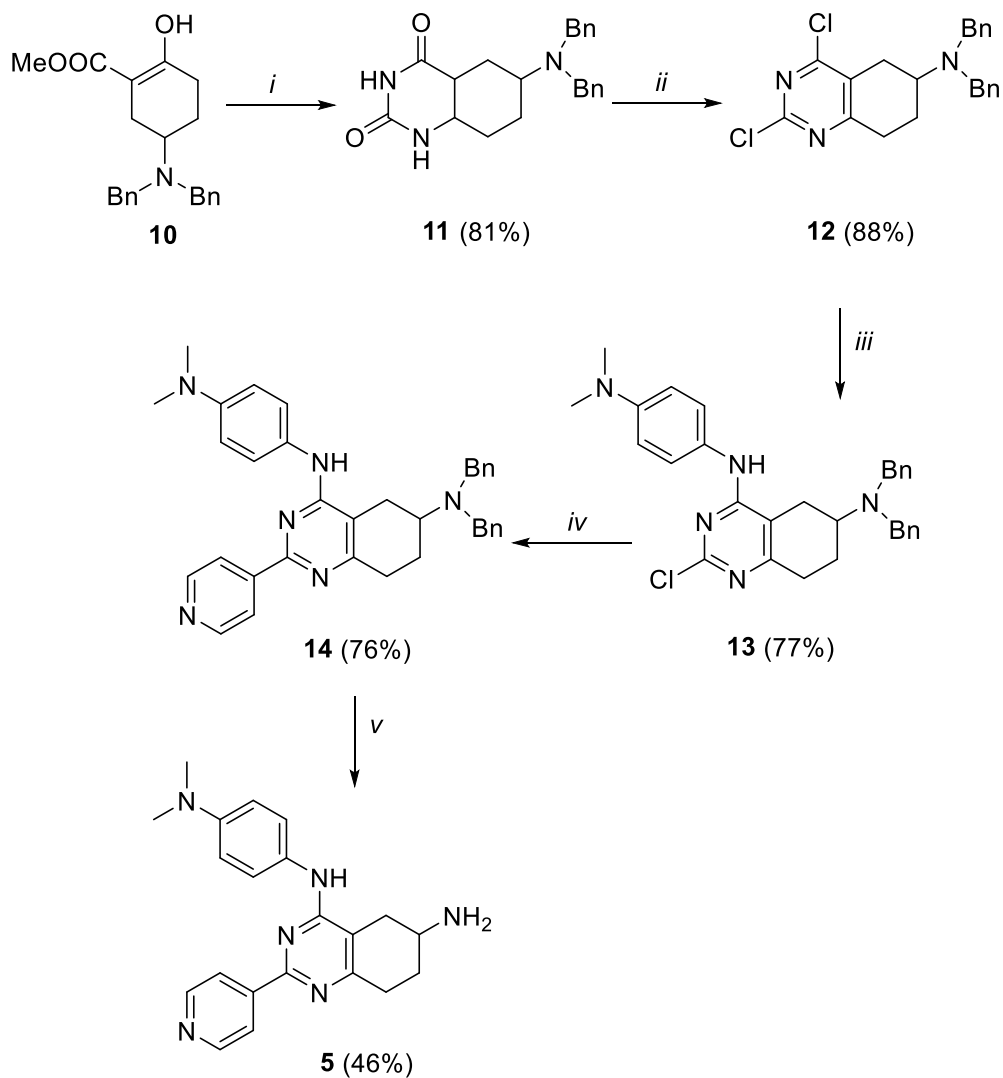
Compound **11** was obtained by amination of compound **10** with urea under basic reaction conditions, following the synthetic procedure reported in literature.²³³ Then, the chlorination of compound **11** was performed by refluxing this intermediate in excess of POCl₃ to provide the desired intermediate **12**, functionalized with chlorine in positions 2 and 4. This reaction results in conversion of the OH⁻ poor leaving group into a good one. The resulted dichloro derivative (**12**) was treated with 4-amino-*N,N*-dimethylaniline in 2-propanol and converted in **13** through the nucleophilic aromatic substitution that was carried out and optimized by microwave assisted synthesis. Even if both chlorinated positions are activated, by carrying out the reaction in the presence of diisopropylethylamine (DIPEA), able to neutralize the hydrochloric acid released during the reaction, and in excess of 4-amino-*N,N*-dimethylaniline we obtained only the 4-substituted compound **13**.

A Suzuki-Miyaura *cross-coupling* protocol was set out leading to the intermediate **14**. The mechanism of palladium-catalyzed *cross-coupling* reaction involves three steps: 1) oxidative addition, 2) transmetalation, and 3) reductive elimination. As a first oxidative step of electrophile (R''-X, where X is a good leaving group) addition to an electron-rich Pd(0)-species producing an organopalladium (II)-complex. Transmetalation of an organometallic reagent (R'M) leads to the formation of a mixed diorgano-Pd(II) complex. The carbon-carbon bond formation upon reductive elimination regenerates the initial Pd(0) catalyst, with subsequent release of the coupling product (R'-R''). This reaction requires the presence of a base, such as K₂CO₃, used to facilitate the otherwise transmetalation of the boronic acid by forming a more reactive boronate species that can interact with the Pd center.²³⁴ In order to increase the yields, the Suzuki reaction was carried out by using the MW apparatus. Finally, the intermediate **14** through a hydrogenolysis of benzyl group by using a Pearlman's catalyst, Pd(OH)₂/C was converted in the final compound **5**.

The intermediate dibenzylate **8** was obtained by reductive amination reaction, from the commercial 1,4-cyclohexanedione monoethylene acetal. This was reacted with dibenzylamine and the obtained Schiff base was reduced to the corresponding amine **8**. Through acidic deprotection **8** was then converted in **9**. Finally, formation of **10** has been accomplished in 98% yield upon treatment of **9** with sodium hydride in dry THF and then with dimethylcarbonate.



Scheme 6.1. Reagents and conditions: (i) HNBn_2 , $\text{NaBH}(\text{OAc})_3$, 1,2-dichloroethane, r.t., 16 hours; (ii) HCl 2M, THF, N_2 , reflux, 4 hours; (iii) dimethylcarbonate, KH , NaH , THF, N_2 , r.t. to reflux, 3 hours.



Scheme 6.2. Reagents and conditions: (i) urea, MeONa, EtOH, N₂, reflux, 5 hours; (ii) POCl₃, N₂, reflux, 5 hours; (iii) 4-amino-*N,N*-dimethylaniline, DIPEA, isPrOH, N₂, MW, 80 °C, 1,4-dioxane; (iv) pyridine-4-boronic acid, PdCl₂(dppf).CH₂Cl₂, K₂CO₃, 1,4-dioxane, Ar, MW., 100 °C, 2 hours; (v) HCOONH₄, Pd(OH)₂-C, MeOH, Ar, reflux, 4 hours.

6.3.2 Biology

All the molecules were tested for their activity against topoisomerase II α . The activity of compound **5** was further investigated in order to determine its mechanism of action.

6.4 Results and discussion

The effect of these compounds (**1-7**) on DNA cleavage and DNA relaxation were assessed. None of the synthesized compounds displayed an ability to increase levels of DNA cleavage, but they all inhibited the overall catalytic activity (as monitored by DNA relaxation assays) of topoisomerase II α (data shown only for compound **5**, Figure 6.7). This result suggested that they act primarily as inhibitors of the enzyme.

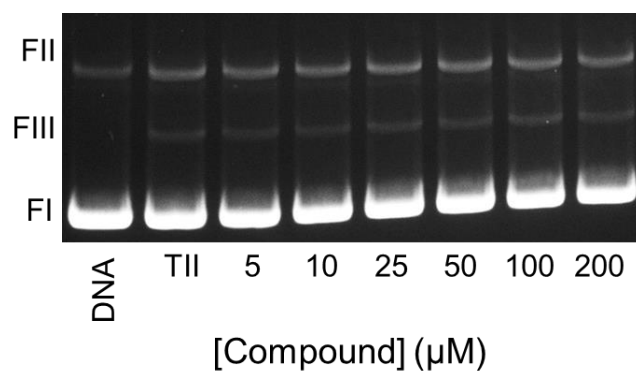


Figure 6.7. Effect of compound **5** (5 μ M, 10 μ M, 25 μ M, 50 μ M, 100 μ M and 200 μ M) on DNA cleavage mediated by topoisomerase II α . DNA cleavage levels were calculated relative to control reaction that contained no drug (TII). The positions of negatively supercoiled (form I, FI), nicked (form II, FII) and linear (form III, FIII) DNA are indicated. Gel is representative of 2 independent experiments.

Among them, compound **5** displayed an $IC_{50} \sim 2 \mu$ M, resulting the most potent derivative (Figure 6.8). These data identify the role of the substituent in position 4. In fact, the inhibitory activity decreased significantly with *m*-fluoroaniline, or piperidine, or morpholine rings, suggesting that the 4-amino-*N,N*-dimethylaniline lead to a derivative (compound **5**) with a better activity profile against topoisomerase II α . To confirm this result, the effect of compound **5** on the overall catalytic activity of the enzyme was monitored also using a decatenation assay (Figure 6.9). Compound **5** was tested up to 50 μ M and, even if the IC_{50} value was relatively higher than observed in the relaxation assay, it was found to be inhibitor of the catalytic activity of topoisomerase II α . As discussed above, topoisomerase II α catalytic inhibitors can be grouped as intercalative or non-intercalative.

To determine whether the inhibition of this compound was due to the activity against the enzyme, rather than to the DNA binding, the ability of **5** to intercalate into relaxed plasmid DNA was determined (Figure 6.10). We found no evidence of DNA intercalation by this derivative.

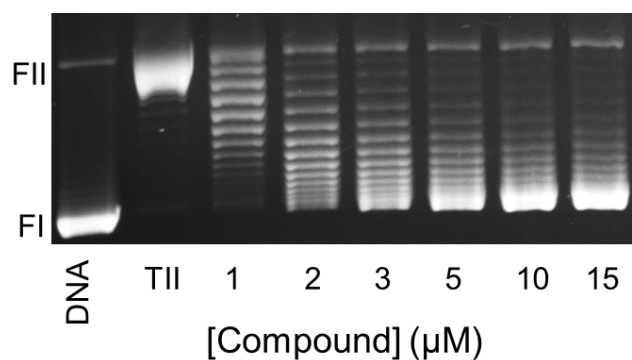


Figure 6.8. Effect of compound **5** (1 μM , 2 μM , 3 μM , 5 μM , 10 μM and 15 μM) on DNA relaxation catalyzed by topoisomerase II α . Assays containing intact negatively supercoiled DNA in the absence of topoisomerase II α (DNA) or negatively supercoiled DNA treated with topoisomerase II α in the absence of compound **5** (TII) are shown as controls. The positions of negatively supercoiled (form I, FI) and nicked (form II, FII) DNA are indicated. Gel is representative of 6 independent experiments.

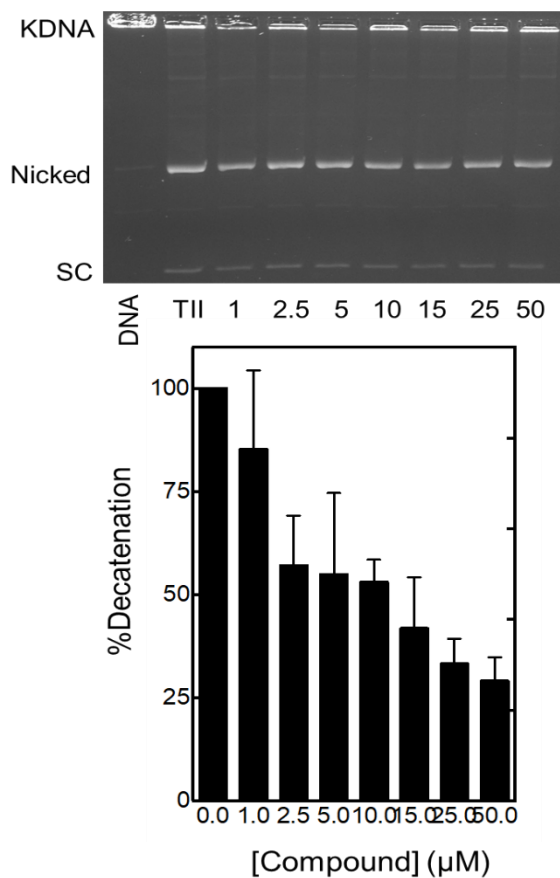


Figure 6.9. Effect of compound **5** (1 μM , 2.5 μM , 5 μM , 10 μM , 15 μM , 25 μM and 50 μM) on DNA decatenation catalyzed by topoisomerase II α . Assays containing intact kDNA in the absence of topoisomerase II α (DNA) or kDNA treated with topoisomerase II α in the absence of compound **5** (TII) are shown as controls. The positions of intact kDNA at the origin (kDNA), decatenated nicked kDNA minicircles, and decatenated supercoiled (SC) kDNA minicircles are indicated. Gel is representative of 5 independent experiments. Quantification of results is shown in the bar graphs at the bottom. Levels of decatenation in the absence of compound **5** was set to 100%. Error bars represent standard deviations for 3 independent experiments.

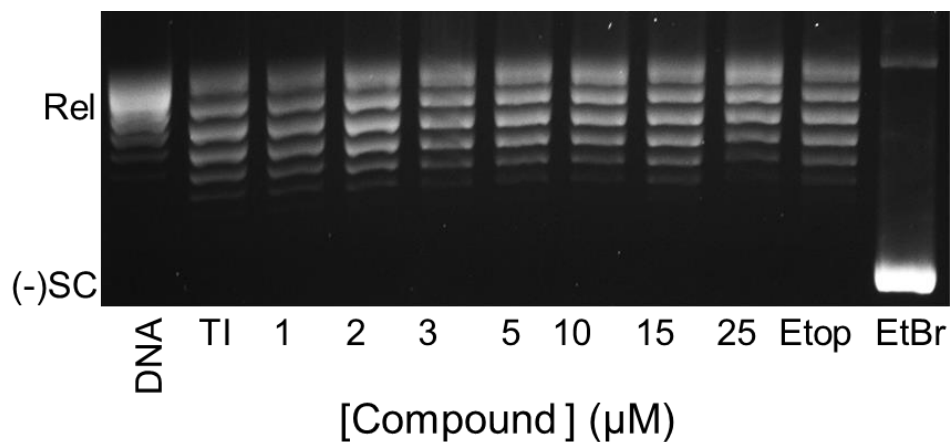


Figure 6.10. Intercalation of compound **5** (1 μM , 2 μM , 3 μM , 5 μM , 10 μM , 15 μM and 25 μM) into relaxed DNA. Result of topoisomerase I-DNA unwinding assay is shown. Intercalation is indicated by the shift in the position of the plasmid from relaxed (Rel) to negatively supercoiled [(-)SC] DNA. A strong intercalator, ethidium bromide (10 μM), and a non-intercalator etoposide (100 μM), are shown as positive and negative controls, respectively. Assays that contained only the relaxed DNA substrate (DNA) or relaxed DNA and topoisomerase I with no compound (TI) are shown. Gel are representative of three independent experiments.

6.5 Conclusion

There is an urgent need for the development of new anticancer drugs. Through the present study we determined that the new scaffold 4-amino-2-pyrido-bicyclic pyrimidine has a good catalytic activity against human topoisomerase II α . In particular, the tetrahydrobenzopyrimidine derivative **5** emerged as the most potent of the series, suggesting the crucial role of the aryl substituent in position 4 of the central core.

Ongoing studies on this compound and its analogues should allow us to shed lights on the mechanism of action, as well as to identify the best substituents for optimal inhibitory activity.

Having a greater understanding of the mechanism may allow us for further synthesis and optimization of more active derivatives.

6.6 Experimental section

6.6.1 Chemistry

Chemical reagents were purchased from Sigma Aldrich. All reactions were performed with dry glassware under a nitrogen atmosphere unless otherwise noted. Nuclear magnetic

resonance spectra (NMR) were recorded at 400 MHz for ^1H and 100 MHz for ^{13}C on Varian VXR 400 spectrometer in CDCl_3 , DMSO or CD_3OD as solvents. Chemical shifts (δ) are given in ppm from tetramethylsilane (TMS) with the solvent resonance as internal standard (CDCl_3 : δ 7.26, DMSO: δ 2.50, CD_3OD : δ 3.31 for ^1H -NMR and CDCl_3 : δ 77.16, DMSO: δ 39.52, CD_3OD : δ 49.00 for ^{13}C -NMR). For ^1H -NMR, data are reported as follows: chemical shift, multiplicity (s = singlet, d = doublet, dd = double of doublets, t = triplet, q = quartet, m = multiplet, p = pentet, dt = doublet of triplets, td = triplet of doublets, tt = triplet of triplets, qd = quartet of doublets, br s = broad singlet), coupling constants (Hz) and integration. Microwave assisted synthesis was performed by using CEM Discover® SP apparatus (2.45 GHz, maximum power of 300W). Electron spray ionization (ESI) mass spectra were recorded on Varian VG 7070E instrument. Chromatographic separations were performed on silica gel columns by flash or gravity column (Kieselgel 40, 0.040-0.063 mm; Merck) chromatography. Reactions were followed by thin-layer chromatography (TLC) on Merck (0.25 mm) glass-packed pre-coated silica gel plates (60 F254) that were visualized in an iodine chamber, or with a UV lamp, KMnO_4 , or bromocresol green. All the names were attributed by Chem BioDraw Ultra 16.0.

N,N-dibenzyl-1,4-dioxaspiro[4.5]decan-8-amine (**8**)

A solution of 1,4-cyclohexanedione monoethylene acetal (5 g, 31.05 mmol) in dry 1,2-dichloroethane (129 mL), dibenzylamine (6.3 mL, 31.05 mmol) and acetic acid (1.8 mL, 31.05 mmol) was stirred for 15 minutes at r.t. Then $\text{NaBH}(\text{OAc})_3$ (10.40 g, 46.58 mmol) was portionwise added and the reaction mixture stirred at r.t. for 16 hours, afterwards was diluted with CH_2Cl_2 (100 mL) and extracted with NaHCO_3 10 % solution (100 mL). The aqueous layer was extracted twice with CH_2Cl_2 (2 x 100 mL), combined organic layers were dried over Na_2SO_4 and concentrated to dryness at low pressure. The crude compound was purified by gravity chromatography on silica gel column, eluting with cyclohexane:TBME (from 10:0 to 9:1) afforded the compound **8** as white solid: 8.07 g (77 %).

^1H NMR (400 MHz, CDCl_3) δ 1.45 (td, $J_1 = 13.0$ Hz, $J_2 = 4.3$ Hz, 2H), 1.67 (td, $J_1 = 12.5$ Hz, $J_2 = 3.5$ Hz, 2H), 1.72-1.81 (m, 2H), 1.82-1.90 (m, 2H), 2.57 (tt, $J_1 = 11.5$ Hz, $J_2 = 3.6$

Hz, 1H), 3.64 (s, 4H), 3.87-3.96 (m, 4H), 7.16-7.24 (m, 2H), 7.28 (dd, $J_1 = 8.5$ Hz, $J_2 = 7.0$ Hz, 4H), 7.33-7.39 (m, 4H). **MS (ESI⁺):** m/z 338 [M+H]⁺.

4-(dibenzylamino)cyclohexanone (9)

HCl 2M solution (62 mL, 124.70 mmol) was added to a of *N,N*-dibenzyl-1,4-dioxaspiro[4.5]decan-8-amine (8.07 g, 23.19 mmol) solution in THF (62 mL). The reaction mixture was stirred under N₂ atmosphere at reflux temperature for 4 hours, then cooled in an ice/water bath, basified with NaOH 5M solution, extracted with ethyl acetate (3 x 50 mL), combined organic layers dried over Na₂SO₄ and concentrated to dryness at low pressure. The crude compound was purified by gravity chromatography on silica gel column, eluting with cyclohexane:TBME (from 10:0 to 9:1) afforded the compound **9** as white solid: 6.46 g (95 %).

¹H NMR (400 MHz, CDCl₃) δ 1.78-1.88 (m, 2H), 2.14-2.20 (m, 2H), 2.22-2.31 (m, 2H), 2.39 (p, $J = 2.4$ Hz, 1H), 2.43 (p, $J = 2.4$ Hz, 1H), 3.02 (tt, $J_1 = 11.5$ Hz, $J_2 = 3.4$ Hz, 1H), 3.66 (s, 4H), 7.20-7.26 (m, 2H), 7.28-7.34 (m, 4H), 7.35-7.40 (m, 4H). **MS (ESI⁺):** m/z 294 [M+H]⁺.

Methyl 5-(dibenzylamino)-2-hydroxy-cyclohexene-1-carboxylate (10)

Under N₂ atmosphere, a solution of 4-(dibenzylamino)cyclohexanone (6.2 g, 20.50 mmol) in THF (2.5 mL) was dropwise added to a suspension of KH (5.26 g, 65.59 mmol) and NaH (0.41 g, 16.40 mmol) in dry tetrahydrofuran (256 mL) at r.t. The reaction mixture was stirred for 30 minutes and dimethyl carbonate was added (5.9 mL, 69.08 mmol), then stirred at reflux temperature under for 3 hours, cooled to r.t., added to cold NaHCO₃ saturated solution (100 mL), the organic layer separated, the aqueous one extracted with ethyl acetate (3 x 100 mL), the combined organic layers dried over Na₂SO₄ and concentrated to dryness at low pressure. The crude compound was purified by gravity chromatography on silica gel column, eluting with cyclohexane:TBME (from 10:0 to 9:1) afforded the compound **10** as white solid: 7.06 g (98 %).

¹H NMR (400 MHz, CDCl₃) δ 1.57-1.74 (m, 1H), 1.94-2.05 (m, 1H), 2.18-2.43 (m, 3H), 2.44-2.54 (m, 1H), 2.73-2.88 (m, 1H), 3.62 (d, $J = 14.0$ Hz, 2H), 3.72 (d, $J = 14.0$ Hz, 2H),

3.76 (s, 3H), 7.18-7.24 (m, 2H), 7.29 (dd, $J_1 = 8.3$ Hz, $J_2 = 6.7$ Hz, 4H), 7.34-7.42 (m, 4H), 12.06 (s, 1H). **MS (ESI⁺):** m/z 352 [M+H]⁺.

6-(dibenzylamino)-5,6,7,8-tetrahydro-1H-quinazoline-2,4-dione (11)

A suspension of **10** (7.04 g, 20.03 mmol) in ethanol (90.14 mL), urea (6.02 g, 100.15 mmol) and sodium methoxide (4.87 g, 90.14 mmol) was stirred at reflux temperature for 16 hours. Afterwards the reaction crude was concentrated to dryness at low pressure, resulting solid triturated in water (10.02 mL), ice cooled, pH adjusted to 8-9 with concentrated HCl and filtered. The crude was then rinsed with MeOH (10.02 mL) and diethyl ether (10.02 mL) to afford **11** as brown solid: 5.87 g (81%).

¹H NMR (400 MHz, DMSO-*d*₆) δ 1.64 (qd, $J_1 = 12.1$ Hz, $J_2 = 5.6$ Hz, 1H), 1.93-2.06 (m, 1H), 2.11-2.25 (m, 1H), 2.22-2.37 (m, 1H), 2.37-2.48 (m, 2H), 2.61-2.76 (m, 1H), 3.59 (d, $J = 14.2$ Hz, 2H), 3.67 (d, $J = 14.2$ Hz, 2H), 7.20 (t, $J = 7.2$ Hz, 2H), 7.30 (t, $J = 7.2$ Hz, 4H), 7.36 (d, $J = 7.2$ Hz, 4H), 10.56 (br s, 1H exchangeable with D₂O), 10.85 (br s, 1H exchangeable with D₂O). **MS (ESI⁺):** m/z 362 [M-H]⁻.

N,N-dibenzyl-2,4-dichloro-5,6,7,8-tetrahydroquinazolin-6-amine (12)

A suspension of **11** (5.86, 16.62 mmol) in POCl₃ (2.32 mL, 24.93 mmol) was stirred at 120 °C under N₂ atmosphere until total solution was observed. POCl₃ was then evaporated under reduced pressure and resulting residue solved in CH₂Cl₂ (50 mL), poured onto ice cold NaHCO₃ saturated solution (300 mL). The pH was adjusted until 7-8 with NaHCO₃ (no gas evolution was observed after addition) and the aqueous layer was extracted with CH₂Cl₂ (3 x 50 mL). The combined organic layers were dried over Na₂SO₄ and concentrated to dryness at low pressure to give **12** as yellow solid: 5.69 g (88%)

¹H NMR (400 MHz, CDCl₃) δ 1.56-2.01 (m, 2H), 2.12-2.42 (m, 1H), 2.65-2.87 (m, 2H), 2.88-3.02 (m, 1H), 3.00-3.19 (m, 1H), 3.69 (d, $J = 13.7$ Hz, 2H), 3.82 (d, $J = 13.7$ Hz, 2H), 7.23 (d, $J = 7.4$ Hz, 2H), 7.32 (t, $J = 7.4$ Hz, 4H), 7.41 (d, $J = 7.4$ Hz, 4H). **MS (ESI⁺):** m/z 398 [M+H]⁺.

*N*₆,*N*₆-dibenzyl-2-chloro-*N*₄-[4-(dimethylamino)phenyl]-5,6,7,8-tetrahydroquinazoline-4,6-diamine (**13**)

A suspension of **12** (250 mg, 0.63 mmol), 4-amino-*N,N*-dimethylaniline (0.09 mL, 0.69 mmol) and DIPEA (0.352 mL, 3.15 mmol) in 2-propanol (1.26 mL) was placed in a microwave apparatus (100 °C, 247 Psi, 200 Watt) for 16 hours. The solvent was removed under reduced pressure and the residue was portioned between CH₂Cl₂ (12.60 mL) and NaHCO₃ saturated solution (12.60 mL). The combined organic phases were dried over with Na₂SO₄ and concentrated under reduced pressure. The crude compound was purified by gravity chromatography on silica gel column, eluting with cyclohexane:ethyl acetate (from 10:0 to 7:3) to give compound **13** as white solid: 240 mg (77%).

¹H NMR (400 MHz, CDCl₃) δ 1.43 (s, 6H), 1.74 (qd, *J*₁ = 12.3 Hz, *J*₂ = 5.1 Hz, 1H), 2.16-2.30 (m, 1H), 2.48 (s, 2H), 2.58-2.73 (m, 1H), 2.81-3.01 (m, 1H), 3.01-3.16 (m, 1H), 3.66 (d, *J* = 14.0 Hz, 2H), 3.84 (d, *J* = 14.1 Hz, 2H), 6.28 (s, 1H), 6.72 (s, 2H), 7.24 (t, *J* = 7.4 Hz, 2H), 7.34 (dt, *J*₁ = 14.7, *J*₂ = 8.1 Hz, 6H), 7.42 (d, *J* = 7.5 Hz, 4H). MS (ESI⁺): *m/z* 498 [M+H]⁺.

*N*₆,*N*₆-dibenzyl-*N*₄-(3-fluorophenyl)-2-(4-pyridyl)-5,6,7,8-tetrahydroquinazoline-4,6-diamine (**14**)

A suspension of **13** (240 mg, 0.48 mmol), pyridine-4-boronic acid (85.7 mg, 0.58 mmol), PdCl₂(dppf) dichloromethane complex (39.20 mg, 0.048 mmol) and K₂CO₃ 2 M solution (0.48 mL, 0.96 mmol) in 1,4-dioxane (4.8 mL) was stirred in a microwave apparatus (120 °C, 247 Psi, 200 Watt) for 2 hours. Resulting crude was portioned between dichloromethane (12 mL) and NaHCO₃ saturated solution (12 mL), the organic layers dried over Na₂SO₄ and concentrated to dryness at low pressure. The crude compound was purified by gravity chromatography on silica gel column, eluting with cyclohexane:ethyl acetate (from 7.5:2.5 to 5:5) to afford **14** as white solid: 197 mg (76%).

¹H NMR (400 MHz, DMSO-*d*₆) δ 1.81 (qd, *J*₁ = 12.3 Hz, *J*₂ = 5.1 Hz, 1H), 2.14 (d, *J* = 12.1 Hz, 1H), 2.60-2.76 (m, 2H), 2.78-2.89 (m, 2H), 2.91 (s, 6H), 2.92-3.02 (m, 1H), 3.69 (d, *J* = 14.2 Hz, 2H), 3.79 (d, *J* = 14.2 Hz, 2H), 6.74-6.84 (m, 2H), 7.17-7.25 (m, 2H), 7.32 (t, *J* = 7.5 Hz, 4H), 7.39-7.47 (m, 4H), 7.49-7.57 (m, 2H), 8.01-8.09 (m, 2H), 8.40 (s, 1H), 8.60-8.68 (m, 2H). MS (ESI⁺): *m/z* 541 [M+H]⁺.

*N*₄-[4-(dimethylamino)phenyl]-2-(4-pyridyl)-5,6,7,8-tetrahydroquinazoline-4,6-diamine (**5**) Under N₂ atmosphere, a suspension of **14** (197 mg, 0.48 mmol), ammonium formate (121.15 mg, 1.92 mmol), Pd(OH)₂/C (39.40 mg, 0.281 mmol) was stirred at reflux temperature until reaction completion. Catalyst was filtered off with trough a celite coarse patch and resulting filtrate concentrated under reduced pressure. The crude compound was purified by gravity chromatography on silica gel column, eluting with CH₂Cl₂:MeOH: aq 33% NH₄OH (9:1:0.1), to afford **5** as white solid: 79 mg (46%).

¹H NMR (400 MHz, DMSO-*d*₆) δ 1.90 (p, *J* = 8.2 Hz, 1H), 2.17 (d, *J* = 19.0 Hz, 1H), 2.60 (dd, *J*₁ = 16.6, *J*₂ = 8.8 Hz, 1H), 2.86 (d, *J* = 6.6 Hz, 2H), 2.91 (s, 6H), 2.97 (dd, *J*₁ = 17.0, *J*₂ = 5.4 Hz, 1H), 3.50-3.60 (m, 1H), 6.75-6.84 (m, 2H), 7.44-7.57 (m, 2H), 8.00-8.12 (m, 2H), 8.52 (s, 1H), 8.61-8.73 (m, 2H). **¹³C NMR** (100 MHz, DMSO-*d*₆) δ 160.97, 158.93, 157.76, 150.11, 142.27, 145.34, 128.75, 123.86, 121.31, 112.32, 109.52, 45.74, 40.50, 29.34, 27.82, 26.26. **MS (ESI⁺)**: *m/z* 361 [M+H]⁺.

6.6.2 Biology

6.6.2.1 DNA Intercalation

DNA intercalation assays were carried out using the protocol of Fortune *et al.*²³⁵ Human DNA topoisomerase I (0.5 U) and 0.3 μg of relaxed pBR322 were incubated in 10 mM Tris-HCl, pH 7.5, 10 mM KCl, 2 mM MgCl₂, 0.02 mM EDTA, 0.1 mM dithiothreitol, 6 μg/mL bovine serum albumin. Ethidium bromide (10 μM), a well-characterized intercalator, was used as positive control, and etoposide (100 μM), a non-intercalative topoisomerase II poison, was used as negative control. Reactions were carried out in the presence of 0-25 μM of compound **5**. Mixtures were incubated for 15 minutes at 37 °C. Samples were extracted using 20 μL of phenol:chloroform:isoamyl alcohol (25:24:1), and the aqueous layer was mixed with 2 μL of agarose loading dye and heated for 5 minutes at 45 °C. Reactions were stopped by the addition of 3 μL of 0.77% SDS-77 mM NaEDTA, pH 8.0. Samples were mixed with 2 μL of agarose loading dye, heated for 2 min at 45 °C, and subjected to electrophoresis in a 1% agarose gel in 100 mM Tris-borate, pH 8.3, and 2 mM EDTA. Gels were stained for 30 minutes using 1.0 μg/mL ethidium bromide and rinsed in deionized water. DNA bands were visualized by UV light and quantified using an

Alpha Innotech digital imaging system. DNA intercalation was monitored by the conversion of relaxed to supercoiled plasmid molecules.

For *Cleavage of Plasmid DNA*, *DNA Relaxation* and *Decatenation of kinetoplast DNA* assays refer to Chapter 4.

Abbreviations

AML: acute myeloid leukaemia
APP(NH)P: adenylyl imidodiphosphate
Boc₂O: di-*tert*-butyl dicarbonate
Bp: base-pair
CD: circular dichroism
Ct DNA: calf thymus DNA
ΔLk: linking difference
DFMO: difluoromethylornithine
DIPEA: *N,N*-diisopropylethylamine
DMAP: 4-dimethylaminopyridine
DMF: *N,N*-dimethylformamide
DMSO: dimethyl sulfoxide
DNA: deoxyribonucleic acid
EGCG: epigallocatechin gallate
ESI: electron spray ionization
Et₃N: triethylamine
kDNA: kinetoplast DNA
Lk: linking number
Lk₀: linking number of relaxed DNA
MAO: monoamino oxidase
MD: molecular dynamics
MLL: mixed lineage leukaemia gene
NMR: nuclear magnetic resonance
ODC: ornithine decarboxylase
PAO: polyaminoxidase
PDB: protein data bank
POCl₃: phosphoryl chloride
PTS: polyamine transport system
r.t.: room temperature
SAM-DC: *S*-adenosylmethionine decarboxylase
SAR: structure activity relationship
SDS: sodium dodecyl sulphate
NaBH(OAc)₃: sodium triacetoxyborohydride
SSAT: spermine/spermidine *N*¹-acetyltransferase enzyme
STD ¹H NMR: saturation transfer difference ¹H NMR
TAE: Tris-Acetate-EDTA buffer
TBE: Tris-Borate-EDTA buffer
TBME: *tert*-butyl methyl ether
THF: tetrahydrofuran
Tw: twist
UV: ultraviolet
Wr: writhe

Bibliography

1. Lehninger, *Principles of Biochemistry* **2013**.
2. <https://training.seer.cancer.gov/disease/categories/classification.html#myeloma>.
3. <http://www.who.int/mediacentre/news/releases/2003/pr27/en/>.
4. Cooper, M. G.; Hausman, R. E., *The cell: A Molecular Approach*. **2000**.
5. Chabner, B. A.; Roberts, T. G., Timeline: Chemotherapy and the war on cancer. *Nat Rev Cancer* **2005**, *5* (1), 65-72.
6. DeVita, V. T.; Chu, E., A history of cancer chemotherapy. *Cancer Res* **2008**, *68* (21), 8643-53.
7. Saijo, N., Progress in cancer chemotherapy with special stress on molecular-targeted therapy. *Jpn J Clin Oncol* **2010**, *40* (9), 855-62.
8. Torigoe, H.; Sato, S.; Yamashita, K.; Obika, S.; Imanishi, T.; Takenaka, S., Binding of threading intercalator to nucleic acids: thermodynamic analyses. *Nucleic Acids Res Suppl* **2002**, (2), 55-6.
9. Watson, J. D.; Crick, F. H., Molecular structure of nucleic acids; a structure for deoxyribose nucleic acid. *Nature* **1953**, *171* (4356), 737-8.
10. Dahm, R., Discovering DNA: Friedrich Miescher and the early years of nucleic acid research. *Hum Genet* **2008**, *122* (6), 565-81.
11. Pommier, Y., *DNA Topoisomerases and Cancer* **2012**.
12. Dewese, J. E.; Osheroff, M. A.; Osheroff, N., DNA Topology and Topoisomerases: Teaching a "Knotty" Subject. *Biochem Mol Biol Educ* **2008**, *37* (1), 2-10.
13. Dewese, J. E.; Osheroff, N., The DNA cleavage reaction of topoisomerase II: wolf in sheep's clothing. *Nucleic Acids Res* **2009**, *37* (3), 738-48.
14. Bauer, W. R.; Crick, F. H.; White, J. H., Supercoiled DNA. *Sci Am* **1980**, *243* (1), 100-13.
15. White, J. H.; Cozzarelli, N. R., A simple topological method for describing stereoisomers of DNA catenanes and knots. *Proc Natl Acad Sci U S A* **1984**, *81* (11), 3322-6.
16. Vologodskii, A. V.; Cozzarelli, N. R., Conformational and thermodynamic properties of supercoiled DNA. *Annu Rev Biophys Biomol Struct* **1994**, *23*, 609-43.
17. Espeli, O.; Marians, K. J., Untangling intracellular DNA topology. *Mol Microbiol* **2004**, *52* (4), 925-31.
18. Falaschi, A.; Abdurashidova, G.; Sandoval, O.; Radulescu, S.; Biamonti, G.; Riva, S., Molecular and structural transactions at human DNA replication origins. *Cell Cycle* **2007**, *6* (14), 1705-12.
19. Wang, J. C., Cellular roles of DNA topoisomerases: a molecular perspective. *Nat Rev Mol Cell Biol* **2002**, *3* (6), 430-40.
20. McClendon, A. K.; Osheroff, N., DNA topoisomerase II, genotoxicity, and cancer. *Mutat Res* **2007**, *623* (1-2), 83-97.
21. Chen, W.; Qiu, J.; Shen, Y. M., Topoisomerase II α , rather than II β , is a promising target in development of anti-cancer drugs. *Drug Discov Ther* **2012**, *6* (5), 230-7.
22. Wang, J. C., DNA topoisomerases. *Annu Rev Biochem* **1996**, *65*, 635-92.
23. Wang, J. C., Moving one DNA double helix through another by a type II DNA topoisomerase: the story of a simple molecular machine. *Q Rev Biophys* **1998**, *31* (2), 107-44.

24. Liu, L. F.; Rowe, T. C.; Yang, L.; Tewey, K. M.; Chen, G. L., Cleavage of DNA by mammalian DNA topoisomerase II. *J Biol Chem* **1983**, *258* (24), 15365-70.
25. Watt, P. M.; Hickson, I. D., Structure and function of type II DNA topoisomerases. *Biochem J* **1994**, *303* (Pt 3), 681-95.
26. Pommier, Y.; Leo, E.; Zhang, H.; Marchand, C., DNA topoisomerases and their poisoning by anticancer and antibacterial drugs. *Chem Biol* **2010**, *17* (5), 421-33.
27. Champoux, J. J., DNA topoisomerases: structure, function, and mechanism. *Annu Rev Biochem* **2001**, *70*, 369-413.
28. Schoeffler, A. J.; Berger, J. M., DNA topoisomerases: harnessing and constraining energy to govern chromosome topology. *Q Rev Biophys* **2008**, *41* (1), 41-101.
29. Pommier, Y., Drugging topoisomerases: lessons and challenges. *ACS Chem Biol* **2013**, *8* (1), 82-95.
30. Pommier, Y.; Pourquier, P.; Fan, Y.; Strumberg, D., Mechanism of action of eukaryotic DNA topoisomerase I and drugs targeted to the enzyme. *Biochim Biophys Acta* **1998**, *1400* (1-3), 83-105.
31. Leppard, J. B.; Champoux, J. J., Human DNA topoisomerase I: relaxation, roles, and damage control. *Chromosoma* **2005**, *114* (2), 75-85.
32. Halligan, B. D.; Edwards, K. A.; Liu, L. F., Purification and characterization of a type II DNA topoisomerase from bovine calf thymus. *J Biol Chem* **1985**, *260* (4), 2475-82.
33. Drake, F. H.; Zimmerman, J. P.; McCabe, F. L.; Bartus, H. F.; Per, S. R.; Sullivan, D. M.; Ross, W. E.; Mattern, M. R.; Johnson, R. K.; Crooke, S. T., Purification of topoisomerase II from amsacrine-resistant P388 leukemia cells. Evidence for two forms of the enzyme. *J Biol Chem* **1987**, *262* (34), 16739-47.
34. Berger, J. M., Type II DNA topoisomerases. *Curr Opin Struct Biol* **1998**, *8* (1), 26-32.
35. Corbett, A. H.; Osheroff, N., When good enzymes go bad: conversion of topoisomerase II to a cellular toxin by antineoplastic drugs. *Chem Res Toxicol* **1993**, *6* (5), 585-97.
36. Wendorff, T. J.; Schmidt, B. H.; Heslop, P.; Austin, C. A.; Berger, J. M., The structure of DNA-bound human topoisomerase II alpha: conformational mechanisms for coordinating inter-subunit interactions with DNA cleavage. *J Mol Biol* **2012**, *424* (3-4), 109-24.
37. Mirski, S. E.; Cole, S. P., Cytoplasmic localization of a mutant M(r) 160,000 topoisomerase II alpha is associated with the loss of putative bipartite nuclear localization signals in a drug-resistant human lung cancer cell line. *Cancer Res* **1995**, *55* (10), 2129-34.
38. Wells, N. J.; Addison, C. M.; Fry, A. M.; Ganapathi, R.; Hickson, I. D., Serine 1524 is a major site of phosphorylation on human topoisomerase II alpha protein in vivo and is a substrate for casein kinase II in vitro. *J Biol Chem* **1994**, *269* (47), 29746-51.
39. Schmidt, B. H.; Osheroff, N.; Berger, J. M., Structure of a topoisomerase II-DNA-nucleotide complex reveals a new control mechanism for ATPase activity. *Nat Struct Mol Biol* **2012**, *19* (11), 1147-54.
40. Drake, F. H.; Hofmann, G. A.; Bartus, H. F.; Mattern, M. R.; Crooke, S. T.; Mirabelli, C. K., Biochemical and pharmacological properties of p170 and p180 forms of topoisomerase II. *Biochemistry* **1989**, *28* (20), 8154-60.
41. Heck, M. M.; Earnshaw, W. C., Topoisomerase II: A specific marker for cell proliferation. *J Cell Biol* **1986**, *103* (6 Pt 2), 2569-81.

42. Hsiang, Y. H.; Wu, H. Y.; Liu, L. F., Proliferation-dependent regulation of DNA topoisomerase II in cultured human cells. *Cancer Res* **1988**, *48* (11), 3230-5.
43. Woessner, R. D.; Mattern, M. R.; Mirabelli, C. K.; Johnson, R. K.; Drake, F. H., Proliferation- and cell cycle-dependent differences in expression of the 170 kilodalton and 180 kilodalton forms of topoisomerase II in NIH-3T3 cells. *Cell Growth Differ* **1991**, *2* (4), 209-14.
44. Grue, P.; Grässer, A.; Sehested, M.; Jensen, P. B.; Uhse, A.; Straub, T.; Ness, W.; Boege, F., Essential mitotic functions of DNA topoisomerase IIalpha are not adopted by topoisomerase IIbeta in human H69 cells. *J Biol Chem* **1998**, *273* (50), 33660-6.
45. Heck, M. M.; Hittelman, W. N.; Earnshaw, W. C., Differential expression of DNA topoisomerases I and II during the eukaryotic cell cycle. *Proc Natl Acad Sci U S A* **1988**, *85* (4), 1086-90.
46. Kimura, K.; Saijo, M.; Ui, M.; Enomoto, T., Growth state- and cell cycle-dependent fluctuation in the expression of two forms of DNA topoisomerase II and possible specific modification of the higher molecular weight form in the M phase. *J Biol Chem* **1994**, *269* (2), 1173-6.
47. Vos, S. M.; Tretter, E. M.; Schmidt, B. H.; Berger, J. M., All tangled up: how cells direct, manage and exploit topoisomerase function. *Nat Rev Mol Cell Biol* **2011**, *12* (12), 827-41.
48. Pendleton, M.; Lindsey, R. H.; Felix, C. A.; Grimwade, D.; Osheroff, N., Topoisomerase II and leukemia. *Ann N Y Acad Sci* **2014**, *1310*, 98-110.
49. Nitiss, J. L., Targeting DNA topoisomerase II in cancer chemotherapy. *Nat Rev Cancer* **2009**, *9* (5), 338-50.
50. Ketron, A. C.; Osheroff, N., Phytochemicals as Anticancer and Chemopreventive Topoisomerase II Poisons. *Phytochem Rev* **2014**, *13* (1), 19-35.
51. Ketron, A. C.; Gordon, O. N.; Schneider, C.; Osheroff, N., Oxidative metabolites of curcumin poison human type II topoisomerases. *Biochemistry* **2013**, *52* (1), 221-7.
52. Austin, C. A.; Marsh, K. L., Eukaryotic DNA topoisomerase II beta. *Bioessays* **1998**, *20* (3), 215-26.
53. Isaacs, R. J.; Davies, S. L.; Sandri, M. I.; Redwood, C.; Wells, N. J.; Hickson, I. D., Physiological regulation of eukaryotic topoisomerase II. *Biochim Biophys Acta* **1998**, *1400* (1-3), 121-37.
54. Christensen, M. O.; Larsen, M. K.; Barthelmes, H. U.; Hock, R.; Andersen, C. L.; Kjeldsen, E.; Knudsen, B. R.; Westergaard, O.; Boege, F.; Mielke, C., Dynamics of human DNA topoisomerases IIalpha and IIbeta in living cells. *J Cell Biol* **2002**, *157* (1), 31-44.
55. Yang, X.; Li, W.; Prescott, E. D.; Burden, S. J.; Wang, J. C., DNA topoisomerase IIbeta and neural development. *Science* **2000**, *287* (5450), 131-4.
56. Ju, B. G.; Lunyak, V. V.; Perissi, V.; Garcia-Bassets, I.; Rose, D. W.; Glass, C. K.; Rosenfeld, M. G., A topoisomerase IIbeta-mediated dsDNA break required for regulated transcription. *Science* **2006**, *312* (5781), 1798-802.
57. Errington, F.; Willmore, E.; Tilby, M. J.; Li, L.; Li, G.; Li, W.; Baguley, B. C.; Austin, C. A., Murine transgenic cells lacking DNA topoisomerase IIbeta are resistant to acridines and mitoxantrone: analysis of cytotoxicity and cleavable complex formation. *Mol Pharmacol* **1999**, *56* (6), 1309-16.
58. Azarova, A. M.; Lyu, Y. L.; Lin, C. P.; Tsai, Y. C.; Lau, J. Y.; Wang, J. C.; Liu, L. F., Roles of DNA topoisomerase II isozymes in chemotherapy and secondary malignancies. *Proc Natl Acad Sci U S A* **2007**, *104* (26), 11014-9.

59. Osheroff, N., Role of the divalent cation in topoisomerase II mediated reactions. *Biochemistry* **1987**, *26* (20), 6402-6.
60. Osheroff, N., Eukaryotic topoisomerase II. Characterization of enzyme turnover. *J Biol Chem* **1986**, *261* (21), 9944-50.
61. Zechiedrich, E. L.; Osheroff, N., Eukaryotic topoisomerases recognize nucleic acid topology by preferentially interacting with DNA crossovers. *EMBO J* **1990**, *9* (13), 4555-62.
62. Roca, J.; Wang, J. C., The capture of a DNA double helix by an ATP-dependent protein clamp: a key step in DNA transport by type II DNA topoisomerases. *Cell* **1992**, *71* (5), 833-40.
63. Corbett, A. H.; DeVore, R. F.; Osheroff, N., Effect of casein kinase II-mediated phosphorylation on the catalytic cycle of topoisomerase II. Regulation of enzyme activity by enhancement of ATP hydrolysis. *J Biol Chem* **1992**, *267* (28), 20513-8.
64. Dewese, J. E.; Osheroff, N., The use of divalent metal ions by type II topoisomerases. *Metallomics* **2010**, *2* (7), 450-9.
65. Laponogov, I.; Pan, X. S.; Veselkov, D. A.; McAuley, K. E.; Fisher, L. M.; Sanderson, M. R., Structural basis of gate-DNA breakage and resealing by type II topoisomerases. *PLoS One* **2010**, *5* (6), e11338.
66. Dewese, J. E.; Burgin, A. B.; Osheroff, N., Human topoisomerase IIalpha uses a two-metal-ion mechanism for DNA cleavage. *Nucleic Acids Res* **2008**, *36* (15), 4883-93.
67. Schmidt, B. H.; Burgin, A. B.; Dewese, J. E.; Osheroff, N.; Berger, J. M., A novel and unified two-metal mechanism for DNA cleavage by type II and IA topoisomerases. *Nature* **2010**, *465* (7298), 641-4.
68. Lindsley, J. E.; Wang, J. C., Proteolysis patterns of epitopically labeled yeast DNA topoisomerase II suggest an allosteric transition in the enzyme induced by ATP binding. *Proc Natl Acad Sci U S A* **1991**, *88* (23), 10485-9.
69. Osheroff, N.; Shelton, E. R.; Brutlag, D. L., DNA topoisomerase II from *Drosophila melanogaster*. Relaxation of supercoiled DNA. *J Biol Chem* **1983**, *258* (15), 9536-43.
70. Baird, C. L.; Gordon, M. S.; Andrenyak, D. M.; Marecek, J. F.; Lindsley, J. E., The ATPase reaction cycle of yeast DNA topoisomerase II. Slow rates of ATP resynthesis and P(i) release. *J Biol Chem* **2001**, *276* (30), 27893-8.
71. Harkins, T. T.; Lewis, T. J.; Lindsley, J. E., Pre-steady-state analysis of ATP hydrolysis by *Saccharomyces cerevisiae* DNA topoisomerase II. 2. Kinetic mechanism for the sequential hydrolysis of two ATP. *Biochemistry* **1998**, *37* (20), 7299-312.
72. Robinson, M. J.; Osheroff, N., Effects of antineoplastic drugs on the post-strand-passage DNA cleavage/religation equilibrium of topoisomerase II. *Biochemistry* **1991**, *30* (7), 1807-13.
73. Burden, D. A.; Osheroff, N., Mechanism of action of eukaryotic topoisomerase II and drugs targeted to the enzyme. *Biochim Biophys Acta* **1998**, *1400* (1-3), 139-54.
74. Fortune, J. M.; Osheroff, N., Topoisomerase II as a target for anticancer drugs: when enzymes stop being nice. *Prog Nucleic Acid Res Mol Biol* **2000**, *64*, 221-53.
75. Kaufmann, S. H., Cell death induced by topoisomerase-targeted drugs: more questions than answers. *Biochim Biophys Acta* **1998**, *1400* (1-3), 195-211.
76. Felix, C. A.; Kolaris, C. P.; Osheroff, N., Topoisomerase II and the etiology of chromosomal translocations. *DNA Repair (Amst)* **2006**, *5* (9-10), 1093-108.
77. Vassetzky, Y. S.; Alghisi, G. C.; Gasser, S. M., DNA topoisomerase II mutations and resistance to anti-tumor drugs. *Bioessays* **1995**, *17* (9), 767-74.

78. Hsiung, Y.; Elsea, S. H.; Osheroff, N.; Nitiss, J. L., A mutation in yeast TOP2 homologous to a quinolone-resistant mutation in bacteria. Mutation of the amino acid homologous to Ser83 of Escherichia coli gyrA alters sensitivity to eukaryotic topoisomerase inhibitors. *J Biol Chem* **1995**, *270* (35), 20359-64.
79. Osheroff, N.; Corbett, A. H.; Elsea, S. H.; Westergaard, M., Defining functional drug-interaction domains on topoisomerase II by exploiting mechanistic differences between drug classes. *Cancer Chemother Pharmacol* **1994**, *34 Suppl*, S19-25.
80. Elsea, S. H.; Hsiung, Y.; Nitiss, J. L.; Osheroff, N., A yeast type II topoisomerase selected for resistance to quinolones. Mutation of histidine 1012 to tyrosine confers resistance to nonintercalative drugs but hypersensitivity to ellipticine. *J Biol Chem* **1995**, *270* (4), 1913-20.
81. Estey, E. H.; Silberman, L.; Beran, M.; Andersson, B. S.; Zwelling, L. A., The interaction between nuclear topoisomerase II activity from human leukemia cells, exogenous DNA, and 4'-(9-acridinylamino)methanesulfon-m-anisidide (m-AMSA) or 4-(4,6-O-ethylidene-beta-D-glucopyranoside) (VP-16) indicates the sensitivity of the cells to the drugs. *Biochem Biophys Res Commun* **1987**, *144* (2), 787-93.
82. Freudenreich, C. H.; Kreuzer, K. N., Localization of an aminoacridine antitumor agent in a type II topoisomerase-DNA complex. *Proc Natl Acad Sci U S A* **1994**, *91* (23), 11007-11.
83. Kerrigan, D.; Pommier, Y.; Kohn, K. W., Protein-linked DNA strand breaks produced by etoposide and teniposide in mouse L1210 and human VA-13 and HT-29 cell lines: relationship to cytotoxicity. *NCI Monogr* **1987**, (4), 117-21.
84. Bender, R. P.; Jablonksy, M. J.; Shadid, M.; Romaine, I.; Dunlap, N.; Anklin, C.; Graves, D. E.; Osheroff, N., Substituents on etoposide that interact with human topoisomerase II α in the binary enzyme-drug complex: contributions to etoposide binding and activity. *Biochemistry* **2008**, *47* (15), 4501-9.
85. Larsen, A. K.; Escargueil, A. E.; Skladanowski, A., Catalytic topoisomerase II inhibitors in cancer therapy. *Pharmacol Ther* **2003**, *99* (2), 167-81.
86. Ishida, R.; Hamatake, M.; Wasserman, R. A.; Nitiss, J. L.; Wang, J. C.; Andoh, T., DNA topoisomerase II is the molecular target of bisdioxopiperazine derivatives ICRF-159 and ICRF-193 in *Saccharomyces cerevisiae*. *Cancer Res* **1995**, *55* (11), 2299-303.
87. Andoh, T.; Ishida, R., Catalytic inhibitors of DNA topoisomerase II. *Biochim Biophys Acta* **1998**, *1400* (1-3), 155-71.
88. Jensen, L. H.; Nitiss, K. C.; Rose, A.; Dong, J.; Zhou, J.; Hu, T.; Osheroff, N.; Jensen, P. B.; Sehested, M.; Nitiss, J. L., A novel mechanism of cell killing by anti-topoisomerase II bisdioxopiperazines. *J Biol Chem* **2000**, *275* (3), 2137-46.
89. Hajji, N.; Mateos, S.; Pastor, N.; Domínguez, I.; Cortés, F., Induction of genotoxic and cytotoxic damage by aclarubicin, a dual topoisomerase inhibitor. *Mutat Res* **2005**, *583* (1), 26-35.
90. Lindsey, R. H.; Pendleton, M.; Ashley, R. E.; Mercer, S. L.; Deweese, J. E.; Osheroff, N., Catalytic core of human topoisomerase II α : insights into enzyme-DNA interactions and drug mechanism. *Biochemistry* **2014**, *53* (41), 6595-602.
91. Pommier, Y.; Marchand, C., Interfacial inhibitors of protein-nucleic acid interactions. *Curr Med Chem Anticancer Agents* **2005**, *5* (4), 421-9.
92. Burden, D. A.; Kingma, P. S.; Froelich-Ammon, S. J.; Bjornsti, M. A.; Patchan, M. W.; Thompson, R. B.; Osheroff, N., Topoisomerase II.etoposide interactions direct the

- formation of drug-induced enzyme-DNA cleavage complexes. *J Biol Chem* **1996**, 271 (46), 29238-44.
93. Bandele, O. J.; Osheroff, N., (-)-Epigallocatechin gallate, a major constituent of green tea, poisons human type II topoisomerases. *Chem Res Toxicol* **2008**, 21 (4), 936-43.
94. Bender, R. P.; Lehmler, H. J.; Robertson, L. W.; Ludewig, G.; Osheroff, N., Polychlorinated biphenyl quinone metabolites poison human topoisomerase IIalpha: altering enzyme function by blocking the N-terminal protein gate. *Biochemistry* **2006**, 45 (33), 10140-52.
95. Bender, R. P.; Ham, A. J.; Osheroff, N., Quinone-induced enhancement of DNA cleavage by human topoisomerase IIalpha: adduction of cysteine residues 392 and 405. *Biochemistry* **2007**, 46 (10), 2856-64.
96. Pogorelčnik, B.; Perdih, A.; Solmajer, T., Recent developments of DNA poisons--human DNA topoisomerase IIa inhibitors--as anticancer agents. *Curr Pharm Des* **2013**, 19 (13), 2474-88.
97. Minotti, G.; Menna, P.; Salvatorelli, E.; Cairo, G.; Gianni, L., Anthracyclines: molecular advances and pharmacologic developments in antitumor activity and cardiotoxicity. *Pharmacol Rev* **2004**, 56 (2), 185-229.
98. Wu, C. C.; Li, T. K.; Farh, L.; Lin, L. Y.; Lin, T. S.; Yu, Y. J.; Yen, T. J.; Chiang, C. W.; Chan, N. L., Structural basis of type II topoisomerase inhibition by the anticancer drug etoposide. *Science* **2011**, 333 (6041), 459-62.
99. Byl, J. A.; Cline, S. D.; Utsugi, T.; Kobunai, T.; Yamada, Y.; Osheroff, N., DNA topoisomerase II as the target for the anticancer drug TOP-53: mechanistic basis for drug action. *Biochemistry* **2001**, 40 (3), 712-8.
100. Tachibana, Y.; Zhu, X. K.; Krishnan, P.; Lee, K. H.; Bastow, K. F., Characterization of human lung cancer cells resistant to 4'-O-demethyl-4beta-(2"-nitro-4"-fluoroanilino)-4-desoxypodophyllotoxin, a unique compound in the epipodophyllotoxin antitumor class. *Anticancer Drugs* **2000**, 11 (1), 19-28.
101. Kruczynski, A.; Barret, J. M.; Van Hille, B.; Chansard, N.; Astruc, J.; Menon, Y.; Duchier, C.; Créancier, L.; Hill, B. T., Decreased nucleotide excision repair activity and alterations of topoisomerase IIalpha are associated with the in vivo resistance of a P388 leukemia subline to F11782, a novel catalytic inhibitor of topoisomerases I and II. *Clin Cancer Res* **2004**, 10 (9), 3156-68.
102. Barret, J. M.; Kruczynski, A.; Vispé, S.; Annereau, J. P.; Brel, V.; Guminski, Y.; Delcros, J. G.; Lansiaux, A.; Guilbaud, N.; Imbert, T.; Bailly, C., F14512, a potent antitumor agent targeting topoisomerase II vectored into cancer cells via the polyamine transport system. *Cancer Res* **2008**, 68 (23), 9845-53.
103. Wilstermann, A. M.; Bender, R. P.; Godfrey, M.; Choi, S.; Anklin, C.; Berkowitz, D. B.; Osheroff, N.; Graves, D. E., Topoisomerase II - drug interaction domains: identification of substituents on etoposide that interact with the enzyme. *Biochemistry* **2007**, 46 (28), 8217-25.
104. Drake, F. H.; Hofmann, G. A.; Mong, S. M.; Bartus, J. O.; Hertzberg, R. P.; Johnson, R. K.; Mattern, M. R.; Mirabelli, C. K., In vitro and intracellular inhibition of topoisomerase II by the antitumor agent merbarone. *Cancer Res* **1989**, 49 (10), 2578-83.
105. Jensen, P. B.; Sørensen, B. S.; Demant, E. J.; Sehested, M.; Jensen, P. S.; Vindeløv, L.; Hansen, H. H., Antagonistic effect of aclarubicin on the cytotoxicity of etoposide and 4'-(9-acridinylamino)methanesulfon-m-anisidide in human small cell lung cancer cell lines and on topoisomerase II-mediated DNA cleavage. *Cancer Res* **1990**, 50 (11), 3311-6.

106. Bojanowski, K.; Lelievre, S.; Markovits, J.; Couprie, J.; Jacquemin-Sablon, A.; Larsen, A. K., Suramin is an inhibitor of DNA topoisomerase II in vitro and in Chinese hamster fibrosarcoma cells. *Proc Natl Acad Sci U S A* **1992**, *89* (7), 3025-9.
107. Tanabe, K.; Ikegami, Y.; Ishida, R.; Andoh, T., Inhibition of topoisomerase II by antitumor agents bis(2,6-dioxopiperazine) derivatives. *Cancer Res* **1991**, *51* (18), 4903-8.
108. Park, S. E.; Chang, I. H.; Jun, K. Y.; Lee, E.; Lee, E. S.; Na, Y.; Kwon, Y., 3-(3-Butylamino-2-hydroxy-propoxy)-1-hydroxy-xanthen-9-one acts as a topoisomerase II α catalytic inhibitor with low DNA damage. *Eur J Med Chem* **2013**, *69*, 139-45.
109. Germe, T.; Hyrien, O., Topoisomerase II-DNA complexes trapped by ICRF-193 perturb chromatin structure. *EMBO Rep* **2005**, *6* (8), 729-35.
110. Pogorelčnik, B.; Perdih, A.; Solmajer, T., Recent advances in the development of catalytic inhibitors of human DNA topoisomerase II α as novel anticancer agents. *Curr Med Chem* **2013**, *20* (5), 694-709.
111. Nitiss, J. L.; Pourquier, P.; Pommier, Y., Aclacinomycin A stabilizes topoisomerase I covalent complexes. *Cancer Res* **1997**, *57* (20), 4564-9.
112. Jensen, P. B.; Jensen, P. S.; Demant, E. J.; Friche, E.; Sørensen, B. S.; Sehested, M.; Wassermann, K.; Vindeløv, L.; Westergaard, O.; Hansen, H. H., Antagonistic effect of aclarubicin on daunorubicin-induced cytotoxicity in human small cell lung cancer cells: relationship to DNA integrity and topoisomerase II. *Cancer Res* **1991**, *51* (19), 5093-9.
113. Petersen, L. N.; Jensen, P. B.; Sørensen, B. S.; Engelholm, S. A.; Spang-Thomsen, M., Postincubation with aclarubicin reverses topoisomerase II mediated DNA cleavage, strand breaks, and cytotoxicity induced by VP-16. *Invest New Drugs* **1994**, *12* (4), 289-97.
114. Natale, R. B.; Cody, R. L.; Simon, M. S.; Wheeler, R. H., An in vivo and in vitro trial of aclarubicin in metastatic breast cancer: a novel approach to the study of analogs. *Cancer Chemother Pharmacol* **1993**, *31* (6), 485-8.
115. Felix, C. A.; Hosler, M. R.; Winick, N. J.; Masterson, M.; Wilson, A. E.; Lange, B. J., ALL-1 gene rearrangements in DNA topoisomerase II inhibitor-related leukemia in children. *Blood* **1995**, *85* (11), 3250-6.
116. Felix, C. A., Secondary leukemias induced by topoisomerase-targeted drugs. *Biochim Biophys Acta* **1998**, *1400* (1-3), 233-55.
117. Cowell, I. G.; Austin, C. A., Mechanism of generation of therapy related leukemia in response to anti-topoisomerase II agents. *Int J Environ Res Public Health* **2012**, *9* (6), 2075-91.
118. Sung, P. A.; Libura, J.; Richardson, C., Etoposide and illegitimate DNA double-strand break repair in the generation of MLL translocations: new insights and new questions. *DNA Repair (Amst)* **2006**, *5* (9-10), 1109-18.
119. Ezoe, S., Secondary leukemia associated with the anti-cancer agent, etoposide, a topoisomerase II inhibitor. *Int J Environ Res Public Health* **2012**, *9* (7), 2444-53.
120. Ross, J. A.; Davies, S. M.; Potter, J. D.; Robison, L. L., Epidemiology of childhood leukemia, with a focus on infants. *Epidemiol Rev* **1994**, *16* (2), 243-72.
121. Canaani, E.; Nowell, P. C.; Croce, C. M., Molecular genetics of 11q23 chromosome translocations. *Adv Cancer Res* **1995**, *66*, 213-34.
122. Hussain, S. P.; Harris, C. C., p53 mutation spectrum and load: the generation of hypotheses linking the exposure of endogenous or exogenous carcinogens to human cancer. *Mutat Res* **1999**, *428* (1-2), 23-32.

123. Bandele, O. J.; Osheroff, N., The efficacy of topoisomerase II-targeted anticancer agents reflects the persistence of drug-induced cleavage complexes in cells. *Biochemistry* **2008**, *47* (45), 11900-8.
124. Meczes, E. L.; Marsh, K. L.; Fisher, L. M.; Rogers, M. P.; Austin, C. A., Complementation of temperature-sensitive topoisomerase II mutations in *Saccharomyces cerevisiae* by a human TOP2 beta construct allows the study of topoisomerase II beta inhibitors in yeast. *Cancer Chemother Pharmacol* **1997**, *39* (4), 367-75.
125. Lyu, Y. L.; Kerrigan, J. E.; Lin, C. P.; Azarova, A. M.; Tsai, Y. C.; Ban, Y.; Liu, L. F., Topoisomerase IIbeta mediated DNA double-strand breaks: implications in doxorubicin cardiotoxicity and prevention by dexrazoxane. *Cancer Res* **2007**, *67* (18), 8839-46.
126. Leeuwenhoeck van, A., Observationes de Anthonii Leeuwenhoeck, de natis e semine genital aminalculis. *Phil.Trans.* **1678**, *12*, 1040-1043.
127. Wallace, H. M., The polyamines: past, present and future. *Essays Biochem* **2009**, *46*, 1-9.
128. Tabor, C. W.; Tabor, H., Polyamines. *Annu Rev Biochem* **1984**, *53*, 749-90.
129. Fredlund, J. O.; Johansson, M. C.; Dahlberg, E.; Oredsson, S. M., Ornithine decarboxylase and S-adenosylmethionine decarboxylase expression during the cell cycle of Chinese hamster ovary cells. *Exp Cell Res* **1995**, *216* (1), 86-92.
130. Bettuzzi, S.; Davalli, P.; Astancolle, S.; Pinna, C.; Roncaglia, R.; Boraldi, F.; Tiozzo, R.; Sharrard, M.; Corti, A., Coordinate changes of polyamine metabolism regulatory proteins during the cell cycle of normal human dermal fibroblasts. *FEBS Lett* **1999**, *446* (1), 18-22.
131. Casero, R. A.; Marton, L. J., Targeting polyamine metabolism and function in cancer and other hyperproliferative diseases. *Nat Rev Drug Discov* **2007**, *6* (5), 373-90.
132. Pegg, A. E., Mammalian polyamine metabolism and function. *IUBMB Life* **2009**, *61* (9), 880-94.
133. Wallace, H. M., The physiological role of the polyamines. *Eur J Clin Invest* **2000**, *30* (1), 1-3.
134. Shantz, L. M., Transcriptional and translational control of ornithine decarboxylase during Ras transformation. *Biochem J* **2004**, *377* (Pt 1), 257-64.
135. Pegg, A. E., Spermidine/spermine-N(1)-acetyltransferase: a key metabolic regulator. *Am J Physiol Endocrinol Metab* **2008**, *294* (6), E995-1010.
136. Wallace, H. M.; Fraser, A. V.; Hughes, A., A perspective of polyamine metabolism. *Biochem J* **2003**, *376* (Pt 1), 1-14.
137. Parchment, R. E.; Pierce, G. B., Polyamine oxidation, programmed cell death, and regulation of melanoma in the murine embryonic limb. *Cancer Res* **1989**, *49* (23), 6680-6.
138. Averill-Bates, D. A.; Agostinelli, E.; Przybytkowski, E.; Mondovi, B., Aldehyde dehydrogenase and cytotoxicity of purified bovine serum amine oxidase and spermine in Chinese hamster ovary cells. *Biochem Cell Biol* **1994**, *72* (1-2), 36-42.
139. Nowotarski, S. L.; Woster, P. M.; Casero, R. A., Polyamines and cancer: implications for chemotherapy and chemoprevention. *Expert Rev Mol Med* **2013**, *15*, e3.
140. Roy, U. K.; Rial, N. S.; Kachel, K. L.; Gerner, E. W., Activated K-RAS increases polyamine uptake in human colon cancer cells through modulation of caveolar endocytosis. *Mol Carcinog* **2008**, *47* (7), 538-53.
141. Chen, K. Y.; Liu, A. Y., Differences in polyamine metabolism of the undifferentiated and differentiated neuroblastoma cells. Metabolic labeling of an 18,000-

M(r) protein by [14C]putrescine and the conversion of putrescine to GABA. *FEBS Lett* **1981**, *134* (1), 71-4.

142. Phanstiel, O.; Kaur, N.; Delcros, J. G., Structure-activity investigations of polyamine-anthracene conjugates and their uptake via the polyamine transporter. *Amino Acids* **2007**, *33* (2), 305-13.

143. Holley, J. L.; Mather, A.; Wheelhouse, R. T.; Cullis, P. M.; Hartley, J. A.; Bingham, J. P.; Cohen, G. M., Targeting of tumor cells and DNA by a chlorambucil-spermidine conjugate. *Cancer Res* **1992**, *52* (15), 4190-5.

144. Mouawad, F.; Gros, A.; Rysman, B.; Bal-Mahieu, C.; Bertheau, C.; Horn, S.; Sarrazin, T.; Lartigau, E.; Chevalier, D.; Bailly, C.; Lansiaux, A.; Meignan, S., The antitumor drug F14512 enhances cisplatin and ionizing radiation effects in head and neck squamous carcinoma cell lines. *Oral Oncol* **2014**, *50* (2), 113-9.

145. Muth, A.; Kamel, J.; Kaur, N.; Shicora, A. C.; Ayene, I. S.; Gilmour, S. K.; Phanstiel, O., Development of polyamine transport ligands with improved metabolic stability and selectivity against specific human cancers. *J Med Chem* **2013**, *56* (14), 5819-28.

146. Hande, K. R., Etoposide: four decades of development of a topoisomerase II inhibitor. *Eur J Cancer* **1998**, *34* (10), 1514-21.

147. Nitiss, J. L.; Liu, Y. X.; Hsiung, Y., A temperature sensitive topoisomerase II allele confers temperature dependent drug resistance on amsacrine and etoposide: a genetic system for determining the targets of topoisomerase II inhibitors. *Cancer Res* **1993**, *53* (1), 89-93.

148. Hande, K. R., Clinical applications of anticancer drugs targeted to topoisomerase II. *Biochim Biophys Acta* **1998**, *1400* (1-3), 173-84.

149. Rezonja, R.; Knez, L.; Cufer, T.; Mrhar, A., Oral treatment with etoposide in small cell lung cancer - dilemmas and solutions. *Radiol Oncol* **2013**, *47* (1), 1-13.

150. Bokemeyer, C.; Kollmannsberger, C.; Harstrick, A.; Beyer, J.; Gerl, A.; Casper, J.; Metzner, B.; Hartmann, J. T.; Schmoll, H. J.; Kanz, L., Treatment of patients with cisplatin-refractory testicular germ-cell cancer. German Testicular Cancer Study Group (GTCSG). *Int J Cancer* **1999**, *83* (6), 848-51.

151. McClendon, A. K.; Osheroff, N., The geometry of DNA supercoils modulates topoisomerase-mediated DNA cleavage and enzyme response to anticancer drugs. *Biochemistry* **2006**, *45* (9), 3040-50.

152. Chow, K. C.; Macdonald, T. L.; Ross, W. E., DNA binding by epipodophyllotoxins and N-acyl anthracyclines: implications for mechanism of topoisomerase II inhibition. *Mol Pharmacol* **1988**, *34* (4), 467-73.

153. Sullivan, D. M.; Latham, M. D.; Rowe, T. C.; Ross, W. E., Purification and characterization of an altered topoisomerase II from a drug-resistant Chinese hamster ovary cell line. *Biochemistry* **1989**, *28* (13), 5680-7.

154. Baldwin, E. L.; Osheroff, N., Etoposide, topoisomerase II and cancer. *Curr Med Chem Anticancer Agents* **2005**, *5* (4), 363-72.

155. Pitts, S. L.; Jablonksy, M. J.; Duca, M.; Dauzonne, D.; Monneret, C.; Arimondo, P. B.; Anklin, C.; Graves, D. E.; Osheroff, N., Contributions of the D-Ring to the activity of etoposide against human topoisomerase II α : potential interactions with DNA in the ternary enzyme--drug--DNA complex. *Biochemistry* **2011**, *50* (22), 5058-66.

156. Beck, W. T.; Danks, M. K.; Wolverson, J. S.; Kim, R.; Chen, M., Drug resistance associated with altered DNA topoisomerase II. *Adv Enzyme Regul* **1993**, *33*, 113-27.

157. Larsen, A. K.; Skladanowski, A., Cellular resistance to topoisomerase-targeted drugs: from drug uptake to cell death. *Biochim Biophys Acta* **1998**, *1400* (1-3), 257-74.
158. Long, B. H., Structure-activity relationships of podophyllin congeners that inhibit topoisomerase II. *NCI Monogr* **1987**, (4), 123-7.
159. Long, B. H., Mechanisms of action of teniposide (VM-26) and comparison with etoposide (VP-16). *Semin Oncol* **1992**, *19* (2 Suppl 6), 3-19.
160. Damayanthi, Y.; Lown, J. W., Podophyllotoxins: current status and recent developments. *Curr Med Chem* **1998**, *5* (3), 205-52.
161. Lee, K. H., Anticancer drug design based on plant-derived natural products. *J Biomed Sci* **1999**, *6* (4), 236-50.
162. Utsugi, T.; Shibata, J.; Sugimoto, Y.; Aoyagi, K.; Wierzba, K.; Kobunai, T.; Terada, T.; Oh-hara, T.; Tsuruo, T.; Yamada, Y., Antitumor activity of a novel podophyllotoxin derivative (TOP-53) against lung cancer and lung metastatic cancer. *Cancer Res* **1996**, *56* (12), 2809-14.
163. Thibault, B.; Clement, E.; Zorza, G.; Meignan, S.; Delord, J. P.; Couderc, B.; Bailly, C.; Narducci, F.; Vandenberghe, I.; Kruczynski, A.; Guilbaud, N.; Ferré, P.; Annereau, J. P., F14512, a polyamine-vectorized inhibitor of topoisomerase II, exhibits a marked anti-tumor activity in ovarian cancer. *Cancer Lett* **2016**, *370* (1), 10-8.
164. Tierny, D.; Serres, F.; Segauola, Z.; Bemelmans, I.; Bouchaert, E.; Pétaïn, A.; Brel, V.; Couffin, S.; Marchal, T.; Nguyen, L.; Thuru, X.; Ferré, P.; Guilbaud, N.; Gomes, B., Phase I Clinical Pharmacology Study of F14512, a New Polyamine-Vectorized Anticancer Drug, in Naturally Occurring Canine Lymphoma. *Clin Cancer Res* **2015**, *21* (23), 5314-23.
165. Gentry, A. C.; Pitts, S. L.; Jablonsky, M. J.; Bailly, C.; Graves, D. E.; Osheroff, N., Interactions between the etoposide derivative F14512 and human type II topoisomerases: implications for the C4 spermine moiety in promoting enzyme-mediated DNA cleavage. *Biochemistry* **2011**, *50* (15), 3240-9.
166. Brel, V.; Annereau, J. P.; Vispé, S.; Kruczynski, A.; Bailly, C.; Guilbaud, N., Cytotoxicity and cell death mechanisms induced by the polyamine-vectorized anti-cancer drug F14512 targeting topoisomerase II. *Biochem Pharmacol* **2011**, *82* (12), 1843-52.
167. Soulet, D.; Gagnon, B.; Rivest, S.; Audette, M.; Poulin, R., A fluorescent probe of polyamine transport accumulates into intracellular acidic vesicles via a two-step mechanism. *J Biol Chem* **2004**, *279* (47), 49355-66.
168. Guminski, Y.; Grousseau, M.; Cugnasse, S.; Imbert, T., Practical demethylation of podophyllotoxin and efficient preparation of 4-Amino-4'-deoxy-4'-demethylepipodophyllotoxin. *Synth Commun* **2012**, *42* (18), 2780-2789.
169. Wellendorph, P.; Jaroszewski, J. W.; Hansen, S. H.; Franzyk, H., A sequential high-yielding large-scale solution-method for synthesis of philanthotoxin analogues. *Eur J Med Chem* **2003**, *38* (1), 117-22.
170. Marom, H.; Miller, K.; Bechor-Bar, Y.; Tsarfaty, G.; Satchi-Fainaro, R.; Gozin, M., Toward development of targeted nonsteroidal antiandrogen-1,4,7,10-tetraazacyclododecane-1,4,7,10-tetraacetic acid-gadolinium complex for prostate cancer diagnostics. *J Med Chem* **2010**, *53* (17), 6316-25.
171. Palermo, G.; Minniti, E.; Greco, M. L.; Riccardi, L.; Simoni, E.; Convertino, M.; Marchetti, C.; Rosini, M.; Sissi, C.; Minarini, A.; De Vivo, M., An optimized polyamine moiety boosts the potency of human type II topoisomerase poisons as quantified by comparative analysis centered on the clinical candidate F14512. *Chem Commun (Camb)* **2015**, *51* (76), 14310-3.

172. Pinto, M. M.; Sousa, M. E.; Nascimento, M. S., Xanthone derivatives: new insights in biological activities. *Curr Med Chem* **2005**, *12* (21), 2517-38.
173. Liou, S. S.; Shieh, W. L.; Cheng, T. H.; Won, S. J.; Lin, C. N., Gamma-pyrone compounds as potential anti-cancer drugs. *J Pharm Pharmacol* **1993**, *45* (9), 791-4.
174. Na, Y., Recent cancer drug development with xanthone structures. *J Pharm Pharmacol* **2009**, *61* (6), 707-12.
175. Shagufta; Ahmad, I., Recent insight into the biological activities of synthetic xanthone derivatives. *Eur J Med Chem* **2016**, *116*, 267-280.
176. Ji, X.; Avula, B.; Khan, I. A., Quantitative and qualitative determination of six xanthenes in *Garcinia mangostana* L. by LC-PDA and LC-ESI-MS. *J Pharm Biomed Anal* **2007**, *43* (4), 1270-6.
177. Mizushima, Y.; Kuriyama, I.; Nakahara, T.; Kawashima, Y.; Yoshida, H., Inhibitory effects of α -mangostin on mammalian DNA polymerase, topoisomerase, and human cancer cell proliferation. *Food Chem Toxicol* **2013**, *59*, 793-800.
178. Zhang, H. Z.; Kasibhatla, S.; Wang, Y.; Herich, J.; Guastella, J.; Tseng, B.; Drewe, J.; Cai, S. X., Discovery, characterization and SAR of gambogic acid as a potent apoptosis inducer by a HTS assay. *Bioorg Med Chem* **2004**, *12* (2), 309-17.
179. Kasibhatla, S.; Jessen, K. A.; Maliartchouk, S.; Wang, J. Y.; English, N. M.; Drewe, J.; Qiu, L.; Archer, S. P.; Ponce, A. E.; Sirisoma, N.; Jiang, S.; Zhang, H. Z.; Gehlsen, K. R.; Cai, S. X.; Green, D. R.; Tseng, B., A role for transferrin receptor in triggering apoptosis when targeted with gambogic acid. *Proc Natl Acad Sci U S A* **2005**, *102* (34), 12095-100.
180. Qin, Y.; Meng, L.; Hu, C.; Duan, W.; Zuo, Z.; Lin, L.; Zhang, X.; Ding, J., Gambogic acid inhibits the catalytic activity of human topoisomerase II α by binding to its ATPase domain. *Mol Cancer Ther* **2007**, *6* (9), 2429-40.
181. Woo, S.; Jung, J.; Lee, C.; Kwon, Y.; Na, Y., Synthesis of new xanthone analogues and their biological activity test--cytotoxicity, topoisomerase II inhibition, and DNA cross-linking study. *Bioorg Med Chem Lett* **2007**, *17* (5), 1163-6.
182. Saraiva, L.; Fresco, P.; Pinto, E.; Sousa, E.; Pinto, M.; Gonçalves, J., Inhibition of protein kinase C by synthetic xanthone derivatives. *Bioorg Med Chem* **2003**, *11* (7), 1215-25.
183. Zou, Y. S.; Hou, A. J.; Zhu, G. F.; Chen, Y. F.; Sun, H. D.; Zhao, Q. S., Cytotoxic isoprenylated xanthenes from *Cudrania tricuspidata*. *Bioorg Med Chem* **2004**, *12* (8), 1947-53.
184. Lin, C. N.; Liou, S. J.; Lee, T. H.; Chuang, Y. C.; Won, S. J., Xanthone derivatives as potential anti-cancer drugs. *J Pharm Pharmacol* **1996**, *48* (5), 539-44.
185. Fellows, I. M.; Schwaebe, M.; Dexheimer, T. S.; Vankayalapati, H.; Gleason-Guzman, M.; Whitten, J. P.; Hurley, L. H., Determination of the importance of the stereochemistry of psorospermin in topoisomerase II-induced alkylation of DNA and in vitro and in vivo biological activity. *Mol Cancer Ther* **2005**, *4* (11), 1729-39.
186. Kwok, Y.; Hurley, L. H., Topoisomerase II site-directed alkylation of DNA by psorospermin and its effect on topoisomerase II-mediated DNA cleavage. *J Biol Chem* **1998**, *273* (49), 33020-6.
187. Cho, H. J.; Jung, M. J.; Woo, S.; Kim, J.; Lee, E. S.; Kwon, Y.; Na, Y., New benzoxanthone derivatives as topoisomerase inhibitors and DNA cross-linkers. *Bioorg Med Chem* **2010**, *18* (3), 1010-7.

188. Woo, S.; Kang, D. H.; Nam, J. M.; Lee, C. S.; Ha, E. M.; Lee, E. S.; Kwon, Y.; Na, Y., Synthesis and pharmacological evaluation of new methyloxiranylmethoxyxanthone analogues. *Eur J Med Chem* **2010**, *45* (9), 4221-8.
189. Su, Q. G.; Liu, Y.; Cai, Y. C.; Sun, Y. L.; Wang, B.; Xian, L. J., Anti-tumour effects of xanthone derivatives and the possible mechanisms of action. *Invest New Drugs* **2011**, *29* (6), 1230-40.
190. Jun, K. Y.; Lee, E. Y.; Jung, M. J.; Lee, O. H.; Lee, E. S.; Park Choo, H. Y.; Na, Y.; Kwon, Y., Synthesis, biological evaluation, and molecular docking study of 3-(3'-heteroatom substituted-2'-hydroxy-1'-propyloxy) xanthone analogues as novel topoisomerase II α catalytic inhibitor. *Eur J Med Chem* **2011**, *46* (6), 1964-71.
191. Wu, G.; Yu, G.; Kurtán, T.; Mándi, A.; Peng, J.; Mo, X.; Liu, M.; Li, H.; Sun, X.; Li, J.; Zhu, T.; Gu, Q.; Li, D., Versixanthones A-F, Cytotoxic Xanthone-Chromanone Dimers from the Marine-Derived Fungus *Aspergillus versicolor* HDN1009. *J Nat Prod* **2015**, *78* (11), 2691-8.
192. Sun, H.; Chen, F.; Wang, X.; Liu, Z.; Yang, Q.; Zhang, X.; Zhu, J.; Qiang, L.; Guo, Q.; You, Q., Studies on gambogic acid (IV): Exploring structure-activity relationship with I κ B kinase-beta (IKK β). *Eur J Med Chem* **2012**, *51*, 110-23.
193. Sousa, M. E.; Pinto, M. M., Synthesis of xanthenes: an overview. *Curr Med Chem* **2005**, *12* (21), 2447-79.
194. Worland, S. T.; Wang, J. C., Inducible overexpression, purification, and active site mapping of DNA topoisomerase II from the yeast *Saccharomyces cerevisiae*. *J Biol Chem* **1989**, *264* (8), 4412-6.
195. Wasserman, R. A.; Austin, C. A.; Fisher, L. M.; Wang, J. C., Use of yeast in the study of anticancer drugs targeting DNA topoisomerases: Expression of a functional recombinant human DNA topoisomerase II α in yeast. *Cancer research* **1993**, *53* (15), 3591-3596.
196. Kingma, P. S.; Greider, C. A.; Osheroff, N., Spontaneous DNA lesions poison human topoisomerase II α and stimulate cleavage proximal to leukemic 11q23 chromosomal breakpoints. *Biochemistry* **1997**, *36* (20), 5934-9.
197. Fortune, J. M.; Osheroff, N., Merbarone inhibits the catalytic activity of human topoisomerase II α by blocking DNA cleavage. *J Biol Chem* **1998**, *273* (28), 17643-50.
198. Miller, K. G.; Liu, L. F.; Englund, P. T., A homogeneous type II DNA topoisomerase from HeLa cell nuclei. *J Biol Chem* **1981**, *256* (17), 9334-9.
199. Sastry, G. M.; Adzhigirey, M.; Day, T.; Annabhimoju, R.; Sherman, W., Protein and ligand preparation: parameters, protocols, and influence on virtual screening enrichments. *J Comput Aided Mol Des* **2013**, *27* (3), 221-34.
200. Ashley, R. E.; Dittmore, A.; McPherson, S. A.; Turnbough, C. L.; Neuman, K. C.; Osheroff, N., Activities of gyrase and topoisomerase IV on positively supercoiled DNA. *Nucleic Acids Res* **2017**, *45* (16), 9611-9624.
201. Shao, Q.; Goyal, S.; Finzi, L.; Dunlap, D., Physiological levels of salt and polyamines favor writhe and limit twist in DNA. *Macromolecules* **2012**, *45* (7), 3188-3196.
202. Thomas, T. J.; Tajmir-Riahi, H. A.; Thomas, T., Polyamine-DNA interactions and development of gene delivery vehicles. *Amino Acids* **2016**, *48* (10), 2423-31.
203. Baird, C. L.; Harkins, T. T.; Morris, S. K.; Lindsley, J. E., Topoisomerase II drives DNA transport by hydrolyzing one ATP. *Proc Natl Acad Sci U S A* **1999**, *96* (24), 13685-90.

204. Minniti, E.; Byl, J. A. W.; Riccardi, L.; Sissi, C.; Rosini, M.; De Vivo, M.; Minarini, A.; Osheroff, N., Novel xanthone-polyamine conjugates as catalytic inhibitors of human topoisomerase II α . *Bioorg Med Chem Lett* **2017**, *27* (20), 4687-4693.
205. Elsea, S. H.; Westergaard, M.; Burden, D. A.; Lomenick, J. P.; Osheroff, N., Quinolones share a common interaction domain on topoisomerase II with other DNA cleavage-enhancing antineoplastic drugs. *Biochemistry* **1997**, *36* (10), 2919-24.
206. Aldred, K. J.; Breland, E. J.; Vlčková, V.; Strub, M. P.; Neuman, K. C.; Kerns, R. J.; Osheroff, N., Role of the water-metal ion bridge in mediating interactions between quinolones and Escherichia coli topoisomerase IV. *Biochemistry* **2014**, *53* (34), 5558-67.
207. Osheroff, N.; Zechiedrich, E. L., Calcium-promoted DNA cleavage by eukaryotic topoisomerase II: trapping the covalent enzyme-DNA complex in an active form. *Biochemistry* **1987**, *26* (14), 4303-9.
208. Friesner, R. A.; Murphy, R. B.; Repasky, M. P.; Frye, L. L.; Greenwood, J. R.; Halgren, T. A.; Sanschagrin, P. C.; Mainz, D. T., Extra precision glide: docking and scoring incorporating a model of hydrophobic enclosure for protein-ligand complexes. *J Med Chem* **2006**, *49* (21), 6177-96.
209. Boritzki, T. J.; Wolfard, T. S.; Besserer, J. A.; Jackson, R. C.; Fry, D. W., Inhibition of type II topoisomerase by fostriecin. *Biochem Pharmacol* **1988**, *37* (21), 4063-8.
210. Utsumi, H.; Shibuya, M. L.; Kosaka, T.; Buddenbaum, W. E.; Elkind, M. M., Abrogation by novobiocin of cytotoxicity due to the topoisomerase II inhibitor amsacrine in Chinese hamster cells. *Cancer Res* **1990**, *50* (9), 2577-81.
211. Dimaggio, J. J.; Warrell, R. P.; Muindi, J.; Stevens, Y. W.; Lee, S. J.; Lowenthal, D. A.; Haines, I.; Walsh, T. D.; Baltzer, L.; Yaldae, S., Phase I clinical and pharmacological study of merbarone. *Cancer Res* **1990**, *50* (4), 1151-5.
212. Chen, M.; Beck, W. T., Teniposide-resistant CEM cells, which express mutant DNA topoisomerase II alpha, when treated with non-complex-stabilizing inhibitors of the enzyme, display no cross-resistance and reveal aberrant functions of the mutant enzyme. *Cancer Res* **1993**, *53* (24), 5946-53.
213. Chen, M.; Beck, W. T., DNA topoisomerase II expression, stability, and phosphorylation in two VM-26-resistant human leukemic CEM sublines. *Oncol Res* **1995**, *7* (2), 103-11.
214. Ranise, A.; Bruno, O.; Bondavalli, F.; Schenone, S.; D'Amico, M.; Falciani, M.; Filippelli, W.; Rossi, F., 5-Substituted 2,3-dihydro-6-mercapto-1,3-diphenyl-2-thioxo-4(3H)-pyrimidinones and their 6-(acylthio) derivatives with platelet antiaggregating, antiinflammatory, antiarrhythmic, antihyperlipidemic and other activities. *Farmaco* **1994**, *49* (9), 551-8.
215. Ranise, A.; Spallarossa, A.; Schenone, S.; Bruno, O.; Bondavalli, F.; Pani, A.; Marongiu, M. E.; Mascia, V.; La Colla, P.; Loddo, R., Synthesis and antiproliferative activity of basic thioanalogues of merbarone. *Bioorg Med Chem* **2003**, *11* (12), 2575-89.
216. Spallarossa, A.; Rotolo, C.; Sissi, C.; Marson, G.; Greco, M. L.; Ranise, A.; La Colla, P.; Busonera, B.; Loddo, R., Further SAR studies on bicyclic basic merbarone analogues as potent antiproliferative agents. *Bioorg Med Chem* **2013**, *21* (21), 6328-36.
217. Baviskar, A. T.; Amrutkar, S. M.; Trivedi, N.; Chaudhary, V.; Nayak, A.; Guchhait, S. K.; Banerjee, U. C.; Bharatam, P. V.; Kundu, C. N., Switch in Site of Inhibition: A Strategy for Structure-Based Discovery of Human Topoisomerase II α Catalytic Inhibitors. *ACS Med Chem Lett* **2015**, *6* (4), 481-5.

218. Palermo, G.; Favia, A. D.; Convertino, M.; De Vivo, M., The Molecular Basis for Dual Fatty Acid Amide Hydrolase (FAAH)/Cyclooxygenase (COX) Inhibition. *ChemMedChem* **2016**, *11* (12), 1252-8.
219. Favia, A. D.; Habrant, D.; Scarpelli, R.; Migliore, M.; Albani, C.; Bertozzi, S. M.; Dionisi, M.; Tarozzo, G.; Piomelli, D.; Cavalli, A.; De Vivo, M., Identification and characterization of carprofen as a multitarget fatty acid amide hydrolase/cyclooxygenase inhibitor. *J Med Chem* **2012**, *55* (20), 8807-26.
220. Cesarini, S.; Spallarossa, A.; Ranise, A.; Bruno, O.; Arduino, N.; Bertolotto, M.; Dallegrì, F.; Tognolini, M.; Gobbetti, T.; Barocelli, E., 6-amino-4-oxo-1,3-diphenyl-2-thioxo-1,2,3,4-tetrahydropyrimidine-5-carbonyl derivatives as a new class of potent inhibitors of Interleukin-8-induced neutrophil chemotaxis. *Bioorg Med Chem* **2009**, *17* (10), 3580-7.
221. Koley, D.; Colón, O. C.; Savinov, S. N., Chemoselective nitration of phenols with tert-butyl nitrite in solution and on solid support. *Org Lett* **2009**, *11* (18), 4172-5.
222. De Vivo, M.; Masetti, M.; Bottegoni, G.; Cavalli, A., Role of Molecular Dynamics and Related Methods in Drug Discovery. *J Med Chem* **2016**, *59* (9), 4035-61.
223. Huang, X.; Traganos, F.; Darzynkiewicz, Z., DNA damage induced by DNA topoisomerase I- and topoisomerase II-inhibitors detected by histone H2AX phosphorylation in relation to the cell cycle phase and apoptosis. *Cell Cycle* **2003**, *2* (6), 614-9.
224. Ortega, J. A.; Riccardi, L.; Minniti, E.; Borgogno, M.; Arencibia, J. M.; Greco, M. L.; Minarini, A.; Sissi, C.; De Vivo, M., Pharmacophore Hybridization To Discover Novel Topoisomerase II Poisons with Promising Antiproliferative Activity. *J Med Chem* **2017**.
225. Jafari, E.; Khajouei, M. R.; Hassanzadeh, F.; Hakimelahi, G. H.; Khodarahmi, G. A., Quinazolinone and quinazoline derivatives: recent structures with potent antimicrobial and cytotoxic activities. *Res Pharm Sci* **2016**, *11* (1), 1-14.
226. Akhtar, J.; Khan, A. A.; Ali, Z.; Haider, R.; Shahar Yar, M., Structure-activity relationship (SAR) study and design strategies of nitrogen-containing heterocyclic moieties for their anticancer activities. *Eur J Med Chem* **2017**, *125*, 143-189.
227. Bonomi, P., Erlotinib: a new therapeutic approach for non-small cell lung cancer. *Expert Opin Investig Drugs* **2003**, *12* (8), 1395-401.
228. Herbst, R. S.; Fukuoka, M.; Baselga, J., Gefitinib--a novel targeted approach to treating cancer. *Nat Rev Cancer* **2004**, *4* (12), 956-65.
229. Katiyar, S. B.; Bansal, I.; Saxena, J. K.; Chauhan, P. M., Syntheses of 2,4,6-trisubstituted pyrimidine derivatives as a new class of antifilarial topoisomerase II inhibitors. *Bioorg Med Chem Lett* **2005**, *15* (1), 47-50.
230. Marzaro, G.; Dalla Via, L.; Toninello, A.; Guiotto, A.; Chilin, A., Benzoquinazoline derivatives as new agents affecting DNA processing. *Bioorg Med Chem* **2011**, *19* (3), 1197-204.
231. Le, T. N.; Yang, S. H.; Khadka, D. B.; Van, H. T.; Cho, S. H.; Kwon, Y.; Lee, E. S.; Lee, K. T.; Cho, W. J., Design and synthesis of 4-amino-2-phenylquinazolines as novel topoisomerase I inhibitors with molecular modeling. *Bioorg Med Chem* **2011**, *19* (14), 4399-404.
232. Khadka, D. B.; Tran, G. H.; Shin, S.; Nguyen, H. T.; Cao, H. T.; Zhao, C.; Jin, Y.; Van, H. T.; Chau, M. V.; Kwon, Y.; Le, T. N.; Cho, W. J., Substituted 2-arylquinazolinones: Design, synthesis, and evaluation of cytotoxicity and inhibition of topoisomerases. *Eur J Med Chem* **2015**, *103*, 69-79.

233. Sun, H. P.; Jia, J. M.; Jiang, F.; Xu, X. L.; Liu, F.; Guo, X. K.; Cherfaoui, B.; Huang, H. Z.; Pan, Y.; You, Q. D., Identification and optimization of novel Hsp90 inhibitors with tetrahydropyrido[4,3-d]pyrimidines core through shape-based screening. *Eur J Med Chem* **2014**, *79*, 399-412.
234. Martin, R.; Buchwald, S. L., Palladium-catalyzed Suzuki-Miyaura cross-coupling reactions employing dialkylbiaryl phosphine ligands. *Accounts of chemical research* **2008**, *41* (11), 1461-73.
235. Fortune, J. M.; Velea, L.; Graves, D. E.; Utsugi, T.; Yamada, Y.; Osheroff, N., DNA topoisomerases as targets for the anticancer drug TAS-103: DNA interactions and topoisomerase catalytic inhibition. *Biochemistry* **1999**, *38* (47), 15580-6.